HZB Helmholtz Zentrum Berlin

FIFTH JOINT BER II AND BESSY II USERS MEETING
Dec. 4-6, 2013

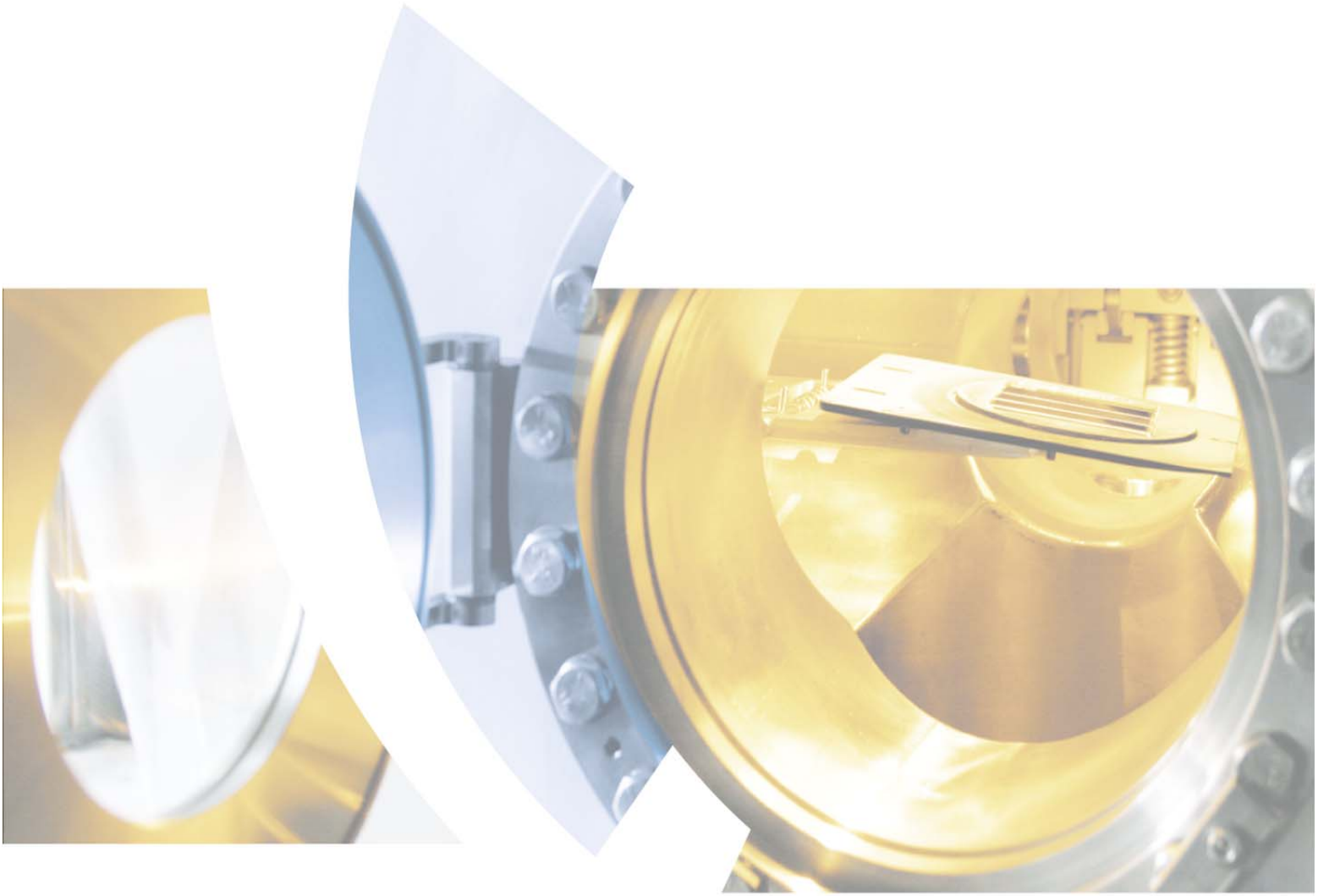

- Neutron Instrumentation Day
- Science Day
- Synchrotron Instrumentation Day
- Vendor Exhibition
- Poster Session

Lise-Meitner-Campus, Berlin-Wannsee and
WISTA and Wilhelm-Conrad-Röntgen Campus, Berlin-Adlershof
https://www.helmholtz-berlin.de/user/usersmeetings/user-meeting-2013/index_en.html

Helmholtz-Zentrum Berlin

für Materialien und Energie GmbH

Lise-Meitner-Campus:

BER II

Hahn-Meitner-Platz 1
14109 Berlin
tel +49 (0)30 8062-42304
fax +49 (0)30 8062-42523
neutrons@helmholtz-berlin.de

Wilhelm-Conrad-Röntgen-Campus:

BESSY II

Albert-Einstein-Str. 15
12489 Berlin
tel +49 (0)30 8062-14666/12981
fax +49 (0)30 8062-14746
photons@helmholtz-berlin.de

htttp://www.helmholtz-berlin.de

Dear friends and users,

Welcome to the 5th *Joint BER II and BESSY II User Meeting of HZB*, which brings together users of our neutron and synchrotron sources at our sites in Berlin Wannsee and Adlershof.

In 2013, the operation of the synchrotron source BESSY II was influenced by the extended summer shutdown, which was used, e.g., to exchange two of four remaining old cavities in the electron storage ring, to start the construction of the EMIL building as well as the building of the new control room for a joint operation of the BESSY II storage ring and the MLS facility of PTB. Till the shutdown at the end of July 2013 the users were served with a stable and brilliant photon flux in full top-up mode, offering more photons than ever to our users. Improvements at individual beamlines included the set-up of a Pilatus detector system at the PX beamline, the commissioning of a new zone plate monochromator at the UE56-1 ZPM, the start of the commissioning of the RICXS beamline at the UE49 SGM as well as the commence of the construction of the KMC-3 diffractometer.

Further investments at BESSY II are made with the purchase of a chopper system for single bunch usage, co-financing a new dedicated VUV and soft X-ray spectroscopy beamline in collaboration with the Humboldt University and the installation of a technology center for highly efficient optical gratings at HZB. A drawback was the failure of the re-installation of the 7T multipole wiggler due to design changes during repair, which delayed the operation of the beamlines EDDI and ASAXS towards 2014.

The construction of the building for the EMIL facility has started and will be finished next year, offering new possibilities for in-situ research in catalysis and energy research together with the Max Planck Society. The BESSY VSR - Workshop "The Variable pulse length Synchrotron Radiation source" in October gave a look into the future of BESSY II and HZB, opening new ideas and options for research. BESSY users enthusiastically endorsed the BESSY VSR concept. A further big step forward to realizing BESSY VSR was the successful pulse-picking experiment.

A successful operation characterized the BER II neutron facility in 2013. Currently sixteen beamlines are in full user operation. An external group of international experts reviewed the beamlines and the general operation of BER II in May 2013. Following the recommendations of these experts and the unanimous decision of HZB's supervisory board to close the BER II reactor in 2020, a strategy on the full user operation of the ten best neutron instruments has been developed and implemented. This secures best operation and service for a suite of instruments for the upcoming six years of user operation. Hence, HZB offers full access to a modern and competitive number of instruments to the community, including new beamlines as the reflectometer BioRef, the VSANS instrument, the neutron Laue diffractometer FALCON, the diffractometer for extreme environment EXED with the High Field Magnet and the future new spectrometer NEAT.

A further improvement of the user service at HZB has been the launch of the new user portal GATE. It worked successfully in the proposal round 2014/I with more than 800 proposals and will help to improve and streamline the common HZB user operation.

The three-part program of the *Joint User Meeting* is highlighted by the keynote lecture by Theo Raising on “Magnetism at the time and length scale of the exchange interaction” and the public lecture by Emil List-Kratochvil on “How bright light is used to improve organic light”. The Verein Freundeskreis Helmholtz-Zentrum Berlin e.V. will bestow the Innovation Award and the Ernst-Eckart-Koch Prize. The Neutron Day and the Synchrotron Day each have a special highlight with young scientists presenting their unique research. The Science Day on Thursday is concluded with a poster session accompanied by the traditional “Berlin Buffet”, kindly sponsored by the companies represented in the industrial exhibition area. Two satellite workshops are organized on industrial use of synchrotron and neutrons and on new methods in protein crystallography. We hope all these meetings will stimulate your interest in photons and neutrons and initiate fruitful new experiments and collaborations. Thank you all for joining us and enjoy the meeting.

Sincerely,

Prof. Dr.-Ing. Anke Kaysser-Pyzalla
Scientific Director and Chief Executive

Contents

Program

Wednesday, December 4th, 2013 : Young Scientists and Neutron Day		Lise-Meitner Campus Hahn-Meitner-Platz 1 14109 Berlin
12:00 – 13:30	Registration and Workshop Lunch	(LMC-Foyer and Café Jahn)
13:30 – 15:00	Neutron Session	(Lecture Hall)
13:30	Welcome	
13:40	*Michael Schöbel (TU München/FRM 2)* Elasto-plastic deformation behavior of heterogeneous materials	
14:00	*Gerald Eisenblätter (Uni Leipzig)* The look inside Roman copper coins: X-ray and neutron tomography experiments	
14:20	*Sascha Oswald (Uni Potsdam)* For your eyes also: Visualizing the secrets of soil	
14:40	*Gail Iles (HZB)* FALCON - Fast Acquisition Laue Diffractometer	
15:00 – 15:30	Coffee Break	(LMC-Foyer)
15:30 – 17:00	Young Scientist Session	(Lecture Hall)
15:30	*Adina Eichner (MLU Halle)* **Ceramid [EOS] and its impact on the lipid membrane** organization of the Stratum corneum - A neutron diffraction study	
15:45	*Leonardo Chiappisi (TU Berlin)* Chitosan-Alkylethoxy Carboxylates - A Surprising Variety of Structures identified by Small Angle Neutron Scattering	
16:00	*Johannes Kähn (HZB)* Comparing the annealing dependency of Al/Si distribution in Sanidine megacrysts from the Eifel region with X-ray and neutron diffraction methods	
16:15	*Rasmus Toft-Petersen (HZB)* Field-induced spin disorder in a doped magneto-electric Ising system	
16:30	*Ariane Hannaske (MPI CPFS Dresden)* $YbCo_2Si_2$ – the reference compound to $YbRh_2Si_2$?!	
16:45	*Mirko Erlkamp (TU Dortmund)* High-pressure studies of lipid and protein films at aqueous-solid Interfaces	
17:00 – 19:00	Poster Session	(Colloquiums room)
19:00	Dinner	(Café Jahn)

Thursday, December 5th, 2013 : Science Day		Wilhelm-Conrad-Roentgen Campus Albert-Einstein-Str. 15 Rudower Chaussee 17 12489 Berlin
9:00 – 18:00	Vendor Exhibition	WISTA Centre
8:30 – 9:30	Registration and Poster Set-up	WISTA Centre
9:30 – 9:40	Opening	Bunsen Auditorium
9:40 – 10:10	Key Note Lecture *Theo Rasing (Raboud University Nijmegen)* *Magnetism at the time and length scale of the exchange interaction*	
10:10 – 10:40	Coffee Break and Vendor Exhibition	WISTA Centre
10:40 – 12:20	Oral Presentations I	Bunsen Auditorium
10:40	*Christian Schüssler-Langeheine (HZB)* *Ultrafast dynamics in antiferromagnets*	
11:00	*Malte Behrens (FHI)* *Surface and bulk analysis of Cu-Composite catalysts for Methanol Synthesis using photons and neutrons*	
11:20	*Lada Yashina (Moscow State University)* *Chemistry of discharge and recharge of Li-air battery: operando XPS studies*	
11:40	*Maria Guerra (Louvre)* *Between the Eurasian steppes and China: provenancing the Xiongnu gold by IBA and SRXRF*	
12:00	*Henrik Ronnow (EPFL, PSI)* *Magnetic order and quantum criticality in dipolar coupled model magnets*	
12:20 – 13:30	Lunch Break	(Canteens on site)
13:30 – 15:10	Oral Presentations II	Bunsen Auditorium
13:30	*Katja Henzler (HZB)* *Electronic Structure of Individual Hybrid Colloid Particles Studied by NEXAFS in the X-ray Microscope*	

13:50	*Harald Schmidt (TU Clausthal)* *Electrode Lithiation in Lithium-Ion Batteries Investigated by In-Operando Neutron Reflectometry*	
14:10	*Andres Santander Syro (CNRS, CSNSM)* *Momentum-resolved reconstruction of the electronic structure across the 'hidden-order' transition in URu_2Si_2*	
14:30	*Roel Van de Krol (HZB)* *Efficient Solar Water Splitting with a $BiVO_4$-Amorphous Silicon Heterojunction Photoanode*	
14:50	*Yeal Politi (MPI Golm)* *A Spider´s Fang: How to Design an Injection Needle Using Chitin-Based Composite Material*	
15:10 – 15:40	Coffee Break and Vendor Exhibition	WISTA Centre
15:40 – 15:50	User Committee	Bunsen Auditorium
15:50 – 17:00	Bestowal of Prizes: Friends of Helmholtz-Zentrum Berlin e.V. *(Chair: M. Richter)*	Bunsen Auditorium
17:00 – 18:00	Public Lecture *Emil List-Kratochvil (TU GRAZ)* *How Bright Light is Used to Improve Organic Light: Research on Organic Light Emitting Diodes at BESSY II*	Bunsen Auditorium
18:00 – 20:00	Poster Session	(BESSY II Experimental Hall)
20:00	Berliner Buffet (sponsored by the companies participating in the vendor exhibition)	(BESSY II Foyer)

Friday, December 6th, 2013
Young Scientists and Synchrotron Day

Wilhelm-Conrad-Roentgen Campus
Albert-Einstein-Str. 15
Rudower Chaussee 17
12489 Berlin

8:30-11:30	Vendor Exhibition and Registration	WISTA Centre
9:00 – 10:30	Young Scientists Session (6 talks, 15 minutes each)	Bunsen Auditorium
9:00	*Nele Thielemann-Kühn (HZB)* *Nonmagnetic linear dichroism in fluorescence spectra from a cubic solid*	
9:15	*Kathrin Koren (TU Graz) Investigation of the Energy Level Alignment in Solution Processed Multilayer PLEDs Utilizing Photoelectron Spectroscopy*	
9:30	*Stephanie Rädel (HZB)* *Investigation of microbunching-instability in energy recovery linacs*	
9:45	*Maxim Erko (MPI of Colloids and Interfaces)* *Deformation mechanism of nanoporous materials upon water freezing and melting*	
10:00	*Andrea Schmidt (Charité) Redox-dependent structural and chemical transformation of the [4Fe3S] cluster in an O_2-tolerant [NiFe] hydrogenase*	
10:15	*Stefanie Winkler (HU Berlin)* *Fermi Level Pinning of Organic Semiconductors on Metaloxides*	
10:30 – 10:40	Poster Prize	Bunsen Auditorium
10:40 – 11:10	Coffee Break and Vendor Exhibition	WISTA Centre
11:10 – 13:00	BESSY II - today and in the future	Bunsen Auditorium
11:10	*Anke Kaysser-Pyzalla (HZB)* *Opening*	
11:20	*Andreas Jankowiak (HZB)* *BESSY II: Status and Perspectives - BERLinPro*	
11:40	*Alexander Föhlisch (HZB)* *BESSY II Status and the BESSY VSR perspective*	
12:00	*Klaus Habicht* *Complementary Spectroscopy at BER II and BESSY II*	
12:20	*Klaus Lips (HZB)* *EMIL (Energy Materials In-Situ Laboratory Berlin) - a novel research platform for next generation solar energy materials at BESSY II*	
12:40	*Christian Jung (HZB)* *DOMINO – the first brick has fallen*	
13:00 – 13:10	*Andreas Jankowiak (HZB)* *Closing of Fifth Joint BER II and BESSY II Users Meeting*	

Abstracts of the invited talks at the Science Day

Thursday, 5th of December

MAGNETISM AT THE TIME AND LENGTH SCALE OF THE EXCHANGE INTERACTION

Theo Rasing[1]

1 Radboud University, Institute for Molecules and Materials, Heijendaalseweg 135, 6525AJ Nijmegen, the Netherlands

From the discovery of sub-picosecond demagnetization over a decade ago to the recent demonstration of magnetization reversal by a single 40 femtosecond laser pulse, the manipulation of spins by ultra short laser pulses has become a fundamentally challenging topic with a potentially high impact for future spintronics, data storage and manipulation and quantum computation. Theoretically, this field is still in its infancy, using phenomenological descriptions of the none-equilibrium dynamics between electrons, spins and phonons. A proper description should include the time dependence of the exchange interaction and nucleation phenomena on the nanometer length scale. A practical challenge is how to bring the optical manipulation of magnetic media to the required nanoscale, which may be possible using plasmonic or wave-shaping techniques. Recent results and an outlook to probe and control magnetic order on the femtosecond time and nanometer length scale will be discussed.

Recent references:

A.Kirilyuk, et al, **Rev. Mod.Phys. 82**, 2731-2784 (2010)
I.Radu et al, **Nature 472**, 205 (2011)
J. Mentink et al, **Phys.Rev.Lett.108,**057202(2012)
T. Ostler et al, **Nature Comm. 3**, 666 (2012)
A.R.Khorsand et al, **Phys.Rev.Lett.108**, 127205 (2012)
C. Graves et al, **Nature Materials12**, 293 (2013)

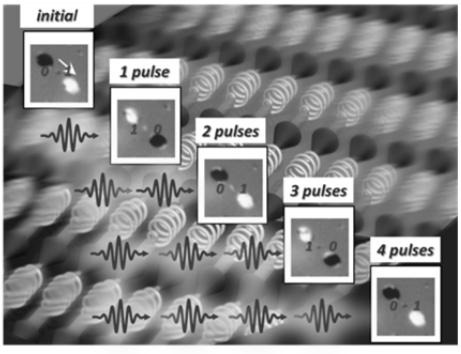

Demonstration of magnetic domain switching by unpolarized laser pulses (T.Ostler et al)

Berlin, 5 December 2013

Ultrafast dynamics in antiferromagnets

Ch. Schüßler-Langeheine, Helmholtz Zentrum Berlin für Materialien und Energie GmbH, Germany

Motivated by the prospect of faster data processing and storage technology, a wealth of experimental and theoretical studies has dealt with ultrafast spin manipulation. It turned out that the speed limit for spin manipulation is defined by the maximum rate, at which angular momentum can be transferred in the system. To manipulate the spin in ferromagnets, angular momentum has to be exchanged between the spin system and another degree of freedom. For antiferromagnets, however, spin manipulation can also be achieved via redistribution of angular momentum within the spin system. We studied ultrafast antiferromagnetic dynamics in a time-resolved resonant soft x-ray diffraction experiment at the FEMTOSPEX slicing facility and found this additional channel to be extremely efficient.

M. Behrens 5.12.13, 11:00

Surface and Bulk Analysis of Cu-Composite Catalysts for Methanol Synthesis Using Photons and Neutrons

Malte Behrens[1], Timur Kandemir[1], Stefan Zander[1,2], Manfred E. Schuster[1], Thomas Lunkenbein[1], Detre Teschner,[1] Michael Hävecker[2], Michael Tovar[2], Dirk Wallacher[2], Robert Schlögl[1]

1 Fritz-Haber-Institut der Max-Planck-Gesellschaft, Department of Inorganic Chemistry, Faradayweg 4-6, 14195 Berlin, Germany
2 Helmholtz-Zentrum Berlin für Materialien und Energie (HZB), Hahn-Meitner-Platz 1, 14109 Berlin and Albert-Einstein-Str. 15, 12489 Berlin, Germany

Methanol is an interesting synthetic fuel that can be synthesized from CO_2 and renewable hydrogen. It is liquid at ambient conditions, can be easily distributed and stored, and is a versatile platform molecule for the chemical industry. The current industrial process used Cu/ZnO-composite catalysts and mixtures of CO_2, CO and H_2 from fossil sources as synthesis gas. Although this is a mature and scalable technology, there still are many challenges and open questions regarding active sites and reaction mechanism of the hydrogenation of anthropogenic CO_2 with renewable H_2. In the last years, we have intensively studied the industrial catalyst using a variety of bulk- and surface-sensitive techniques. In our contribution, we will show how neutron diffraction and X-ray photoelectron spectroscopy (XPS) can help to get a better understanding of complex composite catalysts. These techniques deliver complementary insights into the relevance of the catalyst's defect structure, the critical interplay of the Cu and ZnO components and, finally, the nature of the active sites for methanol synthesis. The results are confirmed by high-resolution transmission electron microscopy. In particular, the concentration of planar defects in the metallic Cu nano-particles was studied under working conditions by in-situ neutron diffraction[1] and the strong interaction of the particles with the reducible ZnO component was analyzed based on in-situ XPS.[2] Both defects and strong Cu-ZnO interaction were found to be essential for a high performance catalyst.[3] The defects are a result of the unique catalyst synthesis route, while the synergetic interactions and the reducibility of ZnO can be promoted by doping of ZnO with trivalent cations.[4] In summary, the case of the industrial methanol synthesis catalyst is an example for the multi-method characterization approach, including diffraction, spectroscopy and imaging techniques, being a pre-requisite for the identification of the crucial (micro-)structural properties of a complex realistic composite catalyst.

1 Angew Chem Int Edit,52,5166,(2013)
2 Angew Chem Int Edit,52,6536,(2013)
3 Science,18,893,(2012)
4 J Am Chem Soc,135,6061,(2013)

Chemistry of discharge and recharge of Li-air battery: *operando* XPS studies

Daniil M. Itkis[1], Dmitry A. Semenenko[1], Elmar Yu. Kataev[1], Vera S. Neudachina[1], Michael Haÿecker[2,3], Detre Teschner[2], Axel Knop-Gericke[2,3], Alexei Barinov[4], Denis Vyalikh[5], Lada V. Yashina[1]

1 Moscow State University, Russia
2 Fritz-Haber Institute of the Max Planck Society, Germany
3 Helmholtz Zentrum Berlin, Germany
4 Sincrotrone Trieste S.C.p.A., Italy
5 TU Dresden, Germany

Power sources that utilize the reaction of lithium and oxygen have become a great challenge since first works in 1996 [1]. Today lithium-air batteries (LAB) attract new wave of attention due to its promise to provide more than 1 kWh/kg and skyrocketing expansion of electric vehicle market [2]. However practical use of LAB is limited by low round-trip efficiency associated with slow kinetics of oxygen reduction on discharge, oxygen evolution on charge and variety of side reactions. Nowadays researcher efforts are focused on different carbon electrode materials. Rather contradictory data on recharge efficiency and cycleablity of a battery with carbon electrode were published last year [3]. In general, the lack of rechargebility is associated with Li_2CO_3 byproduct formation. It appears at the cathode due to lithium superoxide (electrochemical intermediate) or peroxide (discharge product) reactions with the carbon (electrode material). Advanced operando analysis of the processes at the cathode is highly useful in order to resolve such situations and facilitate the search of proper electrode materials. Using *operando* high pressure XPS experiments we show that superoxide radicals generated at the cathode during discharge react with carbon that contains activated double bonds or aromatics to form epoxy groups and carbonates, which limits the rechargeability of Li−O_2 cells [4]. Carbon materials with a low amount of functional groups and defects demonstrate better stability and does not react with Li_2O_2 thus keeping the carbon will-o'-the-wisp lit for lithium−air batteries.

1. J. Electrochem Soc – 143,1(1996)
2. J Phys Chem Let 1,14 (2010)
3. Science 337, 563 (2012)
4. Nano Lett 130904111116007(2013)

Between the Eurasian steppes and China: provenancing the Xiongnu gold by IBA and SRXRF

Maria F. Guerra[1, 2], Martin Radtke[3], Ina Reiche[1], Uwe Reinholz[3], Heinrich Riesemeier[3]

1 Laboratory of Molecular and Structural Archaeology, UMR 8220 CNRS, Paris, France
2 Centre for Research and Restoration of the Museums of France, Paris, France
3 BAM Federal Institute for Materials Research and Testing, Berlin, Germany

Excellent warriors and horsemen, the Xiongnu were a significant military power in the Central Asian steppes, toward the Chinese frontier, who maintained a political relation of "harmony" with the Han. The recent archaeological finds in important sites evidenced a complex economical society for this nomadic tribal league, who left no written documents. Their supplies originated from tribes' tributes and from trade with China together with Chinese offerings. Gol Mod, a Xiongnu necropolis in the north of Mongolia excavated under the aegis of UNESCO by French archaeologists, delivers since 2001 elements typically from both the Chinese and the steppes cultures.

Among the materials found in the burials, gold is a central element. In contrast with the steppes, in China gold jewellery is rare (jade and bronze are the symbols of status and richness) and Chinese texts evoke gold jewellery among the offerings to the Xiongnu. However, many of their sites are situated nearby alluvial gold deposits, which raise questions about the Chinese assertions.

The aim of this work is to establish the provenance of the Xiongnu gold. Are the gold objects found in Gol Mod made by the Chinese or are they a local Xiongnu production?

By coupling IBA data with results obtained by developing at BESSY a SRXRF protocol for this study, we fingerprinted the Xiongnu gold and we could clearly demonstrate that gold metallurgy in the Xiongnu territory is not Chinese, but a local practice by exploiting local and regional alluvial gold resources.

H. Ronnow 5.12.13, 12:00

Magnetic order and quantum criticality in dipolar coupled model magnets

Henrik Ronnow

Combining neutron scattering and low-temperature specific heat and susceptibility measurements, we present results demonstrating surprisingly rich physics emerging from simple dipolar coupled model magnets. Phenomena range from the effect of nuclear spin bath on quantum criticality in LiHoF4 to dimensional reduction in LiErF4 and spin-glass phenomena in mixed Li(Ho/Er)F4 samples.

K. Henzler 5.12.13, 13:30

Individual Hybrid Colloid Particles studied by NEXAFS spectronanoscopy

Katja Henzler[1], Peter Guttmann[1], Yan Lu[1], Frank Polzer[2], Andreas Ott[1,2], Gerd Schneider[1], Matthias Ballauff[1,2]

1 Institute for Soft Matter and Functional Materials, Helmholtz-Zentrum Berlin für Materialien und Energie GmbH, Wilhelm-Conrad-Röntgen-Campus: Albert-Einstein-Str. 15 D-12489 Berlin, Germany Liese-Meitner-Campus: Hahn-Meitner-Platz 1, D-14109 Berlin, Germany
2 Department of Physics, Humboldt University Berlin, Newtonstr. 15, D-12489 Berlin Germany

In the last years the controlled synthesis of complex colloidal hybrid particles has made an enormous progress. Hybrid materials with titanium dioxide as inorganic material are possible candidates for the usage in photocatalysis, like in solar water splitting, or in organic solar cells. However the synthesis of titanium dioxide nanocrystals at room temperature is still a challenge. The anatase nanoparticles are generated in the presence of colloidal microgels. The organic template consists of a solid polystyrene core and a cross-linked poly-N-(isopropylacrylamide) (PNIPAM) network shell. Anatase nanocrystals are generated by a modified sol-gel-process[1], whereas tetraethylorthotitanate is hydrolyzed in the presence of the microgels. These template particles act as nanoreactors which control the hydrolysis of the titanium precursor and leads to the formation of anatase nanocrystals with a diameter of around 6 nm. Until now, the structural analysis of the titanium dioxide on the level of single hybrid particles with statistical significance in aqueous environment is still missing. We will demonstrate that the combination of cryogenic near edge X-ray absorption fine structure (NEXAFS) spectroscopy with transmission X-ray microscopy (TXM)[1,2] provides an unique analytical method to investigate the structure of titanium dioxide nanoparticles on single microgel particles. The NEXAFS spectra show clearly that we have generated anatase nanoparticles with high crystallinity at room temperature. Due to the large field of view of the TXM, it offers the possibility to obtain statistical information about the structural uniformity between individual hybrid particles. Therefore, we are able to analyze the population density of titanium dioxide nanoparticles over many microgel carrier particles. The combination of cryo-TXM with NEXAFS spectroscopy presents a universal method for the structural investigation of hybrid materials.

References:

1. K. Henzler, P. Guttmann, Y. Lu, F. Polzer, G. Schneider, M. Ballauff, Nano Lett. 13, 824, (2013).
2. P. Guttmann, C. Bittencourt, S. Rehbein, P. Umek, XX. Ke, G. Van Tendeloo, C.P. Ewels, G. Schneider, Nat. Photonics 6, 25, (2012).

H. Schmidt 5.12.13, 13:50

Electrode Lithiation in Lithium-Ion Batteries Investigated by *In-Operando* Neutron Reflectometry

Bujar Jerliu[1], Erwin Hüger[1], Beatrix-Kamelia Seidlhofer[2], Roland Steitz[2], Tobias Panzner[3], Jochen Stahn[3], Harald Schmidt[1]

1 Technische Universität Clausthal, Clausthal-Zellerfeld, Germany
2 Helmholtz-Zentrum Berlin, Institut Weiche Materie und Funktionale Materialien, Germany
3 Paul-Scherrer-Institut, Villigen, Laboratory for Neutron Scattering, Switzerland

Lithium-ion batteries are widely developed and used as rechargeable power sources for portable electronic devices and will be essential in the field of automotive transportation. One of their major advantages is their low weight, and therefore the high energy density available. Kinetic processes and interface phenomena at electrodes during charging and discharging cycles play a key role for optimization of these batteries (e.g. for charging times and power density). As negative electrode material, amorphous silicon has become a promising candidate for future Li-ion battery applications due to its high theoretical specific capacity of about 4 Ah/g.

We report on *in-operando* neutron reflectometry experiments on the lithiation of amorphous silicon electrodes, which give insight into fundamental mechanisms and processes. Such studies allow to monitor the modification of Li content and the corresponding volume expansion/contraction of the electrode during lithiation on the nanometer scale. The measurements indicate that during galvanostatic charging Li incorporation takes place in form of a multi-step process, where a moving Li_xSi phase boundary plays an important role. Neutron reflectometry measurements during cyclic voltammetry allow to identify regions (U/I characteristics) where considerable lithium incorporation takes place and where not.

A further important aspect of battery design is the future demand on nanostructured electrode materials, which are more resistant to structural degradation by virtue of their small size. A new approach is discussed that allows to measure lithium transport parameters in nanometer sized silicon layers using isotope labelled multilayer stacks and neutron reflectometry.

B. Jerliu et al. Phys. Chem. Chem. Phys., 15, 7777, (2013)
E. Hüger et al. Nano Lett. 13, 1237, (2013)

Momentum-resolved reconstruction of the electronic structure across the 'hidden-order' transition in URu_2Si_2

C. Bareille[1], F. L. Boariu[2], H. Schwab[2], P. Lejay[3], F. Reinert[2], and A. F. Santander-Syro[1]

1 CSNSM, Université Paris-Sud et CNRS/IN2P3, Bât. 104 et 108, 91405 Orsay, France
2 Lehrstuhl für Experimentelle Physik VII, Universität Würzburg, Am Hubland, D 97074 Würzburg, Germany
3 Institut Néel, CNRS/UJF, B.P. 166, 38042 Grenoble Cedex 9, France

Due to their exceptionally strong correlations, *f*-electron systems present a wide realm of original phase transitions and often poorly understood states of matter. One of the most intriguing is the so-called hidden-order (HO) state forming below T_{HO} =17.5 K in URu_2Si_2. In this material, a heavy-fermion liquid seems to develop at temperatures below about 70 K, where clear experimental signatures of Kondo screening are found. The HO emerges on this pre-formed Kondo lattice, and is characterized a reduction of 60% in the electronic specific heat across the transition, suggesting that a gap of about 10 meV opens over a large portion of its Fermi surface. However, to date, there is no clear momentum-resolved picture showing how the Kondo-lattice evolves into the HO state, and the identification of the associated broken symmetry and gap structure are still longstanding riddles [1-3].

In this talk, I will present our state-of-the-art ARPES measurements imaging the evolution of the electronic structure of URu_2Si_2 across the hidden-order transition [4-6]. In the paramagnetic state, above T_{HO}, we find structures resulting from the hybridization between heavy and light bands, related to the Kondo lattice formation. In the HO state, we observe the opening of an energy gap over 70% of a large heavy-fermion Fermi surface. I will show how these results provide a quantitative microscopic explanation of the large entropy loss observed in thermodynamic data and the quantum-oscillation frequencies determined by Shubnikov–de Haas experiments, and suggest what is the ordering vector associated to the HO state.

[1] T. M. Palstra *et al., Phys. Rev. Lett.* **55**, 2727 (1985).
[2] M. B. Maple *et al., Phys. Rev. Lett.* **56**, 185 (1986).
[3] J. A. Mydosh and P. M. Oppeneer. *Rev. Mod. Phys.* **83**, 1301 (2011).
[4] A. F. Santander-Syro *et al*., *Nature Phys.* **5**, 637-641 (2009).
[5] F. L. Boariu *et al*., *Phys. Rev. Lett.* **110**, 156404 (2013).
[6] C. Bareille *et al*., *Submitted* (2013)

Efficient Solar Water Splitting with a $BiVO_4$-Amorphous Silicon Heterojunction Photoanode

Roel van de Krol[1,2] and Fatwa F. Abdi[1,2]

1 Helmholtz-Zentrum Berlin, Institute for Solar Fuels, Germany
2 Delft University of Technology, the Netherlands

Multinary metal oxides are promising candidates for the conversion of solar energy to chemical fuels. They combine reasonable semiconducting properties with excellent chemical stability and low cost. Bismuth vanadate ($BiVO_4$) is a promising member of this class. It has a bandgap of 2.4 eV, and can be prepared by a low-cost, simple spray pyrolysis technique. Photoelectrochemical measurements were used to identify which processes limit its performance. The slow surface reaction kinetics can be enhanced by applying a cobalt phosphate water oxidation co-catalyst, while the poor conductivity of the material can be improved by doping with tungsten. Intriguingly, W-doping improves the photocurrent, but at the same time also strongly reduces the carrier lifetime and the (already low) carrier mobility. The origin of this apparent discrepancy will be discussed. Further improvements were made by improving the charge carrier separation efficiency by introducing a gradient in the dopant concentration, effectively creating a distributed n^+-n homojunction. These improvements have resulted in photocurrents of 3.6 mA/cm^2 at 1.23 V vs RHE under 1 sun illumination (AM1.5), which is one of the highest photocurrents ever reported for a metal oxide photoanode. Combination with an amorphous silicon tandem cell resulted in a stand-alone water splitting device with a solar-to-hydrogen (STH) efficiency of 4.9% [1].

[1] F.F. Abdi et al., Nat. Commun. 4:2195, 1-7 (2013)

Spider's Fang: how to design an injection needle using chitin biomaterial

Yael Politi[1], Eckhard Pipple[2], Igor Zlotnikov[1], Paul Zaslansky[1], Stefan Siegle[1], Cheghao Li[1], Clara Valverde Serrano[1,] Maxim Erko[1], Friedrich. Barth[3] and Peter Fratzl[1]

1 Dept. Biomaterials, Max Planck Institute of Colloids and Interfaces. 14424 Potsdam (Germany)
2 Max Planck Institute of Microstructure Physics, D-06120 Halle/Saale (Germany)
3 Dept. of Neurobiology, Life Sciences, University of Vienna, Vienna (Austria)

Spiders mainly feed on insects. This means that their fangs, which are used to inject venom into the prey, have to puncture the insect cuticle that is essentially made of the same material, a chitin-protein composite, as the fangs themselves. Here we report a series of structural modifications in the fangs of the wandering spider Cupiennius salei, including texture variation in chitin orientation and arrangement, gradients in protein composition and selective incorporation of metal ions (Zn and Ca) and halogens (Cl). These modifications influence the mechanical properties of the fang in a graded manner from tip to base, allowing it to perform as a multi-use injection needle that can break through insect cuticle, made of a chitin composite as well.

References Calibri 12:
Barth, F. G. Z. Zellforsch. 144, 409 (1973)
(2) Vincent, J. F. V. & Wegst, U. G. K. Arthropod Struct. Dev. 33, 187 (2004)
(3) Y. Politi et al. Adv. Func. Mat. 22, 2519 (2012)

How Bright Light is Used to Improve Organic Light: Research on Organic Light Emitting Diodes at BESSY II

Emil J.W. List-Kratochvil

(1) Institute of Solid State Physics, Graz University of Technology, Graz, Austria
(2) NanoTecCenter Weiz Forschungsgesellschaft mbH, Weiz, Austria

More than 20% of the world's total electricity consumption is used for lighting applications. This number reaches 25% when consumption from display and TV applications is included Therefore innovative, cost and energy effective solutions for display and lighting applications are the focus of an on-going intense world-wide effort in the field of photonics research and development activities. In particular, organic light-emitting diodes (OLEDs), alongside with inorganic solid-state lighting technologies, are the most promising candidates for future display and lighting technologies of the 21st century. The realization of lightweight, potentially flexible and cheap-to-fabricate, highly energy efficient lighting and display applications may help to save hundreds of GWh or millions tons of coal per year.

While the first report on organic electroluminescence from an organic semiconductor – an anthracene crystal - dates back to the 1960s, the discovery of thin film organic light-emitting device from Eastman Kodak by Ching W. Tang and Steven Van Slyke, and three years later, a report of the first polymer light-emitting diode (PLED) by R. Friend and associates triggered enormous efforts, both within academic research as well as industrial development. Yet, despite this first promising commercial success of OLED technologies, a number of challenges need to be further addressed to allow full exploitation of its potential. Along with the ever on-going quest for emitter materials with improved stability and reliable structure to property relations and enhanced processability through printing techniques in particular device related issues are in the focus of current R&D interest.

OLEDs require balanced charge carrier injection from the electrodes, balanced charge carrier transport and defined regions were the recombination of charge carriers takes place. Therefore typically OLEDs are realized in multilayer stacks, where each layer has a certain function such as the transport of holes and electrons or the block of the former. To ensure a proper functioning of the OLED it is now vital that the relative energetic position of each of the layers is properly tuned. Photoelectron spectroscopy as performed at BESSY II directly allows for investigating this energy level positioning in the individual OLED layer as well as the device stack, which makes this experiment an indispensable tool for OLED development.

References:

T. S. Qin, et al. Journal of the American Chemical Society **133** (5), 1301 (2011).
S. Nau, et al. Advanced Materials **25** (32), 4420 (2013).
R. Trattnig, et al. Advanced Functional Materials, DOI: 10.1002/odfm.2013003600 (2013).

Abstracts of the invited talks at the Neutron Day

Wednesday, 4th of December

Elasto-plastic deformation behavior of heterogeneous materials

M. Schöbel[1], G. Requena[2], G. Baumgartner[3], R. Wimpory[4]

1 Forschungs-Neutronenquelle Heinz Maier Leibnitz, TU Munich, Garching, Germany
2 Institute of Materials Science and Technology, TU Vienna, Austria
3 Umformtechnik und Gießereiwesen, TU Munich, Garching, Germany
4 Helmholtz Zentrum Berlin, Wannsee, Germany

The increasing demand on power, light weight and efficiency in engineering applications require materials with sophisticated thermo-mechanical properties. A heterogeneous composite-like microstructure can improve strength, long term stability and creep resistance by load partitioning between its phases (especially at high temperatures). Metal matrix composites and cast alloys were investigated under simulated production and operation conditions to conclude and compare their damage mechanisms. Three examples of systematically different materials, metal matrix composite, low carbon steel and cast Al and Mg alloys with similar micro-mechanical deformation behavior are compared: Diamond particle and SiC fiber reinforced metals, developed for heat sink applications in electronic and fusion power applications, show stress induced (CTE mismatch) matrix deformation and cracking. The interface bonding strength between the matrix and reinforcement is critical for thermal fatigue damage and long term stability under operation conditions. Cast steel components develop micro and macro stresses by austenite to ferrite transformation during cooling after casting. An inverse macro stress state (compared to the conventional thermal models) was observed and explained by a composite-like microstructure in the two-phase region (between Ar_3 and Ar_1) of the low carbon steel.

AlSiMg, AlMgSi and MgAlSi cast lightweight alloys developed for combustion engines suffer high micro stresses amplitudes under operation conditions. Load partitioning between the ductile α-Al / α-Mg matrix phase and stiffer Mg_2Si networks depend on the microstructures morphology. The cooling rate after casting and additional heat treatments are the key issue for crack formation and failure of engine components. In/ex-situ strain scanning experiments on the E3 instrument at HZB were combined with other non-destructive techniques (synchrotron tomography, acoustic emission) to reveal the elasto-plastic deformation during thermal cycling, tensile testing and after casting. The combined results allow conclusions on the deformation mechanisms in metals, obtained by angle dispersive neutron diffraction with its sophisticated experimental capabilities.

G. Eisenblätter 4.12.13, 14:00

A look inside Roman copper coins: X-ray and neutron tomography experiments.

Gerald Eisenblaetter[1], Alexandra Franz[1,2], Nikolay Kardjilov[2], Stefan Zander[2], Gert Kloess[1]

[1] Leipzig University, Faculty of Chemistry and Mineralogy, Institute of Mineralogy, Crystallography and Materials Science, Scharnhorststr. 20, 04275 Leipzig, Germany
[2] Helmholtz-Zentrum Berlin for Materials and Energy, Hahn-Meitner-Platz 1, 14109 Berlin, Germany

Today non-invasive methods are of special interest in historical and archaeological sciences to understand and preserve the cultural heritage. An ideal technique for analysis of ancient artefacts should be non-destructive, non-invasive, fast, universal, versatile, sensitive and able to examine multiple phases. Many archaeometallurgic analyses were done on silver or gold coins due to their value and well preserved state. Copper objects in contrast are highly corrosive. The corrosion takes not only place at the surface but also in the inside of the copper coins showing different paths of corrosion and depletion of alloying elements. With surface analysis only a small amount of the real existing corrosion could be described. First results using X-ray computed microtomography (3D-µXCT) have shown the corrosion inside the copper coins (see figure 1). The combined advantages of Neutron and X-ray imaging data reveal new information about the inner condition of the coins. As our work has shown there is a strong dezincification in parts of the bulk material which can be clearly shown. In addition Neutron diffraction experiments were carried out to proof this dezincification by detecting α-brass as bulk material and copper plus smithsonite in depleted areas.

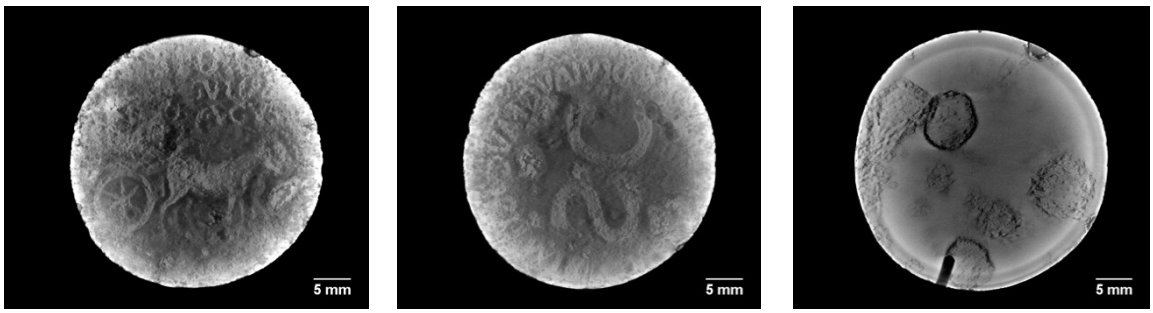

Figure 1 a-c: 3D-µXCT imaging a sestertius of Tiberius obverse (a), reverse (b) and inner part of the coin (c) with drill hole and showing depletion of zinc

The archaeometric studies are carried out on ancient Roman copper coins that are dated to the Julio-Claudian dynasty. The coins are stored at the Leipzig University Library "Bibliotheca Albertina" and the Herzog Anton Ulrich Museum Brunswick in Germany.

G. Iles 4.12.13, 14:40

FALCON: Fast Acquisition Neutron Laue Diffractometer

Gail N. Iles[1], Susan Schorr[1,2]

[1]Helmholtz-Zentrum Berlin, Hahn-Meitner Platz 1, 14109 Berlin, Germany
[2]Freie Universität Berlin, Institute of Geological Sciences, Malteserstr. 74-100, 12449 Berlin, Germany

The Fast Acquisition Laue Camera for Neutrons, FALCON, is a thermal neutron Laue diffractometer situated in the experimental hall of the BER-II reactor at HZB in Berlin. The thermal beamtube, D1S, delivers a stream of neutrons direct to FALCON just 7m from the reactor core but with a low gamma radiation count. Whilst other neutron sources report that guides containing multiple instruments interfere with the intensity and quality of the neutron beam reaching end positions, FALCON will benefit from a beam that does not pass through any objects upstream. A uniquely-designed shutter and beam definer deliver a highly focused neutron beam to the instrument with <1° divergence. The instrument comprises two scintillator plate detectors coupled to four iCCD cameras each. The neutron beam passes through the detector units enabling one detector to be placed in the backscattering position and the second detector in the transmission position. The image-intensified CCDs are capable of obtaining 20-bit digitization Laue images in under ten seconds and variable sample table and detector positions allow a full range of sample environments to be utilised. We invite users to submit proposals for Laue diffraction experiments in the HZB 2014/II round.

Ceramid [EOS] and its impact on the lipid membrane organization of the Stratum corneum – A neutron diffraction study

Adina Eichner[1], Annett Schroeter[1], Thomas Hauß[2], Reinhard H.H. Neubert[1]

1 Martin-Luther-University Halle-Wittenberg, Germany
2 Helmholtz- Zentrum Berlin for Materials and Energy, Germany

The outermost layer of the human skin, the Stratum corneum (SC), represents the main barrier of the mammalian skin [1]. As it became evident, that the main barrier properties can be attributed to the lipid part of the SC [1] the interest of researchers moved towards now its lamellar organization and in particular the impact of different lipid species of the SC lipid matrix for the structural arrangement. Especially the Ceramides (CER) as the main components of the lipid matrix [2] offer a wide range of influencing possibilities. Nevertheless, the elucidation of the SC´s lipid matrix nanostructure is a complex task, due to the variability and the complexity of native SC membranes and its lipids. Consequently, to overcome this variability issue the application of model membranes is the medium of choice for such investigations. Furthermore, by using neutron diffraction, it is possible to investigate nanostructure of the SC components and their interaction. Thus, a structure-function relationship of CER on the molecular level can be established. Additionally, the application of specifically deuterated ceramides, e.g. the long-chain ω-acyl ceramide [EOS] can shed a light to the exact position of the labelled molecule within the lamellar arrangement of the lipids. Experiments carried out at the V1 membrane diffractometer using model membranes composed of the short-chain CER[AP], CER[EOS]-d3, cholesterol [CHOL] and behenic acid [BA] showed a co-existence of three phases. By using the specifically deuterated CERs CER[AP]-d3 or [EOS]-d3 it could be shown that CER[EOS] forms a separate phase in which it is most probably present in its hairpin conformation. Former works showed the model membrane assembling process was significantly driven by CER[AP] [3-5]. Closer insights into its involving process in mixture with long-chain CERs are focussed in further experiments.

[1] P.W. Wertz, Adv Drug Deliver Rev, 18 (1996) 294.
[2] H.J. Yardley, R. Summerly, Pharmacol Ther, 13 (1981) 383.
[3] A. Ruettinger, M.A. Kiselev, T. Hauss, S. Dante, A.M. Balagurov, R.H. Neubert, Eur Biophys J, 37 (2008) 759-771.
[4] A. Schroeter, M.A. Kiselev, T. Hauß, S. Dante, R.H.H. Neubert, BBA Biomembrane, 1788 (2009) 2203.
[5] A. Schröter, D. Kessner, M.A. Kiselev, T. Hauß, S. Dante, R.H.H. Neubert, Biophys J, 97 (2009) 1114.

J. Kähn 4.12.13, 16:00

Comparing the annealing dependency of Al/Si distribution in Sanidine megacrysts $K_{1-x}Na_xAlSi_3O_8$ from Eifel/Germany with X-ray and neutron diffraction methods

Johannes Kähn[1], Daniel Többens[1], Jens-Uwe Hoffmann[2], Manfred Reehuis[2], Susan Schorr[1,3]
[1]Helmholtz-Zentrum für Materialien und Energie, Department Crystallography, Hahn-Meitner-Platz 1, 14109 Berlin, Germany
[2]Helmholtz-Zentrum für Materialien und Energie, Department Quantum Phenomena in Novel Materials, Hahn-Meitner-Platz 1, 14109 Berlin, Germany
[3]Freie Universität Berlin, Institute of Geological Sciences, Malteserstr. 74-100, 12449 Berlin, Germany

Monoclinic sanidine is the high-temperature modification of K-rich alkalifeldspars. Usually, annealing at temperatures above 900°C causes disordering of Al/Si distribution on the two non-equivalent structural sites, but it is possible to disorder samples of sanidine megacrysts from Volkesfeld/Eifel at considerably lower temperatures and shorter times [1]. In order to investigate this behaviour and compare various approaches to obtain Al/Si distribution we studied samples from different locations and determined the Al/Si order with direct and indirect methods, including X-ray and neutron diffraction of powder and single crystal samples. Furthermore, diffuse neutron scattering investigation of a Sanidine single crystal was performed. Neutron scattering experiments were performed at Berlin Research Reactor BERII. Neutron powder diffraction experiments were executed at the Fine Resolution Neutron Diffractometer (E9), single crystal neutron diffraction at the 4-circle Diffractometer (E5) and diffuse neutron scattering experiments at the Flat-Cone Diffractometer (E2). The Al/Si distribution was determined directly, refining site occupancies by applying Rietveld analysis to neutron powder diffraction data and XTAL for neutron single crystal data. This approach is inapplicable when using X-ray diffraction data, due to similar atomic form factors of Al^{3+} and Si^{4+}, thus indirect methods [2,3,4] were applied. X-ray powder diffraction was performed at Helmholtz-Zentrum Berlin, single crystal X-ray diffraction was done at Ruhr-University Bochum and the obtained data were processed using Rietveld refinement and ShelXL software, respectively. The dependency of decreasing Al/Si order on increasing annealing times and temperatures could be verified. We observed that different methods of determining the Al/Si distribution provide different results for our samples. Diffuse scattering of untreated and annealed sanidine samples was successfully detected.

[1] Zeipert&Wondratschek, An unusual annealing behavior of Eifel Sanidine, N.Jb.Miner.Mh. H.9, 407-415 (1981)
[2] Kroll&Ribbe Lattice parameters, composition and Al,Si order in alkali feldspars. Miner.Soc.Amer. Reviews in Mineralogy, 2, 2nd edition, 57-99 (1983)
[3] Kroll&Ribbe, Determining (Al,Si) distribution and strain in alkali feldspars using lattice parameters and diffraction-peak positions, Amer.Miner. Vol.72, 491-506 (1987)
[4] Carpenter&Salje, Thermodynamics of nonconvergent cation ordering in minerals. 3. order-paramenter coupling in potassium-feldspar, Amer.Miner. Vol.79, 1084-1098 (1994)

R. Toft-Petersen 4.12.13, 16:15

Field-induced spin disorder in a doped magneto-electric Ising system

A spin glass is an arrangement of ‘frozen in’ magnetic magnetic moments exhibiting only short range order in spite of its static nature below the freezing temperature T_f . A spin glass is a result of having a non-periodic magnetic ground state, and a very complicated configuration space with many meta-stable states of similar energy. Such a landscape is created by having /both/ random and frustrated magnetic interactions. Many spin glasses are sensitive to applied fields, which essentially enhances order by introducing a preferred direction in space, and destroys the spin glass state. However, by doping the Ising system LiCoPO4 with a substantial amount of nickel, one can create a field induced transition from an long range ordered AFM state to a disordered AFM state producing diffuse diffraction peaks with a very high critical field of 10.5 T. This field induced disordered state could in principle be induced at zero temperature, as further experiments will reveal.

$YbCo_2Si_2$ - a reference compound to $YbRh_2Si_2$?!

Ariane Hannaske[1], Oliver Stockert[1], Cornelius Krellner[2], Andreas Hoser[3], Jens-Uwe Hoffmann[3], Silvia Capelli[4], Karin Schmalzl[5], Diana Quintero Castro[3], Nandang Mufti[1], Christoph Geibel[1], Frank Steglich[1]

1 Max-Planck-Institut für Chemische Physik fester Stoffe Dresden, Germany
2 Goethe Universität Frankfurt am Main, Germany
3 Helmholtz-Zentrum Berlin, Germany
4 Institut Laue-Langevin Grenoble, France
5 Jülich Centre for Neutron Science at Institut Laue-Langevin Grenoble, France

The heavy-fermion compound $YbRh_2Si_2$ has been intensively investigated during the last years due to its vicinity to a quantum critical point (QCP). However, studies about the microscopic magnetic order as well as magnetic excitations are hindered due to the low antiferromagnetic ordering temperature $T_N \approx 70$ mK, the very small ordered magnetic moment ($\approx 10^{-3}$ μ_B/Yb) and the high absorption of neutrons by Rh. We use isostructural $YbCo_2Si_2$ as a reference compound to overcome these problems. Isoelectronic doping of Co on the Rh site in $YbRh_2Si_2$ leads to an increase of the ordering temperature as well as the ordered magnetic moment. $YbCo_2Si_2$ orders antiferromagnetically below $T_N = 1.7$ K and shows a first-order transition at $T_L = 0.9$ K. We used neutron diffraction experiments to shed light on the very complex (B-T) phase diagram. Two different magnetic phases and the occurrence of antiferromagnetic domains are the origin of several transitions observed in macroscopic measurements. To get an idea about magnetic interactions inelastic neutron scattering experiments were performed. Measurements of the critical fluctuations show that $YbCo_2Si_2$ can be tuned to a QCP by the application of a critical magnetic field of $B \approx 2$ T (B || [110]). Well resolved spin excitations, which show dispersion, could be observed in both magnetic phases. A softening of the magnon energy in the vicinity of $Q = (0\ 0\ 1)$ when entering the incommensurate phase might give a hint for quantum critical fluctuations in $YbRh_2Si_2$. Indeed, incommensurate fluctuations have been detected in $YbRh_2Si_2$ along the [110] direction [1].

[1] C. Stock et al., Phys. Rev. Lett. 109, 127201 (2012)

High-pressure studies of lipid and protein films at aqueous-solid Interfaces

Mirko Erlkamp[1], Claus Czeslik[1], Roland Winter[1]

[1] TU Dortmund University, Department of Chemistry and Chemical Biology, D-44221 Dortmund, Germany

The design and performance of a high pressure (HP) cell for neutron reflectivity experiments will be presented.[1] The cell can be used to study solid–liquid interfaces under pressures up to 2500 bar (250 MPa). The sample interface is based on a thick silicon block with an area of about 14 cm2. This area is in contact with the sample solution which has a volume of only 6 cm3. The large accessible pressure range and the low required volume of the sample solution make this HP cell highly suitable for studying pressure-induced structural changes of interfacial proteins, supported lipid membranes, and, in general, biomolecular systems that are available in small quantities, only. To illustrate the performance of the HP cell, we present neutron reflectivity data of protein adsorbates and lipid films under high pressure.[2,3] For example, with increasing pressure, we have found that the degree of protein adsorption is increasing, which can be related to the thermodynamic stability of the folded protein. Furthermore, the pressure-dependent structure of lipids forming lamellar and non-lamellar phases on a silica surface has been analyzed.

References:
1. C. Jeworrek, R. Steitz, C. Czeslik, R. Winter, Rev. Sci. Instrum. 82 (2011) 025106.
2. Y. Zhai, P. L.-G. Chong, L. J.-A. Taylor, M. Erlkamp, S. Grobelny, C. Czeslik, E. Watkins, R. Winter, Langmuir 28 (2012) 5211-5217.
3. J. Koo, M. Erlkamp, S. Grobelny, R. Steitz, C. Czeslik, Langmuir 29 (2013) 8025-8030.

Abstracts of the invited talks at the Synchrotron Day

Friday, 6th of December

Nonmagnetic linear dichroism in fluorescence spectra from a cubic solid

N. Thielemann-Kühn[1,2] , M. W. Haverkort[3] , P. S. Miedema[1], I. Alonso Calafell[1], C. Trabant[1,2,4], M. Gorgoi[1], A. Föhlisch[1,2] and C. Schüßler-Langeheine[1]

1 Institute for Methods and Instrumentation of Synchrotron Radiation Research, Helmholtz-Zentrum Berlin für Materialien und Energie GmbH, Albert-Einstein-Straße 15, 12489 Berlin, Germany
2 Fakultät für Physik und Astronomie, Universität Potsdam, Karl-Liebknecht-Straße 24–25, 14476 Potsdam, Germany
3 Max Planck Institute for Solid State Research, Heisenbergstraße 1, D-70569 Stuttgart, Germany
4 Fachbereich Physik, Freie Universität Berlin, Arnimallee 14, 14195 Berlin, Germany

Fluorescence yield spectra from solids contain different information than X-ray absorption spectra because the involved twofold dipole transitions and the experimental geometry lead to additional selection rules. Even in high-symmetry crystals like rock salt NiO we observed additional nonmagnetic linear dichroism in the fluorescence yield which is absent in the X-ray absorption spectrum. In particular we investigated a NiO bulk sample with cubic symmetry and NiO thin films with different crystal distortions, below and above the Néel temperature. We could distinguish the dichroic effects caused by the fluorescence process from the typical magnetic linear dichroism in XAS [1]. The model calculation of the fluorescence spectra based on ligand field theory predicts the dichroic effects very well.

[1] D.Alders *et al.*,Physical Review B **54**, 7716 (1996)

K. Koren 6.12.13, 9:15

Energy level alignment investigations on solution processed bright blue multilayer PLEDs utilizing photoelectron spectroscopy

Authors: Katrin Koren[1], Roman Trattnig[1] , Leonid Pevzner[2] , Monika Jäger[1] , Raphael Schlesinger[3], Marco Vittorio Nardi[3] , Giovanni Ligorio[3] , Christos Christodoulou[3] , Norbert Koch[3] , Martin Baumgarten[2] , Klaus Müllen[2,5] and Emil J. W. List-Kratochvil[1,4]

1 NanoTecCenter Weiz Forschungsgesellschaft mbH, Franz Pichler Straße 32, A-8160 Weiz, Austria
2 Max-Planck-Institut für Polymerforschung Ackermannweg, Ackermannweg 10, D-55128 Mainz, Germany
3 Institut für Physik, Humboldt-Universität zu Berlin Brook-Taylor-Strasse 6, D-12489 Berlin, Germany
4 Institut für Festkörperphysik, Graz University of Technology Petersgasse 16, A-8010 Graz, Austria
5 Helmholtz Zentrum Berlin für Materialien und Energie GmbH
Elektronenspeicherring BESSY II Albert-Einstein-Strasse 15, D-12489 Berlin, Germany

Abstract: The realization of efficient, stable as well as fully solution processed multilayer polymer light-emitting diodes (PLEDs) is a key topic in worldwide research activities on organic electronic devices. The deposition of several polymeric layers on top of each other without redissolving the layers underneath is still a crucial point in the fabrication of multilayer PLED structures. Besides these fabrication related issue, bright and efficient PLEDs require an alignment of the energy levels of the involved materials in order to get an effective charge carrier injection and blocking at the individual interfaces. Here, we report on the fabrication and properties of bright blue multilayer PLEDs realized by combining different deposition strategies. Photoelectron spectroscopy (PES) was performed on each layer of the device stack. Together with Atomic force microscopy (AFM) images of the several layers a complete picture of the device functionality can be visualized. The AFM investigations exhibit smooth surfaces and the non occurring intermixing of the layers. PES confirms the desired type II band level alignment at each interface leading to a charge carrier confinement in the light emitting diode and further enhancing the exciton formation probability. The resulting solution processed PLED exhibits bright blue light emission with a maximum luminance of 16540 cd/m2 and a maximum device efficiency of 1.42 cd/A, which denotes a five-fold increase compared to corresponding single-layer devices. Based on these results in a next step also solution processed electron injecting and hole blocking layers are studied. This is an important intermediate step towards multilayer OLEDs including solution based electrode manufacturing.

References: R. Trattnig et al, Advanced Functional Materials, 23,39,(2013)

Investigation of microbunching-instability in energy recovery linacs

Stephanie Rädel

Helmholtz Zentrum Berlin für Materialien und Energie GmbH, Berlin,

In an energy recovery linac (ERL), a Photo-injector produces electron bunches with very low emittance und energy spread to feed a superconducting linac section. After the acceleration in the linac, the bunches pass through a transport loop, which for example can include undulators to produce high-brilliance radiation. After the passage through the loop, the bunches pass the linac a second time with a phase shifted by a 180 degree, in this case the linac decelerates the bunches gaining back the energy. The spend bunches are deflected by a dipole magnet to a beam dump. Maintaining the low emittance and energy spread is of major importance in an ERL. Therefore, deep understanding and control of effects which can degrade the emittance and energy spread such as space charge effects are of interest. The microbunching caused by the longitudinal space charge forces can lead to an increase in emittance and energy spread in the arcs of the loop. In this contribution, the impacts of the microbunching instability on the beam quality and its implication for an ERL are discussed.

Deformation mechanism of nanoporous materials upon water freezing and melting

Maxim Erko[1,2], Dirk Wallacher[3], Oskar Paris[1]

1 Institute of Physics, Montanuniversitaet Leoben, Franz-Josef-Strasse 18, 8700 Leoben, Austria
2 Department of Biomaterials, Max-Planck-Institute of Colloids and Interfaces, Am Mühlenberg 1, 14424 Potsdam, Germany
3 Helmholtz Zentrum Berlin fuer Materialien und Energie, Hahn Meitner Platz 1, 14109 Berlin, Germany

The unique structural and dynamic properties of liquid water are most pronounced within the low-temperature region upon strong supercooling. Additional confinement of water within nanometer pores induces new phenomena such as reduced condensation pressure or melting point suppression, and in sufficient small pores water seems even not to freeze at all. The temperature-induced density changes of water in nanopores with width of 2 - 9 nm were studied by combining *in-situ* scattering experiments with X-rays and neutrons. A two-step density model reveals a wall layer covering approximately two layers of water molecules with higher density than the residual core water in the central part of the pores [1]. The simultaneously observed temperature-induced non-monotonous reversible deformation of water-filled nanoporous matrix was treated quantitatively by introducing a model for freezing and melting of fluids in confinement [2]. The physical origin of the melting/freezing induced pore lattice deformation is found to be exactly the same as for capillary condensation/evaporation, namely the curved phase boundary due to the preferred wetting of the pore walls by the liquid phase. Our analytical description is based on the Gibbs-Thomson equation and a generalized Laplace-pressure. As a practical implication, elastic properties of the nanoporous framework can be determined from the temperature-deformation curves.

[1] Erko, M., Hoell, A., Wallacher, D., Hauß, T., Zizak, I., & Paris, O. (2012). *Physical Chemistry Chemical Physics,* **14**, 3852–3858.
[2] Erko, M., Wallacher, D. & Paris, O. (2012). *Applied Physics Letters*, **101**, 181905.

Redox-dependent structural and chemical transformation of the [4Fe3S]-cluster in an O_2-tolerant [NiFe]-hydrogenase

Andrea Schmidt[1], Jacqueline Kalms[1] and Patrick Scheerer[1, §]

[1]*Institut für Medizinische Physik und Biophysik, AG Protein X-ray Crystallography, Charité - Universitätsmedizin Berlin, Charitéplatz 1, D-10117 Berlin, Germany*
[§]*Corresponding author: patrick.scheerer@charite.de*

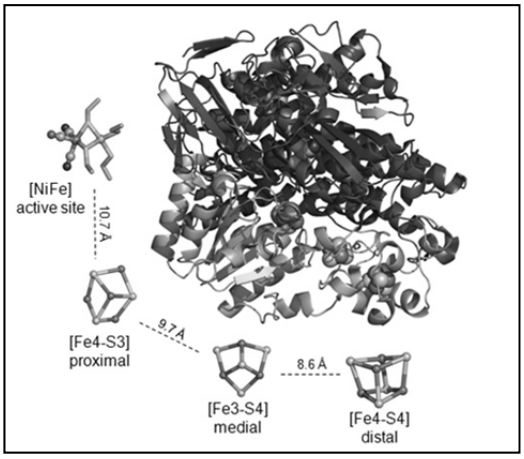

Hydrogenases catalyse the interconversion of H_2 into $2H^+ + 2e^-$. In most hydrogenases their activity is highly sensitive to O_2. To use hydrogenases as tools e.g. in renewable energy technologies, the retention of their activity in presence of O_2 is required [1]. We investigate a membrane-bound [NiFe]-hydrogenase (MBH) from *Ralstonia eutropha*, belonging to a subgroup of hydrogenases, which have evolved O_2-tolerance. MBH consists of a large subunit bearing the [NiFe] active site and a small subunit containing three [FeS]-cluster that direct electron flow to the respiratory chain. In case of MBH, O_2-tolerance relies on exceptional redox-properties of an unprecedented [Fe4S3]-cluster located proximal to the active site. This cluster operates as an electronic switch depending on the nature of the gas molecule at the active site [2]. Redox-dependent structural and chemical rearrangements enable the bidirectional transfer of two electrons within a physiologically relevant potential range [3].

References

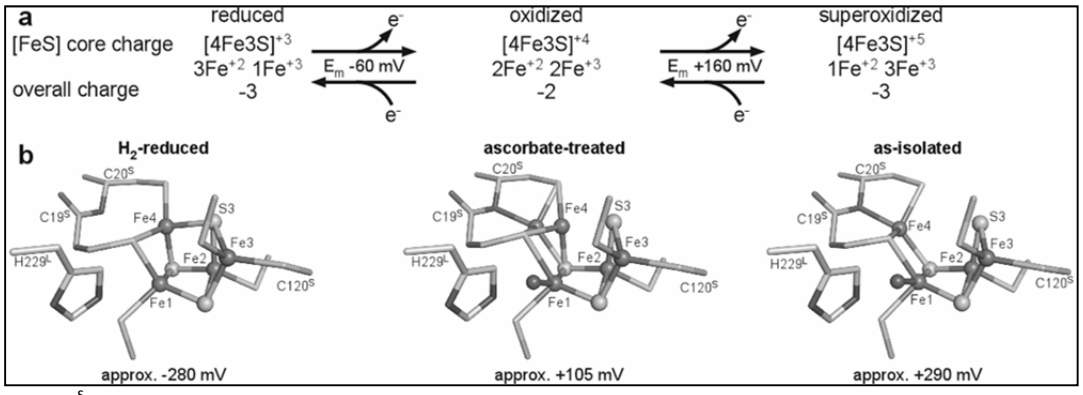

1. Fritsch,J.[§], Lenz,O., Friedrich,B. (2013) **NatRevMicrobiol.** *2*, 106-114.
2. Fritsch,J.*, Scheerer,P.*[,§], Frielingsdorf,S., Kroschinsky,S., Friedrich, B., Lenz,O.[§], Spahn, C.M.[§]. (2011) **Nature** *479(7372)*, 249-52.
3. Frielingsdorf, S., Fritsch, J., Schmidt, A., Hammer, M., Löwenstein, J., Siebert, E., Pelmenschikov, V., Jaenicke T., Kalms J., Lendzian, F., Zebger, I., Teutloff, C., Kaupp, M., Bittl, R., Hildebrandt, P., Friedrich, B., Lenz, O.[§], Scheerer, P.[§] (2013) submitted

Fermi Level Pinning of Organic Semiconductors on Metaloxides

Stefanie Winkler

1 Helmholtz-Zentrum Berlin für Materialien und Energie GmbH, Albert-Einstein-Str. 15, 12489 Berlin, Germany

At a hetero-interface between an organic semiconductor and an electrode vacuum level alignment (VLA) is observed if the substrate Fermi-level (E_F) is located within the energy gap of the semiconductor on top. In contrast, if E_F comes to lie below (above) the (un-)occupied molecular states, an interface dipole ($\Delta\Phi_{pin}$) is formed to reestablish electronic equilibrium across the heterostructure. The critical substrate work function Φ_{crit} at which Fermi-level (E_F)-pinning sets in should in principle be an intrinsic material parameter. However, for one organic semiconductor often different values for pinning have been reported.

In this study on metaloxides substrates, the work function Φ is tailored via employing various submonolayer acceptor-coverages and dipolar monolayer formation. In both cases the electrostatics at the interface to subsequent deposited charge transport materials (CTM) are involved by interface dipoles besides $\Delta\Phi_{pin}$. Φ_{crit} for the acceptor sub-monolayer interlayer is found to be 0.4 eV higher than expected since the simple assumption of VLA does not apply. An electrostatic model that accounts for non-uniformity of the substrate at acceptor sub-monolayer coverages and the associated local work function changes upon CTM-deposition explain the origin of "delayed" E_F-pinning.

If the pristine metaloxide Φ is changed due to a dipolar monolayer formation upon deposition of the CTM, Φ_{crit} is shifted as well, since it can only be determined for the pristine metaloxide.

Abstracts of Poster Session - Young Scientists and Neutron Day

Wednesday, 4th of December

1 High Precision Temperature Regulation for Neutron Scattering Experiments

Klemke B, Sokolowski A, Willenberg B, Ryll H, Gerischer S, Grimm N, Goerigk G, Wallacher D, Kiefer K

Some neutron scattering experiments need very accurate temperature regulation-especially if temperature dependencies near phase transitions are investigated. However, standard sample environment (SE) equipment doesn't meet these requirements. Therefore at the HZB we developed a range of special SE equipment with high precision temperature regulation from room temperature to the Millikelvin range.

2 Flat-Cone Diffractometer E2: 3D diffuse scattering - the ultimate tool for complex structure solution

Hoffmann J-U, Glavatskyi I

The Flat-Cone E2 is a medium resolution single crystal and powder diffractometer with wide sample environment possibilities to study the complicated distributions of superstructure reflections and diffuse scattering arising from structural and magnetic disorder in 3D reciprocal space, which can be scanned in few steps by combining the "off-plane Bragg-scattering" and the Flat-cone layer concept.

3 The Next Generation Humidity Chamber for Biological Samples

Barrett M, Perkins A, Gonthier ., Baudoin S, Deme B, Lelièvre-Berna E, Hauss T, Kiefer K, Wallacher D.

The new generation humidity chamber for neutron scattering has been designed by partners at HZB and ILL. The first prototype will be produced early 2014. We present the features of the new design, as well as the strategies which are employed to bring samples to very high humidity (over 95% R.H.), while having extreme control over the surrounding environment's temperature.

4 A Silicon prism lens for neutrons

Schulz J, Krist Th, Hülsen Ch

We present a prism lens for neutrons. The lens consists of 13 layers of silicon prisms each with a height of 0.25 mm. With this lens we imaged a 0.2mm slit over a distance of 1.7m between the lens and the detector at a wavelength of 4.9 Å at the V14 reflectometer at the HZB. In the FWHM an intensity gain of a factor 7.9 compared to the intensity of the direct beam in the same area was measured.

5 Neutron Optics from HZB

Krist Th, Schulz J, Hoffmann J

Polarizing neutron optical devices have been developed at HZB like solid state polarizing benders, collimators with polarizing walls, 2D polarization analysers and polarizing S-benders showing at a wavelength of 4.4 Å a polarization of 98% and a transmission of 65%. A focusing silicon lens showed a gain of 5.6. Prism systems were shown to work as neutron energy analysers and focusing systems.

6 Sample environment for soft matter and energy research on TOF SANS instruments

Clemens D, Vogtt, K, Siebenbürger M, Hellweg Th, Risse, S, Mascotto, S, Wallacher D, Ballauff, M

HZB is specializing on in-situ techniques that allow to monitor structural states through SANS and in parallel structure driving parameters like temperature, gas concentration, external shear, and electrical (dis-)charging parameters. This is to foster in-house research mainly driven by energy and soft matter topics as well as to attract external users with unique experimental infra-structure.

7 Performance of the Cold Triple Axis Spectrometer V2-FLEXX

Quintero-Castro DL, Toft-Petersen R and Habicht K

FLEXX has been running successfully for almost 2 years. After the upgrade, we find gains of over 10x in intensity, this due to the design of the primary spectrometer. Its characteristics position it among the leading cold TASs. The general performance of FLEXX will be presented, together with important experimental results. M. D. Le, Nuc. Inst. and Meth. in Phy. Res., s. A, 729, 220-226, 2013

8 New 2D detector of SANS instrument V4 at Helmholtz-Zentrum Berlin

Keiderling U, Prevost S, Wilpert Th, Alimov S, Schulz Ch

V4 has been upgraded with a large 2D detector, consisting of an array of 112 linear position sensitive 3He-filled tubes with 8 mm diameter from Reuter-Stokes. Three different tube lengths of 1000, 850 and 600 mm maximize the detection area within the circular cross-section of the existing detector chamber. The poster presents an overview of the detector design, figures of merit, and first results.

9 Three-dimensional Imaging of Magnetic Domains

Manke I, Kardjilov N, Schäfer R, Grothausmann R, Hilger A, Strobl M, Dawson M, Grünzweig C, Behr G, Hentschel M P, David C, Kupsch A, Lange A, Banhart, J

By applying the novel technique of Talbot-Lau neutron tomography with inverted geometry, we have been able to directly image the three-dimensional network of magnetic domains in the bulk of

samples. In particular, the 3D shape and distribution of individual domains in a misoriented magnetic FeSi crystal were visualised and analysed quantitatively.

10 First experimental tests of tensorial neutron tomography for quantitative measurements of magnetic vector fields

Hilger A, Kardjilov N, Manke I, Strobl M, Jericha E, Banhart J

Radiography and tomography with polarized neutrons allows for investigation of magnetic vector field distributions in 2D and 3D. We present quantitative 2D investigations and an approach for real 3D vector field (tensorial) tomography. Results from first experiments and from simulations are compared.

11 The upgrade of the neutron imaging instrument CONRAD 2. Parameters, gains and experimental opportunities.

Kardjilov N, Manke I, Hilger A, Banhart J

Upgrade of the neutron imaging instrument CONRAD2 was performed recently at HZB. The upgrade reflected in increase of flight path up to 10 m providing a larger beam size (field of view) with higher neutron flux density due to the new neutron guides with super mirror coating. The parameters and gains of the new imaging facility will be presented.

12 (3+1) dimensional crystal and antiferromagnetic structures in CeRuSn

Prokes K, Petricek V, Ressouche E, Hartwig S, Ouladdaif B, Mydosh J A, Hoffmann R-D, Huang Y-K, Pöttgen R

CeRuSn adopts at 320K a crystal structure, which is derived from the structure of CeCoAl by a doubling along the c-axis. At low temperature the x and z positions of all elemental sites become incommensurate, while the antiferromagnetic unit cell is doubled along the c-axis direction in respect of this modulated structure. The magnitudes of the nearly collinear Ce moments are modulated as well.

13 Frustrated magnetic order in CePd{1-x}Ni{x}Al

Huesges Z, Woitschach S, Stockert O, Fritsch V, Löhneysen H v, Lemee-Cailleau M-H, Capelli S, Wildes A, Matas S, Prokes K

CePdAl is a model system to study the influence of frustration on quantum phase transitions. Due to the quasi-Kagome lattice structure, only two thirds of the Ce spins order below TN=2.7 K. Doping with Ni suppresses TN; at 14% Ni doping, TN=0. In single crystal neutron diffraction we could show that frustration is manifest in short-range order which co-exists with the long-range order signal.

14 Magnetic order in Tm3Cu4X4 (X = Si, Ge, Sn) compounds.

Baran S, Kaczorowski D, Szytula A, Gil A, Hoser A

Below TN the Tm moment at the 2d site in Tm3Cu4Ge4 and the 2c one in Tm3Cu4Sn4 form a collinear magnetic order with wavevectors (0, 1/2, 0) and (0, 0, œ), respectively. Below Tt the Tm moments at the 4c site (X = Ge) and the 4d one (X = Sn) form a modulated incommensurate structure described by the wavevector k (1/4, 0, kz) for X = Ge and ((1/4, ky, 0) for X = Sn, with kz and ky being close to 0.5.

15 Neutron Diraction Studies of Tb2Ni2-xIn Intermetallic Compounds

Szytula A, Baran S, Hoser A, Kalychak Y M, Penc B, Tyvanchuk Y

Tb2Ni1:78In with the tetragonal Mo2FeB2-type is antiferromagnet below 20 K. Tb moments form collinear magnetic structure commensurate with the crystal, with the wavevector (1/4, 1/4, 1/2). Moment 7.6 μB parallel to c-axis. In Tb2Ni2In with orthorhombic Mn2AlB2-type is antiferromagnetic (100) K with collinear ordering with wavevector (1/2, 1/2, 1/2). At 1.6 K MTb =6.33 μB and is parallel to c-axis.

16 Neutron diffraction studies of magnetism in nanoparticle RMnO3 (R = Pr, Nd, Tb)

Baran S, Bazela W, Dul M, Dyakonov V, Gondek L, Hoser A, Hoffmann J-U, Hofmann T, Penc B, Szytula A

The RMnO3 (R = Pr, Nd, Tb) nanoparticles were studied by means of neutron diffraction with the use of the E6 diffractometer located at HZB. Two intriguing results have been obtained: - magnetic grains have a nonmagnetic shell of a few nm thikness - lowering TbMnO3 grain size leads to lose long-range magnetic order in the Tb sublattice while the Mn magnetic sublattice seems to remain unaffected

17 Pressure induced antiferromagnet-ferromagnet transition in La0.5Ba0.5CoO2.8 cobaltite

Troyanchuk I O, Többens D M, Efimov V V, Bushinksky M V, Ritter C, Hansen T

The anion deficient cobaltite La0.5Ba0.5CoO2.8 by neutron powder diffraction. Applied pressure induces a gradual transition from the antiferromagnetic into a ferromagnetic state through a mixed magnetic state. The transition is not accompanied by obvious changes in the macroscopic crystal symmetry. Possible physical models are discussed

18 Magnetization depth profile of dilute magnetic semiconductor (Ga,Mn)As

Pereira L M C, Steitz R, Augustyns V, Vantomme A, Temst K

Mn-doped GaAs has become the model dilute magnetic semiconductor. Using polarized neutron reflectivity (PNR), we investigated the magnetization depth profile of a Mn-doped GaAs thin film as a function of temperature. Preliminary analysis shows that the ordering temperature decreases close to the interface with the GaAs substrate, potentially due to a higher concentration of interstitial Mn atoms.

19 The Dielectric and Diffraction Studies of Composites NaNO2(1-x)-BaTiO3(x)

Alekseeva O, Al`myasheva O, Koroleva E, Naberezhnov A, Stukova E, Tovar M

The dielectric and diffraction studies of composites NaNO2(x)-BaTiO3(1-x) with x=0.1, 0.05 have been carried out. It is shown that there is temperature range of ferroelectric and incommensurate phases coexistence depending on heating or cooling regimes. The temperature dependencies of order parameter in NaNO2+BaTiO3 have been obtained from x-ray and neutron diffraction data.

20 The ferromagnetic and antiferromagnetic phases in anion deficient La0.5-xPrxBa0.5CoO3-d cobaltites

Efimov V, Sikolenko V, Karpinsky D, Cervellino A, Raveau B and Troyanchuk .O

Neutron powder diffraction studies of crystal and magnetic structures, magnetization and magnetotransport measurements have been performed for La0.5xPrxBa0.5CoO3-d cobaltites. It has been found that the compositions ($0 \leq x \leq 0.35$) are cubic (Pm3m) whereas $x = 0.375$ one is tetragonal (P4/mmm) due to an ordering of rare-earth and barium ions, while the oxygen vacancies are disordered.

21 Neutron diffraction study of Cu2ZnGeSe4 (CZGSe)

Gurieva G, Többens D, Schorr S

CZGSe is considered as potential candidate for photovoltaic applications. Single phase sample was grown by solid state reaction of the elements. Neutron powder diffraction experiments were performed using fine resolution neutron powder diffractometer E9. Structural parameters and cation distribution were determined by Rietveld analysis of the data, providing an insight into point defects in CZGSe.

22 Crystal Chemistry of Manganese containing Perovskites related to Calcium Aluminate Cements

Stöber S, Schorr S, Pöllmann H,

The phase assemblage of calcium iron manganese aluminate cements contains perovskite phases with significant concentrations of Mn3+/Mn4+ ions. Neutron data for structure refinements of brownmillerites (A2BB'O5), ternary (ABO3) and oxygen frustrated perovskites (A3B3O8) were collected at the E9 BER II

23 Temperature and composition-induced structural transitions in Bi1-xPrxFeO3 ceramics

Karpinsky D, Kholkin A, Tovar M, Troyanchuk I, Efimov V, Sikolenko V

Temperature- and composition-induced evolution of the crystal structure of Bi1-xPrxFeO3 ceramics within the morphotropic phase boundary has been studied using X-ray and neutron diffraction techniques. The phase stability regions, three phase coexistence region and features of the structural transitions have been revealed. The temperature-composition structural phase diagram has been constructed.

24 A neutron diffraction study of CZTSSe monograins

Schorr S, Gurieva G, Toebbens D, Muska K, Holopainen T

Studied Cu2ZnSn(S,Se)4 samples are monograins (micrometer scale single crystals), applied in flexible solar cells. Using CZTSSe monograin powder in neutron diffraction (E9), an absorber material directly used in a solar cell is studied. Structural parameters and cation distribution were determined by Rietveld analysis of the data, providing an insight into point defects in the monograins.

25 In Operando Investigation of Lithium Sulfur Cells

Risse S, Clemens D, Lu Y, Mascotto S, Ballauff M

Lithium-sulfur (Li/S) batteries provide a 3 to 5 fold higher theoretical energy density than state-of-art lithium-ion batteries. However, the commercial use of Li/S batteries still cannot be realized due to many unsolved issues. Our goal is the investigation of Li/S cells with three simultaneous "in operando" measurements to get information about the complex reactions of polysulfide.

26 Structure characterization of porous carbon by combination of gas physisorption and SANS.

Mascotto S, Juan J, Wallacher D, Clemens D, Ballauff M

Porous carbon is very attractive for energy applications. However, the clarification of its porous structure can be hardly achieved by standard techiniques. Here we investigated the porosity structure of carbon combining gas physisorption with SANS methods. Taking advantage of the contrast matching between the SLD of carbon and deuterated p-xylene, the porous features can be analyzed in detail.

27 In-Situ Studies of the Lithium Incorporation into Lithium-Ion Batteries Model Systems

Seidlhofer B-K, Jerliu B, Hüger E, Steitz R, Schmidt H

In the field of automotive transportation lithium-ion batteries with high charge/discharge rates and high power densities are required. We monitored the formation and movement of the LixSi phase front by the produced changes in the neutron reflectivity of the electrode/electrolyte interface. The retrieved diffusion pathways are analyzed against optimized charging time and power densities.

28 In-Operando Neutron Reflectometry studies on Lithium Incorporation into Silicon Electrodes in Li-ion Batteries

Jerliu B, Hüger E, Seidlhofer B-K, Steitz R, Schmidt H

Amorphous silicon is a promising negative electrode material for Li-ion battery applications because of its high theoretical specific capacity of about 4200 mAh/g. By neutron reflectometry the insertion/de-insertion of lithium into the amorphous silicon electrode and the corresponding volume expansion can be directly monitored in-operando. Possible lithiation mechanisms are discussed.

29 Combined synchrotron X-ray and neutron imaging for the characterisation of fuel cells

Manke I, Arlt T, Haussmann J, Scholta J, Markötter H, Hilger A, Kardjilov N, Tötzke C, Wippermann K, Lehnert W, Banhart J

Water management is a key problem in state-of-the-art hydrogen driven fuel cells. A fundamental understanding of water distribution and transport in porous carbon fiber gas diffusion layers is a prerequisite for their optimization. In this contribution, we present examples for synchrotron X-ray and neutron imaging studies that help us to understand media transport in fuel cells.

30 Synchrotron X-ray and neutron imaging in DMFC research

Arlt T, Wippermann K, Schröder A, Markötter H, Kardjilov N, Hilger A, Tötzke C, Banhart J, Manke I

Fuel cells are expected to contribute to a sustainable energy supply in future. Direct-methanol fuel cells are promising candidates for several mobile applications. Catalyst layers and gas diffusion layers are objects of current energy research at the Helmholtz-Zentrum Berlin. Complimentary ex-situ and in-operando experiments have been performed at the experimental stations CONRAD 2 and BAMline.

31 Investigating the andhydro-protective effect of sugars with neutron membrane diffraction

Kent B, Garvey CJ, Bryant G, Hunt T, Hauss T

Small solute molecules, particularly di- and mono- saccharides, are associated with an anhydro-protective effect. Existing theories on the mechanisms of membrane protection imply different concentration profiles of sugar molecules between bilayers. We employ neutron membrane diffraction of aligned lipid bilayers to investigate the interaction of sugars with lipid membranes at reduced hydration.

32 Rheo-SANS of colloidal suspensions at V16

Siebenbürger M

In this work, first measurements at V16 with the Rheo-SANS-setup will be shown. The investigated suspensions consist of thermo-sensitive core-shell particles, either in a spherical or dumbbell shape. Here the influence of shear on the structure will be shown for the process of gelation and shear alignement.

33 Using Very Small Angle Neutron Scattering to study complex biological systems.

Yu S, Clemens D, Ballauff M

We aim to study the state of phase and structural changes of complex PE-protein particles using VSANS including contrast variation. First neutron experiments on Human Serum Albumin (HSA) at the V16 reveal its structures by accessing a wide q-range of the scattering pattern. We explore the limits of modern data modeling to reveal its strength and weaknesses.

34 BioRef - combining neutron reflectivity and FTIR for a better understanding of solid-liquid interfaces

Trapp M, Kreuzer M, Dahint R, Steitz R

The time-of-flight reflectometer BioRef is a joint venture of the University of Heidelberg and HZB. It offers the unique possibility to combine neutron reflectivity and in situ ATR-FTIR measurement on a sample at the same time. Using these features, the time dependent interaction of PSS with a model membrane at the solid-liquid interface has been studied as a function of temperature.

35 Shear Cell for Combined In Situ Neutron Reflectivity and ATR-FTIR Measurements

Schwörer F, Trapp M, Steitz R, Dahint R

In our study we demonstrate the potential of BioRef to characterize the structure and molecular conformation of thin lipid films under applied shear using combined neutron reflectivity and infrared analysis. We found enhanced mechanical stability of lipid coatings with polyelectrolyte solutions. The experiments provide first insight in mechanisms of wear reduction in natural joints.

36 Understanding the mode of action of hydrophilic penetration accelerators to the nanostructure of stratum corneum lipid models

Mueller J, Trapp M, Neubert RHH, Schroeter A

To investigate the influence of penetration enhancers on the structure of the Stratum corneum lipid matrix on a molecular scale, neutron reflectivity is an adequate method. With the use of the BioRef it is possible to examine changes in the structure and thickness of the lipid layers (Neutron reflectivity) as well as in the lipid phase state (ATR-FTIR) at the same time with the same sample.

37 Self-aggregation of surfactants in structurally similar room-temperature ionic liquids

Klee A, Prevost S, Gradzielski M

Binary mixtures of CnmimFeCl4 (n=2,4) and CimimCl (i=14,16,18) are investigated. Due to its high light absorption, monomeric surfactant solubility and conductivity, classical methods as light scattering, surface tension, conductivity or ITC are unusable. Neutron scattering is unaffected by these particularities and hence is an irreplacable tool to get information on aggregate existence and shape.

38 Controlling vesicles; morphology and size with telechelic polymers

Malo de Molina P, Tran Dang N, Poltzer F, Prevost S, Grazielski M

Vesicles are widely used as drug delivery carriers and model systems for biological membranes. In all cases a precise control over their morphology and size is crucial. We show that the addition of telechelic polymers with two (resp. 4) sticky ends to vesicles results in small uni-(resp. multi-) lamellar vesicles, the size of which can be fine-tuned via concentration and polymer architecture.

39 The versatility of biopolyelectrolyte-surfactant complexes for microstructures formation explored by SANS

Chiappisi L, Prevost S, Gradzielski M

Mixtures of bio-derived polyelectrolytes and oppositely charged surfactants have a large potential for pharmaceutical and food-grade applications for solubilisation of water-insoluble compounds and as viscosity enhancers. By mixing chitosan with surfactants from the CiEjCOOH family, a large variety of structures can be produced, controllable via pH and by surfactant hydrophobic/hydrophilic ratio.

40 Polyglycerol surfactants: the nonionic amphiphiles from sustainable chemistry

Heunemann H, von Lospichl B, Prevost S, Gradzielski M

While nonionic surfactants are typically represented by the class of alkyloligoethoxylates, produced from the carcinogenic, mutagenic and flammable ethylene oxide, the industry starts to adopt polyglycerol surfactants whose polar headgroups are based on glycerol, the byproduct of biodiesel. We present the investigation of this recent class of nonionic surfactant, with low temperature sensitivity.

41 Control of vesicles; morphology and size via telechelic polymers

Malo de Molina P, Tran Dang N, Poltzer F, Prevost S, Gradzielski M

Vesicles are widely used as drug delivery carriers and model systems for biological membranes. In all cases a precise control over their morphology and size is crucial. We show that the addition of telechelic polymers with two (resp. 4) sticky ends to vesicles results in small uni-(resp. multi-) lamellar vesicles, the size of which can be fine-tuned via concentration and polymer architecture.

42 The self-assembly of inorganic ions: theta-amphiphiles as a new class of surfactants

Bauduin P, Prevost S, Brusselle D, Farras P, Teixidor F, Diat O, Zemb T

The sandwich ion COSAN, with Cobalt (III) trapped between two hydrophobic boron-based cages (dicarbollides), is a rigid molecule, the acidic form of which unexpectedly exhibits self-aggregation in

water, forming small micelles and large vesicles in equilibrium with monomers. The driving force is believed to be molecular forces, the missing piece among our understanding of colloidal forces.

43 Influence of Polycation Molecular Weight and Barrier Layers on the Polyanion Diffusion within Polyelectrolyte Multilayers

Passvogel M, Nestler P, Köhler R, Helm C A

Polyelectrolyte multilayers consisting of a protonated and a deuterated block are annealed in 1M NaCl. Neutron reflectivity shows that interdiffusion broadens the internal interface. The polyanion (prot. and deut. PSS) diffusion constant depends on the polycation (PDADMA) polymer weight assuming PDADMA/PSS move as a complex. A layer consisting of branched PEI serves as diffusion barrier for PSS.

44 Characterization of S-I-S Josephson junctions with reflectometry

Qviller A, Østreng E, Steitz R, Seidlhofer B, Meckback M, Ilin K, Siegel M, Fjellvåg H, Frommen C, Hauback B

Neutron and x-ray reflectometry are ideal techniques for probing buried interfaces. They can be utilized to measure the insulating barrier thickness in S-I-S Josephson junctions. We report measurements on Nb-AlOx junctions with the use of the V6 reflectometer at BER II and x-rays. The relationship between the barrier thickness and the critical current is then determined.

45 Direct Visualization of the Influence of Penetration Enhancer Molecules to Planar SC Lipid Model Bilayers at the Lipid/Liquid Interface Applying Neutron Reflectivity

Schroeter A, Mueller J, Koehler R, Neubert RHH

The Neutron reflectivity experiment on soft-supported lipid bilayers can offer insights into the mode of action of penetration enhancer. Thus, the system consists of a silicon crystal backing, pre-coated with a polyelectrolyte multilayer (PE) to which SC lipid bilayers is adsorbed in situ. The PE layer is needed to separate the lipid membrane from the hard matter support.

46 In vivo study of embolism formation in lianas stems using cold neutron radiography

Tötzke C, Miranda T, Konrad W, Gout J, Kardjilov N, Dawson M, Manke I, Roth-Nebelsick A

Cold neutron imaging was used for in vivo studies of water relations in plants. Using D2O as tracer substance we could visualize the water ascent in liana stems. We were able to directly observe the formation of gas embolism in the water conducting tissue under water stress conditions. Cold neutron radiography has proven to be a useful tool for studying water relations in plant stems.

Poster Abstracts – Science Day at BESSY II

Thursday, 5th of December

1 RZPA Optimization for Parallel Fluorescence Spectrometers

Löchel H, Loukas P, Fernandez Herrero A, Vadilonga S, Avramenko A, Braig C, Rehanek J, Erko A

The performance of a reflection zone plate array (RZPA) for parallel X-ray spectroscopy was optimized using the programs REFLEC and RAY. The procedure evaluates an optimal input angle for a given energy resolution, the pixel size and the geometrical dimensions. The variable depth of profile is also important. LOOPER, a program attachment, allows the calculation with several independent variables.

2 In situ observation of gating phenomena in the flexible porous coordination polymer Zn2(BPnDC)2(bpy) (SNU-9) in a combined diffraction and gas adsorption experiment

Bon V, Senkovska I, Wallacher D, Többens D M, Zizak I, Feyerherm R, Müller U, Kaskel S

The intrinsic structural dynamic during the adsorption of CO2 and N2 on flexible porous coordination polymer Zn2(BPnDC)2(bpy) was studied in situ by powder and ex situ by single crystal XRD. The formation of intermediate phase during the CO2 adsorption could be postulated, while the transformation from narrow pore form to the open structure occurs in quasi one step in the case of N2 adsorption.

3 Investigation of piezoelectric domain patterns in NaNbO3 thin films by grazing incidence x-ray diffraction

Schmidbauer M, Schwarzkopf J, Kwasniewski A, Sellmann J, Braun D

Tensely strained NaNbO3 epitaxial thin films grown on (110) DyScO3 substrates by pulsed laser deposition show a regular one-dimensional piezoelectric domain pattern. The lateral domain sizes, the in-plane monoclinic distortion angles and the in-plane strain distribution were investigated by 3D grazing incidence x-ray diffraction as a function of the film thicknesses (1.5 nm .. 28 nm).

4 Identification of non-agglomerated nanodiamonds inside metal matrix composites by synchrotron radiation

Popov V, Többens D, Prosviryakov A

The study demonstrated that the application of synchrotron radiation could effectively identify non-agglomerated nanodiamonds in an aluminum matrix at a volume fraction as low as 3%. Composites were produced by a mechanical alloying process that allowed a uniform distribution of individual non-agglomerated primary nanodiamond particles in the metal matrix.

5 Momentum-Dependent Charge Correlations in YBa2Cu3O6+δ Superconductors Probed by Resonant X-Ray Scattering: Evidence for Three Competing Phases

Blanco-Canosa S, Frano A, Loew T, Lu Y, Porras J, Ghiringhelli G, Minola M, Mazzoli C, Braicovich L, Schierle E, Weschke E, Le Tacon M, Keimer B

We use resonant x-ray scattering to determine the momentum-dependent charge correlations in YBa2Cu3O6+δ samples. The results reveal nearly critical, biaxial in-plane charge density wave (CDW) correlations for high doping levels. However, the corresponding scattering intensity exhibits a strong uniaxial anisotropy for low oxygen concentrations.

6 MAXYMUS - Features, Results and Upcoming Upgrades

Weigand M, Bechtel M,Bykova I, Goering E, Schütz G

MAXYMUS is a scanning X-ray microscope operating as permanent endstation at BESSY II. It features UHV compatibility for surface sensitive measurement as well as a unique pump and probe system for time resolved measurements. Upcoming upgrades including an in-vacuum camera for ptychography and X-ray fluorescence microscopy as well as a new interferometer and control system will be shown.

7 Dynamic control of the ground state and excitation spectra in patterned ferromagnets

Novosad V

The system of interacting vortices is employed to demonstrate a Resonant-Spin-Ordering approach for manipulating the ground state and excitation spectra [1, 2]. The experimental and micromagnetic data are in an agreement, and could serve as a basis for planning future synchrotron imaging experiments at BESSY. [1] APL, 102, 052401 (2013). [2] Nat.Comm. DOI: 10.1038/ncomms2331 (2012).

8 Magnetic Order of Randomly Distributed Fe in Multiferroic YMn1.93Fe0.07O5

Partzsch S, Hamann-Borrero J-E, Schierle E,Weschke E, Souptle D, Büchner B, Geck J

We present a resonant x-ray diffraction study on multiferroic YMn1.93Fe0.07O5 at the MnL- and FeL edges. Surprisingly the randomly Fe impurities follow the magnetic ordering of the Mn host. The determination of the magnetic ordering of the Fe impurity by detailed azimuthal dependencies at two different temperatures reveals an unexpected spin reorientation.

9 Magnetic Coupling of Gd3N@C80 Endohedral Fullerenes to a Substrate

Bernien M, Hermanns C F, Krüger A, Kuch W, Schmidt C, Wasserroth S T, Ahmadi G, Heinrich B W, Franke K J, Schneider M, Brouwer P W, Weschke E

XMCD measurements of Gd3N@C80 adsorbed on a Cu surface reveal that the magnetic moments of the encapsulated Gd atoms couple ferromagnetically to each other. When the molecules are in contact with a ferromagnetic Ni substrate, we detect two different Gd species, one that couples antiferromagnetically to the Ni, whereas the other one exhibits a stronger and ferromagnetic coupling to the substrate.

10 Ultrafast magnetic and structural dynamics in antiferromagnetic Europium-Telluride

Trabant C, Pontius N, Holldack, Schierle E, Weschke E, Kachel T, Mitzner R, Beye M, Springholz G, Dakovski G, Turner JJ, Moeller S, Wang T, Gray A, Hantschmann M, Dürr HA, Minitti M, Schick D, Bargheer M, Lee WS, Chuang YD, Hussain Z, Shen ZX, Foehlisch A & Schuessler-Langeheine C

We studied ultrafast magnetic and structural dynamics in thin films of the antiferromagnetic semiconductor EuTe using resonant-magnetic-scattering with ultrashort x-ray pulses from the BESSY II Femtoslicing and LCLS. The momentum resolved data show a loss of antiferromagnetic magnetic order before the structural changes through strain waves become visible.

11 Spin manipulation in antiferromagnetic Holmium

Trabant C, Pontius N, Zabel H, Mitzner R, Holldack K, Freemont J, Foehlisch A, Schuessler-Langeheine C

The speed limit for ultrafast spin manipulation is given by the achievable angular momentum transfer rate. Antiferromagnets have been predicted to be considerably faster than ferromagnets, because a loss of magnetic order does not necessarily require a transfer of angular momentum out of the spin system. We present experimental data from the antiferromagnet holmium that support this prediction.

12 Study of GeTe and Sb2Te3-GeTe alloys by time resolved XANES

Wang R.-N, Boschker J E, Bragaglia V, Giussani A, Calarco R, Le Guyader L, Beye M, Radu I, Holldack K, Fons P, Kolobov A V

Time-resolved pump-probe XANES was performed on crystalline GeTe and Sb2Te3-GeTe alloy samples with an excitation below the amorphization threshold to study the dynamics behind optical switching. Although a difference in the absorption spectra could be measured by static XANES between the crystalline and optically-amorphized phases, no trend could be observed with the pump-probe experiments.

13 Towards single bunch access in hybrid mode operation

Kühn D, Holldack K, Ovsyannikov R, Kuske P, Müller R, Scheer M, Gorgoi M, Sorgenfrei F, Lindenau B, Leyendecker M, Leitner T, Svensson S, Mårtensson N and Föhlisch A

In this contribution we will present our ongoing efforts on providing single bunch pulse picking in hybrid mode operation of BESSY II storage ring at full 1.25 MHz frequency.

14 Ongoing developments of the ArTOF - a novel type of angular resolved time-of-flight photoelectron spectrometer

Leitner T, Ovsyannikov R, Stråhman C, Gorgoi M, Öhzelt M, Volmer A, Sorgenfrei F, Kühn D, Bauer M, Lundqvist M, Karlsson P, Holldack K, Kuske P, Sankari R, Mårtensson N, Svensson S, Föhlisch A

The ArTOF instrument is a recently developed new type of high resolution, high transmission, angular resolved photoelectron spectrometer based on the combination of an electrostatic electron lens system with the time-of-flight principle of electron energy detection. In this contribution our latest instrument developments will be presented and future plans will be outlined.

17 In-Operando Neutron Reflectometry studies on Lithium Incorporation into Silicon Electrodes in Li-ion Batteries

Jerliu B, Hüger E, Seidlhofer B-K, Steitz R, Schmidt H

Amorphous silicon is a promising negative electrode material for Li-ion battery applications because of its high theoretical specific capacity of about 4200 mAh/g. By neutron reflectometry the insertion/de-insertion of lithium into the amorphous silicon electrode and the corresponding volume expansion can be directly monitored in-operando. Possible lithiation mechanisms are discussed.

18 In-Situ Studies of the Lithium Incorporation into Lithium-Ion Batteries Model Systems

Seidlhofer B-K, Jerliu B, Hüger E, Steitz R, Schmidt H

In the field of automotive transportation lithium-ion batteries with high charge/discharge rates and high power densities are required. We monitored the formation and movement of the LixSi phase front by the produced changes in the neutron reflectivity of the electrode/electrolyte interface. The retrieved diffusion pathways are analyzed against optimized charging time and power densities.

20 Beamlines for the Energy Material in Situ Laboratory (EMIL) at BESSY II

Hendel S, Schäfers F, Follath R, Scheer M, Bahrdt J, Hävecker M, Reichardt G, Lips K

The Energy Material in Situ Lab will include two beamlines with twenty optical elements: The hard X-ray beamline consists of a plane grating monochromator for the first harmonic and a double crystal monochromator for the energy range up to 10 keV. The radiation of the soft X-ray beamline is dispersed by another PGM operating in collimated light. Several mirrors are foreseen to shape the beam.

21 In Operando Analysis of Materials by Nanoscale X-ray Spectromicroscopy

Henzler K, Werner S, Guttmann P, Rehbein S, Schneider G, Ballauff M

The analysis of materials for renewable energies and storage is a major challenge to optimize the materials for the respective application. New analyzing tools will be needed to characterize the structural changes of the materials during the working cycle of the respective devices. Nanoscale X-ray Spectromicroscopy is a suitable technique for such studies.

22 Semi-automatic Segmentation of Cellular Structures from Cryo Soft X-ray Transmission Microscopy Images

Cardenes R, Klementieva O, Crispi F, Gratacos E, Schneider G, Bijnens B

Segmentation of cellular structures is crucial for the quantification of biological samples. Here, we introduce concepts for 3D segmentation of spherical cellular structures and membranes in reconstructed cells from Cryo Soft X-ray Transmission microscopy (cryo-TXM), to optimize manual user interaction, achieving successful results.

23 X-ray spectromicroscopy analysis of organic solar energy materials at the nanoscale: Domain dimensions, in-plane orientation and chemical contrast

Zykov A, Steyrleuthner R, Schubert M, Mete T, Fostiropoulos K, Guttmann P, Werner S, Henzler K, Neher D, Schneider G, Kowarik S

We investigated the in-plane nanomorpholgy of the polymer P(NDI2OD-T2) and of diindenoperylene (DIP) heterostructures as applied in organic solar cells and OFET's by X-ray transmission microscopy with sub 30nm resolution. The device relevant domain sizes and polymer backbone orientations are visible in x-ray dichroism and domains in heterostructures can be assigned to different molecules.

24 Combining nanoscale cryo X-ray tomography with SERS and laser ablation ICP-MS for the investigation of nanoparticle-cell interactions

Drescher D, Guttmann P, Büchner T, Zeise I, Traub H, Jakubowski N, Schneider G, Kneipp J

To understand the interactions of Au and Ag nanoparticles with biomolecules and cells, we combine 3D information about nanoparticle distribution in cellular substructures from cryo X ray tomography using synchrotron radiation with the chemical characterization of the particle environment obtained by surface-enhanced Raman scattering (Drescher et al., Nanoscale 2013).

25 On the Nature of the Chemical Bond in Aqueous Ferrocyanide

Engel N, Bokarev S, Suljoti E, Garcia-Diez R, Lange K, Atak K, Golnak R, Kothe A, Dantz M, Kühn O, Aziz E

Resonant inelastic X-ray scattering and X-ray absorption experiments at the iron L- and nitrogen K-edge are combined with ab initio calculations for a systematic investigation of the nature of the chemical bond in potassium ferrocyanide in aqueous solution. The atom- and site-specific nature of RIXS allows for a direct observation of ligand-to-metal and metal-to-ligand charge transfer bands.

26 N K-edge NEXAFS of aqueous para-aminobenzoic acid solutions

Gainar A, Stevens J S, Suljoti E, Xiao J, Golnak R, Suljoti E, Brandenburg T, Aziz E F, Schroeder S L M

Speciation studies of molecular solutes represent a stepping stone for understanding molecular self-assembly during crystal nucleation. By N K-edge absorption measurements we have determined the electronic structure of para-aminobenzoic acid (PABA) in its crystalline polymorphs, in aqueous solution as a function of pH. The results can be interpreted by ground-state DFT calculations.

27 Proton transfer in aqueous NH3 solution

Unger I, Thürmer S, Slavíček P, Kryzhevoi N, Winter B

Core-excited NH3 and ND3 in aqueous solution may, in contrast to the gas phase, decay via delocalized channels such as intermolecular Coulombic decay (ICD). Spectral differences between the two samples suggest a prominent role of protons in the delocalization processes and can be explained by a recently proposed model of proton transfer assisted (PTA) charge delocalization.

28 Laser-assisted electron scattering in strong-field ionization of water by few-cycle laser pulses

Wilke M, Al-Obaidi R, Moguilevski A, Brandtstätter R, Kothe A, Engel N, Metje J, Kiyan I, Yu, Aziz E F

Strong-field ionization of dense water gas was studied by means of angle-resolved time-of-flight electron spectroscopy. In contrast to diluted gases where above-threshold ionization (ATI) and high-order ATI (HATI) of single molecules dominate electron emission a collective effect of radiation absorption by neighboring particles known as laser-assisted electron scattering (LAES) was observed.

29 Continuous wafer-scale graphene on cubic-SiC(001)

Chaika A, Molodtsova O, Zakharov A, Marchenko D, Sanchez-Barriga J, Varykhalov A, Shvets I

The graphene synthesized on commercially available cubic-SiC(001)/Si(001) wafers have been studied. We prove the wafer-scale continuity and uniform thickness of the graphene overlayer, which consists of only a few monolayers with physical properties of quasi-freestanding graphene. A realistic way of bridging the gap between the outstanding properties of graphene and their applications was shown.

30 Atomic structure and chemical bonding at the interface between Fe and topological insulator probed by photoeletron diffraction

Yashina LV, Kuznetsov MV, Volykhov A A, Sanchez-Barriga J, Sirotina AP, Neudachina VS, Varykhalov A,Rader O

Phenomena that occur during prototypical TI Bi2Te3-ferromagnetic metal Fe interface formation are studied by XPD and STM,XPS,ARPES,XPD, DFT. Adatoms relax strongly into the Bi2Te3 lattice and form chemical bonds both with Bi and to Te. Iron clusters are randomly distributed, but the ordered structure is formed at the interface, which includes interstitial and surface Fe atoms.

33 Electron pair emission using time-of-flight spectrometers: new perspectives

Huth M, Chiang C-T, Trützschler A, Schumann F O, Kirschner J, Widdra W, Mähl S, Kampen T

An instrument consisting of a pair of commercial time-of-flight spectrometers and a lab based UV source is described. The light source delivers photons up to 45 eV with a repetition rate of 1 MHz. We determined the performance of the instrument via photoemission and electron excited pair emission from surfaces. The feasibility to perform double photoemission experiments from solid surfaces is demonstrated.

34 Modification of induced spin-orbit splitting of n- states of graphene under joint intercalation of Bi and Au

Zhizhin EV, Varykhalov A, Rybkina AA, Rybkin AG, Marchenko DE, Vladimirov GG, Rader O, Shikin AM

Spin-orbit splitting of valence band states of graphene is negligible. Intercalation atoms of Au leads to the effect of SO splitting of pi-states of MG above 60 meV. This effect caused by two reasons:1) process of pi–d hybridization, 2) influence of a high intra-potential gradient. In this work was interesting Bi because his characterized by the sp-valence band structure and high atomic number.

35 Photoemission of Bi2Se3 with Circularly Polarized Light: Probe of Spin Polarization or Means for Spin Manipulation?

Sanchez-Barriga J, Varykhalov A, Braun J, Xu S-Y, Alidoust N, Kornilov O, Minar J, Hummer K, Springholz G, Bauer G, Schumann R, Yashina L V, Ebert H, Hasan M Z, Rader O

The peculiar in-plane spin texture of topological insulators is believed to enable control of the electron spin by circularly polarized light in photoemission. We show for Bi2Se3 that with VUV light we measure the ground state spin texture. A 6 eV laser, however, flips the spins out of the surface plane with the sense of circular polarization.

37 Structural and Biochemical Characterization of the Folyl-poly-γ-L-glutamate Hydrolysing Activity of Human Glutamate Carboxypeptidase II

Navratil M, Ptacek J, Starkova J, Lubkowski J, Barinka C, Konvalinka J

Human glutamate carboxypeptidase II acts as folate hydrolase in small intestine. However there is limited knowledge of folate recognition and processing by the enzyme as well as virtually no information on the consequence of GCPII H475Y polymorphism on folate hydrolysis. Here we present a series of structural, kinetic and mutagenesis studies aimed at dissecting GCPII role in folate metabolism.

38 The new fragment screening facillity at the HZB MX-beamline BL14.2

Mueller U, Sparta K, Ühlein M, Linnik J, Heine A, Klebe G, Weiss MS

Fragment based drug discovery is a very modern and powerful new experimental technique to analyse the funtional surface of medically relevant proteins at atomic detail level. This presented project is developed in strong collaboration with AG Klebe from University Marburg and is aiming for the establishment of a new screening facility using the upgraded MX-beamline BL14.2.

39 Structure-functional analysis of novel haloalkane dehalogenases DbeA from Bradyrhizobium elkanii USDA94 and DpcA from Psychrobacter cryohalolentis K5

Tratsiak K, Prudnikova T and Kuta Smatanova I University of South Bohemia, South Bohemian Research Center of Aquaculture and Biodiversity of Hydrocenoses, Zamek 136, 37333 Nove Hrady, Czech Republic School of Complex Systems Institute of Systems Biology and Ecology Academy of Science of the Czech Republic, Zamek 136, 373 33 Nove Hrady, Czech Republic

DbeA and DpcA enzymes (EC 3.8.1.5), were isolated from Bradyrhizobium elkanii USDA94 and Psychrobacter cryohalolentis K5. DpcA, exhibiting unique temperature profiles, has substrate specificity prefered brominated and terminally substituted substrates, while DbeA protein towards brominated and iodinated compounds. The DpcA crystals belong to space group P21 (1.05 Å) and DbeA to P212121 (2.2 Å).

40 X-ray vs. NMR structure of the N-terminal domain of delta-subunit of RNA polymerase

Demo G, Papouškova V, Komarek J, Kaderavek P, ídek L, Sklenar V, Wimmerova M

The crystal structure of the N-terminal domain of delta-subunit of RNA polymerase from Bacillus subtilis solved at the resolution of 2.0 Å is presented. The X-ray structure shows significant differences from the average NMR structure. We systematically investigated the cause of the discrepancies between the NMR and X-ray structures, as the pH, presence of metal ions and crystal packing forces.

41 How does the membrane-bound [NiFe] hydrogenase of Ralstonia eutropha achieve oxygen-tolerance? - Structural and chemical transformation of the unprecedented [4Fe-3S] cluster.

Kalms J, Schmidt A, Frielingsdorf S, Fritsch J, Hammer M, Lenz O, Scheerer P

Hydrogen is the most promising clean energy carrier and therefore O2-tolerant hydrogenases are on special interest as tools in renewable energy technologies. Only a small subgroup of [NiFe] hydrogenases is qualified for this application due to a unique [4Fe-3S] cluster. Cluster architecture regarding to O2-tolerance of membrane-bound [NiFe] hydrogenase has been analyzed by X-ray crystallography.

42 Tailoring of network dimensionality and porosity adjustment in Zr- and Hf-based MOFs

Bon V, Senkovska I, Weiss MS, Kaskel S

Three Zr and Hf based metal–organic frameworks, namely DUT-52, DUT-53 and DUT-84 (DUT = Dresden University of Technology) were synthesized using linear 2,6-naphtalenedicarboxylate as a linker. By adjusting the modulator concentration only, the connectivity of Zr6O8 cluster can be reduced from 12 to 8 and even to 6, which is reflected in different crystal structures and BET specific surface area.

43 Observation of the hydride bridge in the NiFe active site of [NiFe] hydrogenase by high-resolution crystallographic analysis

Ogata H, Nishikawa K, Lubitz W

Hydrogenases catalyze the reversible hydrogen oxidation process by cleaving dihydrogen heterolytically. We present a crystallographic analysis of the reduced state of [NiFe] hydrogenase from D. vulgaris Miyazaki F at 0.9 Å resolution. It revealed the presence of the hydride bridge at the NiFe active site in the catalytic active state. Furthermore the CO and CN ligands could be identified.

44 A G protein-coupled receptor at work – Structural insights from the rhodopsin model

Szczepek M, Park JH, Kim YJ, Hildebrand PW, Krauss N, Ernst OP, Choe, H-W, Hofmann KP, Scheerer P

To transmit extracellular signals into living cells, nature has evolved membrane-spanning receptor proteins (G-protein-coupled-receptors or GPCRs), that connect the extracellular environment to the cell interior. Our crystal structures of various activated states of the GPCR-photoreceptor rhodopsin receptor can serve as model for activation and inactivation processes in the large GPCR family.

45 High throughput screening identifies novel inhibitors of histone lysine demethylase enzymes KDM4A-E

Carter DM, Specker E, Przygodda J, Neuenschwander M, Seyffarth C, Von Kries J, Gohlke U, Heinemann U

KDM4A-F enzymes stimulate cancer cell growth. We identified small molecules that inhibit KDM4 activity. Crystal structures of similar compounds bound to a KDM4 isoform reveal modes of binding, and regions within the active site that can be exploited to enhance potency. We aim to use this information to further engineer our compounds and to test their ability to halt cancer cell growth in vivo.

46 Activation of AMPA-type glutamate receptors by their ligand binding domains

Chebli M, Baranovic J, Salazar H, Faelber K, Lau A, Daumke O, Plested A

The AMPA-type of ionotropic glutamate receptors is a ligand-gated ion channel and mediates fast excitatory synaptic transmission in the central nervous system. AMPA receptors form tetrameric structures but to date only one full-length tetrameric structure exists bound to an antagonist. Here we describe a tetrameric receptor assembly of neurotransmitter binding domains fully bound to glutamate.

47 Facilities for Macromolecular Crystallography at the HZB

Weiss MS, Förster R, Hellmig H, Röwer M, Sparta K, Steffien M, Ühlein M, Mueller U

The Macromolecular Crystallography (MX) group at the HZB is operating three state-of-the-art beamlines (BL14.1-3) for MX. The beamlines represent the most productive MX-stations in Germany, with more than 1000 PDB depositions. BLs14.1 and 14.2 are energy tunable, while BL14.3 is a fixed-energy side station. On the poster, a summary on the experimental possibilities of the beam lines will be given.

48 S-SAD structure determination of a spliceosomal protein

Schütze T, Apelt L, Weber G, Ulrich A, Stelzl U, Weiss M, Wahl M

Orthorhombic crystals of a spliceosomal protein (179 amino acids, 4 Cys, 6 Met) were used for anomalous diffraction data collection on the HZB-MX beamline BL14.2. Using a wavelength of 2.0 Å, data were collected from four crystals. For three of the four crystals 270 degrees of data turned out to yield anomalous differences of sufficiently high quality, so that the structure was solved using S-SAD.

49 On the structure-function relationship between surface chemistry and catalytic activity of cobalt and manganese oxides towards oxygen evolution reaction (OER)

Hillebrand P, Zajac D, Ramirez Caro A, Bogdanoff P, Fiechter S

Electrodeposited amorphous cobalt and crystalline manganese oxide catalysts were investigated studying their surface after oxygen evolution with a combined electrochemical-UPS setup and ex-situ EXAFS/XANES measurements. While manganese oxide appear unchanged after electrochemical treatment of the electrode surface, the cobalt oxide films show potential depending changes in their valence band.

50 The Efficiency of the ICD Process

Förstel M, Arion T, Hergenhahn U

We have determined the efficiency of Interatomic / Intermolecular Coulombic Decay in Neon and water clusters. In water clusters, we find a difference between clusters of deuterated to those of normal water, which hints towards a competition between ICD and proton transfer processes. In Neon clusters, earlier findings of unit efficiency are corroborated.

51 Time-of-flight multi-electron-ion coincidence spectroscopy studies of acetaldehyde

Zagorodskikh S, Squibb RJ, Mucke M, Zhaunerchyk V, Linusson P, Eland JHD, Feifel R

Single-photon multiple ionization processes of acetaldehyde have been investigated using a versatile multi-particle coincidence technique utilising a time-of-flight magnetic bottle. Photon energies of 95, 307-350 eV and 550-600 eV were chosen to investigate multiple-ionization processes involving emission of multiple valence and core electrons and the emission of multiple Auger electrons.

52 Investigation of the Hydrogenation of Graphene on Ni(111) via Temperature Programmed X-Ray Photoemission Spectroscopy and Temperature Programmed Desorption

Späth F, Zhao W, Gotterbarm K, Gleichweit C, Steinrück H-P, Papp C

We studied the reaction of graphene prepared on a Ni(111) crystal with atomic hydrogen in detail, with XPS and TPD. We find a single-side fully hydrogenated graphene layer and, depending on coverage, two H2 desorption maxima at 360 and 650 K. This behavior is confirmed by both methods. The data are compared to gold-intercalated graphene on Ni(111).

53 Modeling catalytic reactions: graphene-supported Pd nanoclusters studied with high resolution XPS

Gotterbarm K, Bronnbauer C, Bauer U, Papp C, Steinrück H-P

Corrugated graphene layers grown on Rh(111) served as template for the deposition of palladium nanoclusters. The growth and thermal stability of the clusters and their interaction with adsorbates was studied by fast high-resolution XPS at beamline U 49/2-PGM1. We found a cluster-by-cluster growth mechanism. With increasing temperatures restructuring and agglomeration of the clusters occur.

54 Hard diamond-like carbon coatings on soft olefinic polymers

Fischer CB, Rohrbeck M, Wehner S, Richter M, Städter M, Schmeisser D

Hard diamond-like carbon (DLC) layers with different thickness have been coated on soft conventional olefinic polymers, e.g. high density polyethylene (HDPE). Synchrotron radiation is used for a detailed understanding of the interlayer formation between these unequal materials (by NEXAFS). The specific topographies of the carbon coatings are examined by SEM and AFM microscopy.

55 A spectroscopic comparison of AOS thin films and TCO single crystals

Haeberle J, Gaspar D, Barquinha P, Machulik S, Janowitz Ch, Galazka Z, Schmeisser D

AOS have a bright future for commercial electronics. We compare the electronic properties of a-GIZO and a-SnOx films with those of the corresponding (In, Ga, Zn, Sn) single Xtal-TCOs. We report on the core levels, the VB PES data, pIY, and the XAS absorption data. From these we are able to derive the elemental ratio, the pDOS, the band schemeas well as the contributions of defect states.

56 FeRh on Cu(100): Cluster substrate interaction viewed by photoelectron spectroscopy

Baev IV, Beeck T, Jänkälä K, Martins M, Wurth W

We studied small FeRh clusters deposited on Cu to understand the electronic structure changes induced by cluster substrate interaction. The band structure of Cu serves as a map for the orbitals involved. Band structure changes depend on the cluster size and the type of atoms involved. Theoretical models to describe the coupling are developed within the SFB 668.

57 Metal contacts on the Ga2O3 single crystal (100) surface

Machulik S, Nazarzadehmoafi M, Siebert A, Mohamed M, Janowitz C, Galazka Z, Manzke R

Results of band structure measurements on Ga2O3 single crystals agreed well with theoretical calculations. Previous ARPES measurements performed on Au-Ga2O3 contacts confirmed Schottky behavior with a barrier height of 1.01 eV. We performed an ARPES study of Ag-Ga2O3, yielding barrier height of 0.55 eV. The results point to a lower barrier, which is in agreement with theoretical predictions.

58 Schottky barrier height of Ag on In2O3 (111) single crystal

Nazarzadehmoafi M, Machulik S, Neske F, Janowitz C, Galazka Z, Manzke R

We studied schottky barrier height of metal-semiconductor contact, implemented through Ag evaporation on In2O3 single crystals by ARPES. ARPES was used to determine the barrier height by following band bending of valence band and core level of Ag deposition, which was in consistent with theoretical prediction. Diffuse band-gap states and Fermi level shift with Ag deposition were detected.

59 The problem of XANES spectrum interpretation measured by TEY technique at different photon glancing angles

Andreeva M, Repchenko Yu, Domashevskaya E,Terekhov V, Seredin P, Kashkarov V

The strange shape of TEY XANES spectra from GaInP measured at the phosphorus L2,3 edges as a function of photon glancing angle of incidence is explained by taking into account the energy dependence of the non-resonant photoelectron background. We perform detailed analysis of the resonant white line shape depending on the optical parameters and the relative amount of the nonresonant contribution.

60 Theoretical descrirption of X-ray absorption spectroscopy of the graphene-metal interfaces

Voloshina E, Ovcharenko R, Shulakov A, Dedkov Y

The NEXAFS spectra for the selected graphene-based systems are calculated in the framework of the approach, which includes the effects of the dynamic core-hole screening. The obtained results are compared with available experimental data demonstrating the excellent agreement between theory and experiment.

61 The theoretical description XES/NEXAFS of metal-like systems including dynamical effects

Ovcharenko R, Voloshina E, Dedkov Y, Shulakov A

We propose improved calculation scheme for XES/NEXAFS spectra calculation of metal-like systems including dynamical core-hole screening. Described formalism was applied to K/L emission bands of Mg and Al metals as well as K emission and absorption of graphene. Excellent agreement between theory and experiment is achieved.

62 Electronic and spin structure of Graphene on Pt(111)

Klimovskikh II, Rybkin AG, Rybkina AA, Rusinova MV, Zhizhin EV, Shikin AM

Main aim of our work is to study electronic and spin structure of Graphene on Pt(111). System was investigated by angle- and spin- resolved photoelectron spectroscopy (ARPES and SARPES). Hybridization of Pt states with pi-states of graphene is observed. Spin resolved spectra show that pi-state is spin split near Fermi edge.

63 Electronic Structure and Many-Body Effects in Heavily Doped Graphene

Fedorov A, Verbitskiy N, Haberer D, Struzzi C, Knupfer M, Büchner B, Fink J, Pettaccia L, Grüneis A

Here we performed a comprehensive study of electronic structure of alkali and earth-alkaline doped quasi-free-standing graphene using XPS and high resolution ARPES measurements of the spectral function to extract the underlying Eliashberg functions and ascribe the measured fine structure to peaks in the phonon dispersion relation of graphene.

64 Controlled assembly of graphene-capped nickel, cobalt and iron silicides.

Vilkov O, Fedorov A, Usachov D, Yashina LV, Generalov A, Verbitskiy N, Grueneis A, Vyalikh DV

Starting from thin films of Ni, Co and Fe, we were able to form high-quality metal silicides with a variety of stoichiometries under a CVD-grown graphene layer. The coupling between graphene and silicides is rather weak and quasi-freestanding properties of graphene are preserved. The silicides are reliably protected by grahene and can cover a wide range of electronic materials/device applications.

65 Understanding the effects of sputter damage in W-S thin films by HAXPES

Sundberg J, Lindblad R, Gorgoi M, Rensmo H, Jansson U, Lindblad A

In this study, hard X-ray photoelectron spectroscopy (HAXPES) has been used to study W-S films deposited by magnetron sputtering. High-resolution reference measurements for crystalline WS2 and metallic W are also presented. Argon sputtering of the surface not only removes the outermost oxidized material, but also leads to preferential sputtering of sulfur and the formation of metallic tungsten.

66 A study of structure and microstructural development during Deformation and/or recrystallization processes taking place in natural and synthetic polycrystalline halite

Tommaseo C E

The microstructural and structural properties in synthetic pure and SiO2 gel-doped polycrystalline halite and in natural salt samples are presented. Local structural rearrangements take place during textural development, obviously due to the different deformation and recrystallization behavior of adjacent grain orientations influencing finally the bulk texture.

67 XPS studies of the influence of the polarization state on binding energies in ferroelectric BaTiO3

Welke M, Huth P, Schindler K-M, Denecke R

BaTiO3 has several phase transitions. The biggest change occurs during the phase transition from tetragonal to cubic where the electrical polarization disappears. In conventional XPS jumps in binding energies occurred at transition temperatures. Using HIKE this could be shown not to be a surface effect only. Additionally, 100 Å thick layers of CoFe2O4 and NiFe2O4 on BaTiO3 also showed these jumps.

68 HAXPES study of electronic structure and its effect on magnetic properties in (001) and (110) oriented LSMO thin films

Elovaara T, Kooser K, Granroth S, Majumdar S, Huhtinen H, Paturi P

LSMO is grown c-axis out-of-plane (001) and in-plane (110) without polar discontinuity at the substrate-film interface which improves FM interaction. XRD, HAXPES and magnetic study reveals that (110) lattice is more relaxed leading to less deformation of electronic density around the La atom or in the MnO(6) octahedra. This improves also FM, making (110) orientation attractive for spintronics.

69 NiFe2O4: a candidate for efficient spin filtering at room temperature?

Hoppe M, Döring S, Gorgoi M, Schneider CM, Müller M

The spinel NiFe2O4 (NFO) is ferrimagnetic and insulating at room temperature, which makes this material intriguing for the realization of spin-filtering tunnel barriers. To investigate the suitability of NFO for this purpose, we deposited ultra-thin films (2 nm < d < 10 nm) on Nb:SrTiO3 and studied their structural, magnetic and electronic properties via XRD, SQUID, NEXAFS, HAXPES and XMCD.

70 Ultrathin EuO films grown on ITO by reactive molecular beam epitaxy

Zijlstra B, Caspers C, Hoppe M, Zander W, Schubert J, Schneid C M, Müller M

The magnetic insulator EuO offers a novel approach for generating highly spin polarized currents. Ultrathin EuO films were grown by reactive-MBE on conductive and lattice-matched SnO2-doped In2O3. The crystalline and magnetic properties of the hetero-structure were characterized by RHEED, XRD and SQUID; and the local electronic structure was probed by a depth-dependent HAXPES study.

71 X-ray spectroscopic nondestructive methods for thin films and interfaces study. Application to SrTiO3 based heterostuctures

Filatova EO, Kozhevnikov IV, Sokolov AA, Egorova YV, Konashuk AS, Vilkov OY, Schaefers F, Gorgoi M

Air-exposed systems SrTiOx/B/Si with different interlayers (B) grown by ALD technique were studied using NEXAFS, XPS, HAXPES and SXR. We are focusing on the study of the influence of interlayer material on the atomic and electronic structure of the SrTiOx film. Also the atomic and chemical composition profiles across the heterostructure with in-depth resolution better than 1 nm are discussed.

72 Modeling of the impact of surface band bending on core-level lines in HAXPES

Wippler D, Gerlach D, van Albada SJ, Wilks RG, Pieters B, Wimmer M, Gorgoi M, Huepkes J, Baer M, Rau U

We have studied p-doped hydrogenated amorphous silicon (a-Si:H) by depth-resolved HAXPES at KMC-1 and observed energy-dependent core-level shifts. Using a computational model including a pronounced surface band bending and considering the Lambert-Beer law, we are able to effectively model the position and shape of the measured Si 1s and Si 2s core-level lines.

73 Band alignment at the interface between transparent conductive oxides and p-doped amorphous silicon

Rössler R, Korte L, Wilks RG, Starr D, Alsmeier J, Gorgoi M, Rech B, Bär M

We present an HAXPES analysis of the contact between degenerated n-type transparent conductive oxides (TCOs) and p-type hydrogenated amorphous silicon (a-Si:H) as used for contacts in high efficiency a-Si:H/c-Si heterojunction solar cells. In addition to insights into the chemical interface structure, the band alignment between the TCOs, namely ZnO:Al and ITO, and the (p)a-Si:H layer was derived.

74 Dopant Activation and Diffusion During Solid-Phase Crystallization of Thin-Film Silicon Solar Cell Structures

Wilks RG, Wimmer M, Gerlach D, Felix R, Ruske F, Lips K, Gorgoi M, Blum M, Yang W, Weinhardt L, Rech B, Heske C, Bär M

Thin-film p/n junctions for photovoltaic devices can be formed by solid-phase crystallization (SPC) and rapid thermal processing (RTP) of amorphous silicon (a-Si) to form poly¬crystalline silicon. Hard x-ray photoemission (HAXPES) at KMC-1 was used to study the chemical and electronic structure of these Si-based p/n junctions revealing SPC- and RTP-induced activation and diffusion of the dopants.

75 Small and wide angle x-ray scattering studies on bone, polymer composites and calcium carbonate at the BESSY II µspot beamline

Wagermaier W, Benecke G, Hoerth R, Lee K, Li C, Schmidt I, Seidt B, Siegel S, Fratzl P

The BESSY II µspot beamline provides a unique combination of simultaneous microbeam scanning SAXS/WAXS together with XRF to study (i) structure and composition of bone material during healing in an osteotomy rat model, (ii) structural changes in polymer – metalfluoride particle composites during in-situ tensile testing and (iii) the structure of crystallized calcium carbonate microlens arrays.

76 Chronic impairment of the vagus nerve function leads to changes in elemental composition of dopamine related brain structures in rats.

Szczerbowska-Boruchowska M, Krygowska-Wajs A, Ziomber A, Thor P, Zizak I, Wrobel P

We determine whether vagus nerve (VN) dysfunction may affect elemental composition of dopamine related brain structures in rats. Tissue slices were studied using the micro-XRF at the mySpot beamline (BESSY II). We found significantly increased levels of P, S, Cl, K, Fe and Zn in corpus striatum and lower contents of Ca, Zn and Rb in substantia nigra as a result o electrical stimulation of VN.

77 Monitoring Mechanochemical Syntheses by in situ X-ray Diffraction

Wilke, Fischer, Tröbs, Rademann, Emmerling

A method is presented to follow milling reactions using pseudo in situ synchrotron X-ray diffraction measurements. This method enables to follow the reaction time-resolved and offers the possibility to detect crystalline or amorphous intermediates. As model systems transition metal phenylphosphonates and different cocrystals were analyzed.

78 In situ characterization of crystallization processes

Nguyen Thi Y, Gnutzmann T, Rademann K, Emmerling F

Simultaneous application of in situ WAXS and Raman spectroscopy allows monitoring of crystallization processes starting from a solution via transient metastable phases, amorphous or crystalline, to finally stable crystalline forms. The influence of different solvents on the crystallization of organic polymorphic compounds was investigated using an acoustic levitator as contact-free sample holder.

79 Investigations of Degradation of Cementitious Materials by in-situ Structure Analysis

Stroh J, Emmerling F

The objective of our investigation is to unravel the mechanism of sulfate attack on cements depending on salt concentrations and exposure times. Synchrotron X-ray Diffraction analysis of thin cement sections was carried out with high spatial resolution. The extrapolation of the results to lower concentrations and furthermore the prediction of service life of cement constructions will be available.

80 Investigation of local structural changes in LiFeMnF6 cathode of Li-ion battery during electrochemical cycling by in-operando X-ray absorption spectroscopy

Fischer B, Lieser G, de Biasi L, Gesswein H, Rana J, Scher T, Binder J, Schumacher G

X-ray absorption spectroscopy measurements were performed in operando on Li ion batteries containing LiFeMnF6 as cathode material. It is observed that Fe participates in the redox reaction while Mn remains inactive. The structural changes are not completely reversible which might be one of the reasons for the capacity fading observed by electrochemical measurements.

81 Combined synchrotron X-ray and neutron imaging for the characterisation of fuel cells

Manke I, Arlt T, Haussmann J, Scholta J, Markötter H, Hilger A, Kardjilov N, Tötzke C, Wippermann, K, Lehnert W, Banhart J

Water management is a key problem in state-of-the-art hydrogen driven fuel cells. A fundamental understanding of water distribution and transport in porous carbon fiber gas diffusion layers is a prerequisite for their optimization. In this contribution, we present examples for synchrotron X-ray and neutron imaging studies that help us to understand media transport in fuel cells.

82 3D Analysis of transport structures in realistically compressed gas diffusion layers

Tötzke C,Gaiselmann G, Osenberg M, Bohner J, Arlt T, Markötter H, Hilger A, Wieder F, Kupsch A, Müller BR, Hentschel MP, Banhart J, Schmidt V, Lehnert W, Manke I

Water and media transport in gas diffusion layers (GDLs) plays a major role in the water management of fuel cells. We studied the 3D microstructure of realistically compressed GDLs by synchrotron X-ray tomography and found marked differences in the local morphology due to the channel-land pattern of the flow field. Morphologic changes occur upon compression and influence the gas and fluid flow.

83 VUV optical functions of SrTiO3 and NdGaO3 crystals determined by spectroscopic ellipsometry

Dorywalski K, Andriyevsky B, Piasecki M, Lemee N, Patryn A, Cobet C, Esser N

Complex dielectric functions were experimentally determined within the broad spectral range E = 2–25 eV and E = 2–20 eV for SrTiO3 and NdGaO3 single crystals, respectively, using synchrotron-based spectroscopic ellipsometry. The ellipsometric spectra were evaluated within a framework of optical layer model taking into account sample surface roughness and anisotropy of NdGaO3.

84 Investigation of diamond-like carbon structure using a combination of synchrotron and conventional ellipsometry and spectrophotometry

Necas D, Franta D, Ondracka P, Zajickova L, Muresan M, Perina V, Miksova R

A series of diamond-like carbon films with varying hydrogen concentration (as measured by ERDA + RBS) was prepared using PECVD. Their dielectric response was investigated in wide spectral range from 0.009 to 50 eV using a combination of synchrotron and conventional ellipsometry and spectrophotometry, utilising dielectric function models based on the Thomas–Reiche–Kuhn sum rule.

85 Spin-orbit coupling on quantum well states in noble metal films on W(110) and Mo(110) surfaces

Rusinova M, Rybkina A, Klimovskikh I, Rybkin A, Zhizhin E, Shikin A

The spin structure of quantum well states in noble metals overlayers on W(110) and Mo(110) is studied experimentally by SARPES. It was shown that spin-orbit coupling effects lead either to spin-orbit splitting of delocalized sp- states or to surface-localized spin polarization of atomic-like d-states depending on how strongly the states are influenced by the substrate.

86 Magnetocrystalline Anisotropy of X-ray Magnetic Linear Dichroism at the 3p edges of Crystalline Fe, Co, and Ni thin Films

Tesch M F, Mertins H-Ch,Legut D, Gilbert MC, Jansing C, Bürgler D E, Schneider C M, Oppeneer P M, Hamrle J, Gaupp A

We present first measurements of X-ray magnetic linear dichroism in reflection (XMLD-R) on crystalline Fe, Co and Ni thin films across the 3p edges. A strong dependence of the XMLD-R spectra on the magnetocrystalline anisotropy is observed. Theoretical spectra were calcuated for Fe and Co within the framework of the density-functional theory and agree well with the experiment.

87 Epitaxial Polymorphism of La2O3 Studied by in vivo X-ray Diffraction

Proessdorf A, Grosse F, Niehle M, Hanke M, Kaganer V, Bierwagen O, Trampert A

La2O3 is known to be stable in its hexagonal crystal structure.In this contribution we investigate the growth of thin films by molecular beam epitaxy on Si(111). The formation of a kinetically stabilized low temperature cubic phase followed by the stable hexagonal phase is detected by in situ x-ray diffraction. This transformation dynamics is discussed on the base of elastic energy considerations.

88 Structure of stimuli-responsive polymer films at variable temperature and hydrostatic pressure

Reinhardt M, Dzubiella J, Trapp M, Köhler R, Gutfreund P, Kreuzer M, Gröschel A, Müller A, Ballauff M, Steitz R

Stimuli responsive PDMAEMA brushes were analyzed with neutron reflectometry, NR, at the solid-liquid interface in the temperature range 20 to 60 °C for hydrostatic pressures from 1 to 1000 bar. A novel theoretical model of the brush density profile (structure) as a function of grafting density, temperature and hydrostatic pressure was used to fit the experimental NR data.

89 Brushes of weak Polyelectrolytes (PE): Complex interactions with Solvent and Gold Nanoparticles

Yenice Z, Genzer J, v. Klitzing R, Köhler R

Charge gradients along PDMAEMA brushes were investigated using Neutron reflectometry, to see the charge distribution along the polymer chains. The results show that stronger charged brushes appear thicker due to stronger inter- and intra-molecular electrostatic repellence. The water content in higher charged brushes is greater and we found hints of lateral molecular transport in brushes.

90 Self-aggregation of surfactants in structurally similar room-temperature ionic liquids

Klee A, Prevost S, Gradzielski M

Binary mixtures of CnmimFeCl4 (n=2,4) and CimimCl (i=14,16,18) are investigated. Due to its high light absorption, monomeric surfactant solubility and conductivity, classical methods as light scattering, surface tension, conductivity or ITC are unusable. Neutron scattering is unaffected by these particularities and hence is an irreplacable tool to get information on aggregate existence and shape.

91 Controlling vesicles' morphology and size with telechelic polymers

Malo de Molina P, Tran Dang N, Poltzer F, Prevost S, Grazielski M

Vesicles are widely used as drug delivery carriers and model systems for biological membranes. In all cases a precise control over their morphology and size is crucial. We show that the addition of telechelic polymers with two (resp. 4) sticky ends to vesicles results in small uni-(resp. multi-) lamellar vesicles, the size of which can be fine-tuned via concentration and polymer architecture.

92 The versatility of biopolyelectrolyte-surfactant complexes for microstructures formation explored by SANS

Chiappisi L, Prevost S, Gradzielski M

Mixtures of bio-derived polyelectrolytes and oppositely charged surfactants have a large potential for pharmaceutical and food-grade applications for solubilisation of water-insoluble compounds and as viscosity enhancers. By mixing chitosan with surfactants from the CiEjCOOH family, a large variety of structures can be produced, controllable via pH and by surfactant hydrophobic/hydrophilic ratio.

93 Polyglycerol surfactants: the nonionic amphiphiles from sustainable chemistry

Heunemann H, von Lospichl B, Prevost S, Gradzielski M

While nonionic surfactants are typically represented by the class of alkyloligoethoxylates, produced from the carcinogenic, mutagenic and flammable ethylene oxide, the industry starts to adopt polyglycerol surfactants whose polar headgroups are based on glycerol, the byproduct of biodiesel. We present the investigation of this recent class of nonionic surfactant, with low temperature sensitivity.

94 Control of vesicles' morphology and size via telechelic polymers

Malo de Molina P, Tran Dang N, Poltzer F, Prevost S, Gradzielski M

Vesicles are widely used as drug delivery carriers and model systems for biological membranes. In all cases a precise control over their morphology and size is crucial. We show that the addition of telechelic polymers with two (resp. 4) sticky ends to vesicles results in small uni-(resp. multi-) lamellar vesicles, the size of which can be fine-tuned via concentration and polymer architecture.

95 The self-assembly of inorganic ions: theta-amphiphiles as a new class of surfactants

Bauduin P, Prevost S, Brusselle D, Farras P, Teixidor F, Diat O, Zemb T

The sandwich ion COSAN, with Cobalt (III) trapped between two hydrophobic boron-based cages (dicarbollides), is a rigid molecule, the acidic form of which unexpectedly exhibits self-aggregation in water, forming small micelles and large vesicles in equilibrium with monomers. The driving force is believed to be molecular forces, the missing piece among our understanding of colloidal forces.

96 The Influence of the Relative Humidity on the Internal Structure of Polyelectrolyte Multilayers

Zerball M, Köhler R, v. Klitzing R

The swelling behavior of 2-Block Polyelectrolyte Multilayers (one protonated and one deuterated block) in water vapours was investigated by Neutron Reflectometry. The Block-Structure creates an additional interface inside the film, serving as an extra structural unit for neutrons. This way, the swelling of the inner and the outer part of the PEMs and variations of the inner structure can be tested

99 Gold nanoparticles on oxygen-free support in CO oxidation

Klyushin A, Rocha T, Hävecker M, Knop-Gericke A, Schlögl R

The active sites on Au catalysts are still not comprehensively understood and the field remains controversial. In-situ NAP-XPS measurements of electronic structure of Au nanoparticles on oxygen-free support was made during CO oxidation. Untreated samples were totally inactive, but after the O3 treatment the samples showed high reactivity, however the active site was O-functionalized carbon.

100 Strong Metal Support Interactions (SMSI) studied by XPS on Pd/FeOx and Pd/ZnO

Kast P, Friedrich M, Teschner D, Behrens M, Schlögl R

Pd/FeOx and Pd/ZnO present a special class of catalysts due to the reducibility of their supports. Hydrogen treatment can lead to partial reduction of the oxides, resulting in overgrowth of the Pd particles. CO oxidation as model reaction identified the reversibility of the respective catalyst states. Electronic modification of Pd and quantification of its content was investigated by in situ XPS.

103 Photooxidation of Graphene: Adsorption and Dissociation of NO2 on Graphene/Ir(111)

Böttcher S, Vita H, Horn K

We report the formation of graphene oxide (GrO) by adsorption and photon induced dissociation of NO2 on graphene/Ir(111) at 100K. GrO is measured with Auger yield NEXAFS as well as core level XPS. Two modifications exist, consisting of different oxide species, depending on the photon flux. Graphene is recovered upon annealing to 500°C. This chemical oxidation method is simple and non destructive.

104 Electronic structure of graphene on pseudomorphic Cu/Ir(111)

Vita H, Böttcher S, Horn K, Voloshina E N,, Kampen T, Thissen A, Dedkov Y S

The crystallographic and electronic structures of graphene on Cu/Ir(111) was studied by means of STM/AFM and photoelectron spectroscopy (XPS/ARPES) in combination with DFT calculations. These results permit an understanding of the mechanisms that determine the interface properties of graphene/metal systems and allow to discriminate between different contributions in the bonding in these systems.

105 Adsorbate and Substitutional Doping of Epitaxial Graphene on SiC(0001) and Ni(111)

Wanke M, Raidel C, Koch R, Tadich A, Edmonds M, Fromm F, Smets Y, Mazej Z, Ley L, Pakes C, Gebhard J, Zhao W, Höfert O, Gotterbarm K, Mammadov S, Papp C, Görling A, Steinrück H-P, Seyller T

The doping of epitaxial graphene on SiC and on Ni surface were studied using ARPES and XPS at BESSY with various experimental methods in addition. During growth on SiC ammonia was used to incorporate nitrogen into graphene, while on Ni(111) only one precursor each, for boron and nitrogen doping was used. Adsorbate doping could be achieved by the use of fluorinated fullerenes on monolayer graphene.

106 Electronic and magnetic properties of cobalt intercalated in graphene on Ir(111)

Vita H, Böttcher S, Horn K

Graphene on ferromagnetic substrates such as Ni(111) and Co(0001) can act as a spin filter [1]. Here we present the interaction of ferromagnetic Co sandwiched between Ir(111) and graphene with consequences for the expected magnetic properties. We find a transfer of magnetic moment from the Co film onto the grapheme layer beyond a Co thickness of 2ML. [1] Karpan et al. Phys. Rev. B 78 (2008)

107 XMCD studies on indicator layer to see current density of YBCO in SC state

Audehm P, Stahl C, Schmidt M, Albrecht J, Schütz G, Goering E

We want to quantitatively monitor the internal current density of a YBCO thin film high-TC-superconductor (SC) via the corresponding magnetic stray field. The magnetic stray field is large enough to influence the CoFeB therefore serving as a probe for the local field strength. Reflectometry-setups like our setup “ERNSt” have the advantage of a variable orientation of the magnetic field.

115 Band-bending in organic semiconductors: the role of alkali-halide interlayers

Wang H, Amsalem P, Heimel G, Salzmann I, Koch N, Oehzelt M

Band-bending in organic semiconductors, occurring at metal/alkali-halide cathodes in organic-electronic devices, is experimentally revealed and electrostatically modeled. Metal-to-organic charge transfer through the insulator, is identified as the origin of the observed band-bending, which is in contrast to the localized interface dipole occurring without the insulating buffer layer.

116 Influence of graphene interlayers on the interaction between cobalt phthalocyanine and Ni(111)

Uihlein J, Adler H, Polek M, Glaser M, Ovsyannikov R, Bauer M, Chasse T, Peisert H

The influence of graphene interlayers on electronic interface properties of cobalt phthalocyanine (CoPc) on Ni(111) is studied using both photoemission (XPS) and X-ray absorption spectroscopy (XAS). It is shown that a graphene buffer layer cannot prevent charge transfer processes at the interface to Ni(111), however, the detailed electronic configuration is different.

117 Doping of C60 (sub)monolayers by Fermi-level pinning induced electron transfer

Niederhausen J, Amsalem P, Wilke A, Heimel G, Winkler S, Schlesinger R, Vollmer A, Rabe JP, Koch N

Fermi-level pinning of C60 (sub)-monolayers on thin films of sexithiophene (6T) grown on Ag(111) is shown to induce electron transfer from the metal to a fraction of the C60 molecules. The charge transfer causes a potential drop within the 6T interlayer and dipole-dipole repulsion, leading to a disproportionation into coexisting neutral and charged C60 molecules.

118 Synchrotron based analysis on the formation of the Cu(In,Ga)Se2/CdS and Cu(In,Ga)Se2/ZnS interface using soft x-ray photoemission spectroscopy (SXPS) and near edge x-ray absorption fine structure spectroscopy (NEXAFS).

Ümsür B, Calvet W, Steigert A, Höpfner B, Lauermann I, Lux-Steiner M Ch

We have investigated Cu(In,Ga)Se_2 absorbers which were initially covered by thin films of CdS and ZnS as buffer layers. In order to study the relevant interface region the thin films have been removed again by etching in diluted HCl prior to the investigation using SXPS and NEXAFS at the SURICAT and the HIKE end stations at Bessy II. Only marginal traces of Zn and Cd were found in the nearest surface region of the absorber. However, it seems that there is more Cd in the absorber than Zn.

119 Nonmagnetic linear dichroism in fluorescence spectra from a cubic solid

Thielemann-Kühn N, Haverkort M W, Miedema P S, Alonso Calafell I, Trabant C, Gorgoi M, Föhlisch A, Schüssler-Langeheine C

Fluorescence yield spectra from solids contain different information than X-ray absorption spectra because the involved twofold dipole transitions and the experimental geometry lead to additional selection rules. Even in high-symmetry crystals like rock salt NiO we observed additional nonmagnetic linear dichroism in the fluorescence yield which is absent in the X-ray absorption spectrum.

120 A study of the polarization anisotropy in resonant inelastic soft X-ray emission from liquid acetonitrile

Kooser K, Käämbre T, Quevedo W, Kunnus K, Wernet Ph

We studied the valence electronic structure of liquid acetonitrile using N 1s RIXS (from microjet) with detection at parallel or perpendicular to the incident linear polarization. We observe anisotropy of both intensity and spectral shape of the valence spectrum (at level with gaseous acetonitrile), and a relative intensity anisotropy of the vibronic energy loss features.

121 At the interface between organic radicals and TiO2(110) single crystals: electronic structure and paramagnetic character

Kakavandi R, Savu S.-A, Caneschi A, Chasse T, Casu M B

Organic radicals are metal-free molecules with at least one unpaired electron that originates a magnetic moment. We find that in a pyrene derivative of the nitronyl nitroxide radical deposited on rutile TiO2(110) the molecules keep/lose their paramagnetic character depending on the local substrate hydroxylation. The first molecular layer act as a “buffer” on which to grow intact organic magnets.

121a XMCD study of the magnetism of size-selected free cobalt oxide clusters

Lawicki A, Krach P, Langbehn B, Langenberg A, Hirsch K, Zamudio-Bayer V, Terasaki A, Möller T, Issendorff B v, Lau JT

Magnetic spin and orbital moments of size-selected free cobalt oxide cluster ions with stoichiometry of CoxOy+ (x=2-6, y=2-8) have been determined via XMCD spectroscopy. In the case of two cobalt oxides (Co2O2+, Co3O3+) high magnetic spin moments have been measured. All the others exhibit only weak magnetic moments. The magnetic moments seem to scale with the formal oxidation states of clusters.

122 The New XUV Optics Beamline at BESSY II

Schäfers F, Sokolov AA, Senf F, Mast M, Schmidt J-S, Eggenstein F, Siewert F, Erko A

Presently a new Optics Beamline equipped with a versatile 9-axes UHV-Reflectometer is set into operation at BESSY-II. This setup is dedicated to at-wavelength characterization and calibration of large-scale precision gratings, mirrors, multilayered systems and novel nano-optical devices. The beamline operates in the UV- and XUV-range with very high spectral purity and will be operational in 2014.

123 Monochromatization of femtosecond XUV light pulses with the use of reflection zone plates

Metje J, Borgwardt M, Moguilevski A, Kothe A, Engel N, Wilke M, Al-Obaidi R, Tolksdorf D, Firsov A, Brzhezinskaya M, Erko A, Aziz E F

We present the first study of the temporal performance of reflection zone plates used for monochromatization of XUV light. The pulses were generated in our newly built laser-based tabletop setup that employs high-order harmonic generation (HHG). By using laser pulses of 25 fs length to pump the HHG process, a pulse duration of 45 fs for monochromatized XUV light was achieved.

124 Innovative Diffractive Optics for 4th Generation Synchrotron Radiation Sources (FELs and ERLs)

Brzhezinskaya M, Firsov A, Erko A

The diffraction optics based on total external reflection gives the unique possibility for spectroscopy and monochromator design in application to 4th generation synchrotron radiation sources with high power density such as FELs and ERLs. We focus on the elaboration of new approaches for design and fabrication of focusing elements working in the entire energy range, from THz up to hard X-rays.

125 Imaging spin detector for electron spectroscopy

Johansson M, Funneman D, Bahr S, Kampen T, Schaff O

The design and first results of a new imaging spin-detector with rotator in combination with a PHOIBOS 150 analyzer are presented. By detection principle spin filtered images of the analyzer exit plane can be obtained. A patented magnetic rotator lens mounted between the analyzer exit and the scattering crystal enables for rotation of the transversal component of the polarization vector.

126 Novel Developments in Near Ambient Pressure XPS – the route towards standard analysis tools in synchrotron and laboratory environments

Thissen A, Bahr S, Kampen T, Maehl S, Schaff O

Nowadays advanced materials analysis means Photoelectron Spectroscopy in extreme environments like elevated pressures or electrochemical cells. Thus, in operando analysis of devices can be realized. NAP-XPS is already used at synchrotrons with growing success. Attempts are made to develop this to a user-friendly standard analysis tool at synchrotrons and in laboratory environments.

127 UNIFIT 2014 - the new spectrum processing, analysis and presentation software for XPS and XAS

Hesse R, Denecke, R

Main focus of the advancement to UNIFIT 2014 was in the realization of a dynamical memory management for the reduction of the necessary main memory using the software UNIFIT. As the result of the software optimization the used main memory can be reduced up to 100-fold and therefore the number of simultaneously processable spectra could be increased from 300 to 1200.

128 VEKMAG - a vector magnet for BESSY II

Ryll H, Radu F, Back C, Kuch W, Tennant A, Zabel H

VEKMAG is a Vector Superconducting Magnet station, which will be installed at the dipol beamline PM2 at BESSY II. It is designed for XAS/XMCD measurements and for resonant and-off resonant soft X-ray scattering methods, in a temperature range of <2K-500K. It will provide a 9T field in the beam direction, a 2T field in the horizontal plane and a 1T field in the perpendicular direction.

129 High Precision Temperature Regulation for Neutron Scattering Experiments

Klemke B, Sokolowski A, Willenberg B, Ryll H, Gerischer S, Grimm N, Goerigk G, Wallacher D, Kiefer K

Some neutron scattering experiments need very accurate temperature regulation-especially if temperature dependencies near phase transitions are investigated. However, standard sample environment (SE) equipment doesn't meet these requirements. Therefore at the HZB we developed a range of special SE equipment with high precision temperature regulation from room temperature to the Millikelvin range.

130 Flat-Cone Diffractometer E2: 3D diffuse scattering - the ultimate tool for complex structure solution

Hoffmann J-U, Glavatskyi I

The Flat-Cone E2 is a medium resolution single crystal and powder diffractometer with wide sample environment possibilities to study the complicated distributions of superstructure reflections and diffuse scattering arising from structural and magnetic disorder in 3D reciprocal space, which can be scanned in few steps by combining the "off-plane Bragg-scattering" and the Flat-cone layer concept.

131 Comparison of CD measurements by EUV-Scatterometry and CD-AFM

Laubis Ch, Haase A, Soltwisch V, Dai G, Henn MA, Gross H, Scholze F

Reconstructed geometry profile parameters on an EUV test mask like CD or sidewall angle (SWA) as derived from EUV scatterometry are compared to the results of a fully traceable CD-AFM at PTB. The comparison yields a linear relation within a spread of about 1 nm and an offset of the absolute values below 3 nm. The variation of the SWA can be traced to real variations of the SWA as measured by AFM.

132 The new XPP/KMC3-Beamline at BESSY II

Gaal P, Sander M, Leitenberger W, Bargheer M

We present properties and prospects of the new XPP/KMC3-Beamline for pico second resolution "laser-pump X-ray probe" experiments. In first measurement the new beamline optics was characterized. In addition we present plans for an in-vacuum diffractometer for low temperature diffraction experiments and an experimental endstation for EXAFS in the energy range of 2- 16 keV.

133 Sample Environment Advancements at BESSY

Wallacher D, Grimm N, Gerischer S, Kiefer K

In the last years we made some efforts to provide SE for XRD, SAXS and EXAFS studies at BESSY-II. With TU-Dresden and MPI-Golm gas loading setups were designed for in-situ investigations on nanostructured materials, which request precise gas dosing at low Temperature. If no commercial solutions are available, tailored tools were built, i.e. a cryogenic sample changer or a set-up for microfluidics.

134 A Ruler for the Nanoworld: EUV and Gisaxs Scatterometry

Soltwisch V, Wernecke J, Haase A, Laubis C, Krumrey M, Scholze F

The continuous shrinking in feature size of integrated circuits in the semiconductor industry is a huge technical challenge. Angle resolved scatterometry is based on the analysis of light scattered from a periodic structure. We show first results of preliminary GISAXS and FEM studies of the reconstruction of a silicon grating with a nominal critical dimension of 50 nm.

135 Characterisation of diffraction gratings by EUV scatterometry and GISAXS

Scholze F, Soltwisch Victor , Wernecke J, Krumrey M

EUV scatterometry and GISAXS are used for the characterization of commercial gratings and gratings from Fraunhofer IOF with laminar or blazed structure. Although the diffraction efficiency of all gratings is comparable, the diffuse scatter background in-between the diffraction orders differs by orders of magnitude. The determination of duty cycle and blaze angle by GISAXS is demonstrated.

136 Diffuse EUV Scattering from Rough Multilayer Mirrors

Haase A, Soltwisch V, Laubis Ch, Scholze F

We present the characterization of high-quality Mo/Si multilayer mirrors with reflectivities well above 60% with respect to to interface roughness using diffuse EUV scattering. Two dimensional off-specular reciprocal space maps serve to extract the average power spectral density considering dynamic effects. Our theoretical analysis is based on the fully dynamic distorted wave Born approximation.

137 The in-vacuum PILATUS 1M detector: Characterisation and Applications

Wernecke J, Müller P, Gollwitzer C, Soltwisch V, Scholze F, Krumrey M

A PILATUS 1M detector for windowless in vacuum operation was developed by PTB and Dectris Ltd. and is now routinely used at the FCM beamline of PTB. The measured quantum efficiency,in particular below 5 keV,is sufficient for small-angle X-ray scattering (SAXS,GISAXS) down to 1.7 keV. This gives access to low q-values and anomalous scatting of important elements like Si, P, S, Cl (examples shown).

138 A Ruler for the Nanoworld: SAXS on nanoparticle suspensions

Gollwitzer C, García-Diez R, Krumrey M

Accurate length measurements are difficult for objects in the nanometre size range (1 nm to 100 nm). Small-angle X-ray scattering (SAXS) using X-rays with a wavelength below 1 nm is suitable to determine the size and size distribution of nanoparticles in suspension. SAXS is used at the four-crystal monochromator beamline of PTB in a number of projects of the European Metrology Research Programme.

139 **A Ruler for the Nanoworld: Small-angle X-ray scattering on nanostructured polymer thin films**

Wernecke J, Okuda H, Wang C, Krumrey M

Grazing-incidence small-angle X-ray scattering is a very powerful tool to characterise nm-sized structures on and beneath surfaces. The setup and unique capabilities for (GI)SAXS at the FCM beamline are highlighted along with examples of advanced anomalous scattering techniques on polymer thin films such as ASAXS at the sulfur K-edge and scattering contrast matching GISAXS at the silicon K-edge.

140 Experimental station for complementary X-ray analytics of nanoscaled materials allowing for geometries from total reflection to normal incidence

Lubeck J, Beckhoff B, Fliegauf R, Holfelder I, Weser J

The 9-axis manipulator of the experimental station allows for a flexible beam geometry and reproducible sample alignment. The unique design enables measurements for determining layer thicknesses and elemental or spatial compositions, elemental depth profiles, chemical bonding states as well as the molecular orientation of bonds by means of X-ray spectrometry combined with X-ray reflectometry.

141 SIMS correction and depth profiling of ion implantations using Grazing Incidence XRF

Hönicke P, Beckhoff B, Kayser Y, Kayser S

An X-ray based depth profiling method using Grazing Incidence X-Ray Fluorescence analysis was adapted to shallow ion implantations into silicon and other semiconductors. The determined profiles are in good agreement with complementary results. Additionally, the method was used to derive corrections for SIMS, which can suffer from various effects leading to artefacts in the depth profiles.

142 Reference-free Quantification of elemental depth gradients in Cu(In,Ga)Se2 absorbers by grazing incidence X-ray fluorescence analysis

Streeck C, Pollakowski B, Herzog C, Lubeck J , Gerlach M, Hönicke P, Unterumsberger R, Brunken S, Beckhoff B, Kanngiesser B, Schock H-W, Mainz R

To determine both the absolute composition and the in-depth gradient in Cu(In,Ga)Se2 thin films calibrated instrumentation qualifies non-destructive methods such as grazing incidence x-ray fluorescence analysis to address this analytical challenge. Varying the angle of incidence over a broad range provides quantitative access to the elemental in-depth distributions of interest.

145 Structural characterization of P1’-diversified urea-based inhibitors of glutamate carboxypeptidase II

Pavlicek J, Ptacek J, Cerny J, Byun Y, Skultetyova L, Pomper M, Lubkowski J, Barinka C

We characterize six complexes between GCPII and P1’-diversified urea-based inhibitors that have the C-terminal glutamate replaced by a more hydrophobic moiety. Our results provide the description of interactions governing the recognition of non-glutamate residues in the P1’ pocket of the enzyme. Presented data can be used for the design of glutamate-free GCPII inhibitors with modified properties.

146 Automatic data processing using XDSAPP v1.0

Sparta K, Müller U, Weiss M, Heinemann U

XDSAPP is an expert python-based user interface for the fast processing of X-ray diffraction images from single crystals with XDS. Additional software like SFCHECK, Pointless, XDSSTAT and phenix.xtriage are used for automatic decision making. We present the latest developments and features of the soon to be released version 1.0 of XDSAPP.

147 A Microspectrophotometer for BL14.2

Röwer M, Steffien M, Förster R, Scheerer P, Müller U, Weiss M S

In 2014 the HZB-MX experimental end station BL14.2 will receive a major upgrade. The poster shows the new nano-diffractometer with configuration of devices around the sample position. This includes the option for UV/vis absorption spectrometry. The new spectrometer will be available directly at the beamline or in a dedicated 'Spectro-Lab' room.

148 Crystallographic validation of a small fragment library on endothiapepsin

Heine A, Radeva N, Park A, Köster H, Craan T, Krug M, Ühlein M, Weiss M,Sparta K, Müller U, Klebe G

Fragment-based approaches have become increasingly popular for lead development in pharmaceutical drug research. Here, a small nonrule of 3 compatible fragment library consisting of 364 compounds was designed and validated using endothiapepsin as model protease. A high hit rate was observed when we started a crystallographic screening of the entire library showing different fragment binding modes.

149 Unique rearrangement of human muscle fructose-1,6-bisphosphatase tertiary structure

Barciszewski J, Kolodziejczyk R, Rakus D, Dzugaj A, Jaskolski M

Fructose-1,6-bisphosphatase catalyzes an irreversible hydrolysis reaction of fructose-1,6-bisphosphate. It is the regulatory enzyme of glyconeogenesis. FBPase activity is modulated allosterically by low molecular-weight inhibitor AMP. We have crystallized human muscle FBPase in active and inactive states. Comparison of these two structures let us to propose the mechanism of enzyme inhibition.

150 ProMs in tune: inhibiting proline rich motif-mediated protein-protein interactions - application to EVH1 domains of Ena/VASP proteins

Barone M, Roske Y, Opitz R, Müller M, Reuter C, Soicke A, Piotukh K, Huy P, Beyermann M, Schmieder P, Oschkinat H, Schmalz HG, Kühne R

VASP and zyxin are associated with stress fibers as well as with focal adhesions. Zyxin recruits Ena/VASP- family members via its FPPPP motifs by EVH1 domains. Here we present novel small-molecule fragments for replacing protein segments adopting a polyprolin helix to address protein-protein interactions. X-ray data demonstrate that the new EVH1 inhibitors occupy the canonical binding site.

151 A guide to data collection using the beamline 14.1 Pilatus 6M detector

Bommer M, Dobbek H, Weiss MS, Müller, U

While the introduction of the Pilatus 6M detector has brought automatic benefits, a few changes in data collection strategy maximise its potential. Fine phi slicing and high multiplicity benefit the isolation of anomalous scatterers, SAD phasing and high resolution data collection. We also explain Rmerge, Rsym, Rmeas, Rrim, Rpim, I/sig(I), CC½.

152 Is detergent a factor in the drastic change in photosystem II crystal packing upon dehydration

Bommer M, Hellmich J, Ibrahim M, Kern J, Burkhardt A, Meents A, Zouni A, Dobbek H

As is the case for many complex biological membrane proteins, photosystem II crystals, while often simple to obtain, present a nightmare in optimisation. In an attempt to produce consistently highly diffracting crystals, we explore the interplay of detergent and dehydration leading to an increase in resolution from 6 to 2.9 Å based on an internal rearrangement to a Type I like crystal packing.

154 Electronic Properties of Clathrate Compounds in the Sn-In-As-I System

Neudachina VS, Sirotina AP, Volykhov AA, Kataev EY, Senkovsky B, Shevelkov AV, Yashina LV

Current interest to clathrate compounds is attributed to their prospective thermoelectric properties. We report electronic properties and chemical bonding of the Sn24–x–δInxAs22–yI8 clathrates probed by valence-band and core-level photoemission as compared to DFT modeling.

155 Direct evidence of the zero surface reactivity of Li-air battery discharge products (Li2O2 and Li2O) towards grapheme

Kataev E, Itkis D, Verbitskiy N, Fedorov A, Tsukanova D, Neudachina V, Senkovsky B, Grueneis A, Vyalikh D, Yashina L

We examine surface chemistry of lithiated carbon nanowalls and graphene/Ni using in situ XPS during oxygen exposure up to 256 L and annealing up to 550 °C. We observed delithiation of the CNW/graphene and formation of the Li2O2 on carbon surface with increasing of oxygen dosage and Li2O2 decomposition to Li2O after annealing. No chemical reaction between lithium peroxide and carbon was observed.

156 Anisotropy in the X-ray absorption of room-temperature fluorinated graphite C2F

Asanov I, Vyalikh D, Bulusheva L

The NEXAFS CK- and FK-edge spectra measured at different incidence angles of radiation beam showed that room-temperature produced semifluorinated graphite is highly anisotropic material, where the fluorine atoms are subsequently attached to both sides of a graphene sheet forming the covalent bonds with carbon atoms. More probable fluorine pattern was determined for quantum-chemical modeling.

157 Chemistry in Metal-Protein Systems under Vacuum

Makarova AA, Neudachina VS, Grachova EV, Yashina LV, Blüher A, Mertig M, Molodtsov SL, Laubschat C, Vyalikh DV

In recent years an increasing interest in the design of bio-metal hybrid structures and their application in electronics and robotics has lead to a need of understanding of the mechanisms involved in chemical interaction between metals and biosystems under vacuum. Herein by means of photoelectron spectroscopy we characterize interaction between protein and technologically essential metals (Cu,Fe).

158 NEXAFS study of Ca-based biominerals of Antarctic ice fishes.

Petrova O,Sivkov V, Nekipelov S, Vialykh D, Molodtsov S, Ehrich H

Using NEXAFS – spectroscopy the atomic, chemical and mineral composition of ice fish bones, scales, teeth and otoliths as well as some Сa-based minerals was investigated.

159 Manipulating the Electronic Properties of Manganese Phthalocyanine Thin Films by Potassium Intercalation

Haidu F, Smykalla L, Salvan G, Knupfer M, Hietschold M, and Zahn D R T

MnPc is a promising candidate for future spintronic devices due to its high spin state of S=3/2. We investigated the changes of the electronic properties of K intercalated MnPc by UPS, XPS, IPS, and NEXAFS. According to the Mn L edge branching ratio the spin state of S=5/2 could be achieved. From the UP and IP spectra the evolution of the transport band gap was revealed.

160 Electronic properties of Al and Ag nanoparticles embedded into organic matrix.

Babenkov S, Molodtsova O, Aristova I, Aristov V

We present study of metal nanoparticles embedded into organic matrix of fluorinated copper phthalocyanines (CuPCF4). The evolution of morphology and electronic properties as a function of nominal silver and aluminum content were studied by x-ray photoelectron spectroscopy at RGBL on BESSY II.

161 High Definition and Synchrotron Radiation Based IR-Microspectroscopy Approach to Reveal Kidney Stones History

Blanco F, Ortiz-Alías P, Valiente M, López-Mesas M

The heterogeneous group of compounds that form kidney stones leaves a particular distribution which depends on the metabolic disturbances experienced by the patient. In this work,IR microspectroscopy has been used for a complete characterization of some stone samples. This technique has made available novel information,which allows a better assessment for tracking kidney stone formation history.

162 Application of Hyper Spectral Imaging and Synchrotron IR Microscopy for the characterization of functional materials with application in odontology.

Kotkowska O, Ortiz Alías P, Lumbreras F , Serranti S, Bonifazi G, Valiente M

In order to understand better the process of remineralization/demineralization that takes place in the interface saliva/enamel Hyper Spectral Imaging (HSI) and Synchrotron IR microscopy have been applied. The distribution maps were obtained by applying HSI methods, detailed study of different forms of apatite were performed by IR Miscroscopy with synchrotron source of light

163 High flux cluster deposition setup with atomic size resolution

Picot T, Hillion A, Houben K, Couet S, Temst K, Vantomme A, Van Bael MJ, Janssens E, Lievens P

We present a magnetron sputtering cluster source allowing to produce clusters with a size ranging from a diameter of several nanometers down to a few atoms with an ultimate size resolution. Several techniques based on synchrotron radiation such as far-infrared spectroscopy and X-Ray Magnetic Circular Dichroism are discussed to investigate superconducting and magnetic properties of small clusters.

165 Synchrotron X-ray and neutron imaging in DMFC research

Arlt T, Wippermann K, Schröder A, Markötter H, Kardjilov N, Hilger A, Tötzke C, Banhart J, Manke I

Fuel cells are expected to contribute to a sustainable energy supply in future. Direct-methanol fuel cells are promising candidates for several mobile applications. Catalyst layers and gas diffusion layers are objects of current energy research at the Helmholtz-Zentrum Berlin. Complimentary ex-situ and in-operando experiments have been performed at the experimental stations CONRAD 2 and BAMline.

166 Direct X-Ray Refraction of Micro Structures

Kupsch A, Lange A, Hentschel MP, Bruno G, Müller BR

For the purpose of X-ray optical analysis by scanning micro structured samples, refracted 30 keV X-rays are imaged on a 2D detector in presence of a 50 µm primary beam. At 3” angular resolution fibres, capillaries and monospheres reveal deflection according to geometrical optics (100% cross section) and up to 20-fold beam broadening. Diffraction fringes of nanoparticles are detected simultaneously

167 Structure and Local Toughening Effects in Zirconia Ceramics – What can be seen in Synchrotron Light?

Zehbe R, Mochales Palau C, Zaslansky P, Müller WD, Fleck C

Tooth dentine features a distinct hierarchical structure and composition, which are well adapted to absorb mechanical loads. This natural template serves as model for zirconia-based materials, containing hierarchical features determined important for improving toughness. Synchrotron µCT allows imaging these materials, although challenges remain open for these highly absorbing structures.

168 µ-SRXRF characterization of Brazilian emeralds

Curado J, Radtke M, Buzanich G, Reinholz U, Riesemeier H, Guttler R, Rizzutto M

Emerald is one of the most important precious stone and the identification and quantification of elements as Cr, Fe and V allows the determination of their region of provenance and veracity.The aim of the present study is characterize emeralds from different mines of Brazil by using µ-SRXRF, identifying the fingerprint according to the provenance of the material.

169 Slicing – A New Method For Non Destructive 3D Elemental Sensitive Characterization Of Materials

Radtke M, Buzanich G, Curado J, Reinholz U, Reisemeier H, Scharf O

The non-destructive three-dimensional elemental sensitive characterization of samples is still a challenge. Using the Color X-Ray Camera allows real 3D measurements on larger objects for the first time. Therefore the sample is excited with a sheet beam and moved stepwise to get the element distribution per layer with one measurement. This layers can be combined to a full 3D image afterwards.

170 Non-Sexual Abdominal Appendages in Adult Insects Challenge a 300 Million Year Old Bauplan

Hoch H, Wessel A, Asche M, Baum D, Beckmann F, Bräunig P, Ehrig K, Mühlethaler R, Riesemeier H, Staude A, Stelbrink B, Wachmann E, Weintraub P, Wipfler B, Wolff C, Zilch M

The bauplan of adult winged insects is conserved since more than 300 Mya. Our discovery of an exception in planthoppers disprove two long-held paradigms and reveals the hidden potential of the ancient genetic and developmental tool-kits. The lateral appendage bears highly organized sensory and secretory units and is probably an enemy-detection device against small predators.

171 Evaluation of total reflection x-ray fluorescence (txrf) analysis using a color x-ray camera (cxc)

Fittschen UEA, Menzel M, Scharf O, Radtke M, Reinholz U, Buzanich G, Montoya V, McIntosh K, Horntrich C, Streli C, Havrilla G J

Shading in TXRF was evaluated directly using a CXC available at Bamline. The device allows monitoring the illuminated and shaded parts of the sample at the same time. Arrays composed of 8x8 uniform Ni pL-droplet residues were analyzed “edge on” and “side on”. A decline of 40% fluorescence intensity between the first and the last deposit printed in one row was found only for “side on” illumination.

172 Absorption of the primary beam in sr-txrf analysis: experimental visualization using a color x-ray camera (cxc)

Menzel M, Fittschen UEA, Scharf O, Radtke M, Reinholz U

In this work µL-droplets containing different elements were analyzed by SR-TXRF combined with a CXC. This analytical technique allows localizing of the absorption effects directly. The absorption of the incoming beam by the sample material “up stream” and shading of specimen located “down stream” can be determined and compared to model calculations. This cannot be achieved by scanning µ-XRF.

173 Characterization and application of HAPG mosaic crystals in high-resolution X-ray spectroscopy with synchrotron radiation

Gerlach M, Anklamm L, Antonov A, Beckhoff B, Grigorieva I, Holfelder I, Kanngiesser B, Legall H, Malzer W, Schlesiger C

HAPG is a novel type of mosaic crystal with a high integral reflectivity and a very low mosaicity. In a joint research project of PTB, TUB and the manufacturer Optigraph its diffraction properties were investigated. A wavelength-dispersive spectrometer based on HAPG crystals was set-up at the laboratory of PTB and first high-resolution X-ray spectroscopy experiments were carried out successfully.

174 Properties of the inner structure of ammonium nitrate prills

Staude A, Ehrig K, Krebs H

We report on Computed Tomography (CT) measurements of an ammonium nitrate prill. These prills are the essential part of modern explosives for mining and civil construction. Certain properties of the inner structure of the prills determine the quality of the explosive. In our measurements these properties could easily be measured.

175 Synchrotron x-ray imaging for characterization of fuel cell components

Markötter H, Haussmann J, Klages M, Seidenberger K, Wilhelm F, Arlt T, Manke I, Scholta J, Banhart J

The water distribution and evolution in a PEM fuel cell was studied via synchrotron imaging. The method development towards fuel cell research is presented in this poster. Water quantification and the identification of liquid water transport paths were conducted using radiography and tomography. Additionally the role of cracks in the microporous layer is demonstrated.

176 Pore Structure Analysis of Cordierite Diesel Particulate Filter Materials

Bruno G, Lange A, Hentschel MP, Onel Y, Wolk T, Staude A, Ehrig K, Müller BR, Kupsch A

Laboratory and Synchrotron X-ray refraction techniques, computed tomography, Fast Fourier Transform, and a new statistical approach (DIVA) reveal porosity and pore orientation of honeycomb cordierite ceramics for diesel particulate filter applications. The bi-continuous microstructure of such materials governs their excellent thermal shock resistance and thermal expansion anisotropy.

177 Electrolyte distribution and discharge time – a combined study of X-ray tomography and electrical measurements of a commercially available lithium-ion capacitor

Wieder F, Kallfass Ch, Manke I, Hilger A, Tötzke C, Hoch C, Schier H, Graf K, Banhart J

A lithium-ion capacitor (LIC) was studied during a charge/discharge procedure. Changes in the interior structure were investigated by means of X-ray tomography during electrical cycling of the LIC. With increasing number of cycles we found electrolyte accumulating at the bottom of the capacitor. A correlation between electrolyte distribution at the bottom and performance of the LIC was determined.

178 A NEXAFS and XPS study of the controlled Layer-by-Layer Self Assembly of organic Tetralactam Macrocycles based on Coordination Chemistry

Darlatt E, Traulsen C H-H, Richter S, Poppenberg J, Heinrich T, Schalley C A, Unger W E S

Organic macrocycles are useful building blocks for molecular machines. In our study a multilayer stack of tetralactam macrocycles was assembled stepwise under exploitation of coordination chemistry. Evidence for complex formation, for the presence of aromatic and amide groups and for preferential orientation of macrocycles was achieved by XPS and NEXAFS. Layer thicknesses were estimated by XPS.

179 XPS and NEXAFS studies of epoxy surfaces

Nietzold C, Dietrich PM, Ivanov-Pankov S, Weigel W, Unger WES

Epoxy-terminated silicon oxide surfaces were derivatized to determine the amount of reactive epoxy surfaces functionalities. Surface chemical analysis was performed using photoelectron and NEXAFS spectroscopy at the HE-SGM beamline. Furthermore carbohydrates with amine functionalities were immobilized on these epoxy-modified silicon surfaces.

180 Pentacene on Epitaxial Graphene: XPS and NEXAFS Investigations

Nefedov A, Zhang W, Sezen H, Fedorov A, Verbitskiy N, Grüneis A, Wöll C.

In this study the adsorption of pentacene on a single layer of graphene grown epitaxially on Ni(111) has been investigated by means of near-edge X-ray absorption fine structure (NEXAFS) spectroscopy and X-ray photoelectron spectroscopy (XPS) at room temperature. It was found that pentacene molecules demonstrate a dependence of their orientation on the coverage.

181 Theoretical NEXAFS investigation of structural defects in graphene: A density functional theory study

Ehlert Ch, Unger WES, Saalfrank P

Lippitz et al. used a bromine plasma to treat and modify the surface of highly oriented pyrolytic graphite (HOPG). The NEXAFS spectra show unknown resonances between 286 eV and 291 eV. We show, using DFT, that defects can explain these new features in this energy region.

182 Investigation of the Surface Structure of Ionic Liquids by ERXPS and NEXAFS

Holzweber M, Lippitz A,Unger WES

The liquid surface structure and the orientation respectively of ionic liquids at the liquid-vacuum interface were investigated in dependence of the side chain length. Therefore energy resolved XPS (ERXPS) depth profiling and NEXAFS was used. The sample system consisted of the ionic liquids 1-butyl-3-methyimidazolium and 1-hexyl-3-methylimidazolium N,N-bis(trifluoromethylsulfonyl)imide (NTf2).

183 Synchrotron-Radiation XPS Study of Nitrogen-containing Films on Silicon: Amino- vs. Amidosilanes

Dietrich PM, Glamsch S, Gross T, Lippitz A, Unger WES

Films made from two benzamidosilanes were studied using combined variable X-ray energy / angle-resolved XPS at the HE-SGM beamline. Thereby a sub-surface chemical characterization and non-destructive chemical depth profiling of the very thin organic layers was achieved. Silane-related silicon species at the silicon oxide-silane interface could be specified and quantified as silane molecules/nm².

114h Chemical bonding of porous SiO2-based low-k dielectrics

Konashuk AS, Konyushenko MA, Sokolov AA, Schaefers F, Filatova EO

Nanoporous low-k Organo-Silicate Glass films were studied by means of X-ray reflection spectroscopy. Formation of chemical bonds of –CH3 groups with Si and O atoms is discussed. It was established that –CH3 groups substitute O atoms in SiO4 tetrahedron forming of Si-C bond that reduces value of permittivity. Creation of cross-linking due to C=C bond prevents the further decrease of permittivity.

114i NEXAFS study of opened and buried Al2O3 layers

Konyushenko MA, Konashuk AS, Sokolov AA, Schaefers F, Filatova EO

Influence of bottom electrode material and its thermal annealing on the lowest unoccupied states and microstructure of the annealed Al2O3 film in the Al2O3-based heterostructures have been studied using soft X-ray reflection spectroscopy. Also the effect of post deposition annealing and Al2O3 interlayer between the film and substrate on the intermixing in TiN/SiO2/Si structures is discussed.

CR1 Spectro-microscopy on Pt Nanoparticle supported on Fe3O4

Genuzio F, Sala A, Schmidt Th, Freund H-J

Supported Pt nanoparticles on Fe3O4 are a promising catalytic system. Their properties depend on preparation conditions, e.g. annealing in UHV leads to encapsulation by an FeO skin, rising their activity in CO oxidation. We present a combined LEEM/LEED/XPS study (SMART microscope) on the influence of preparation parameters (deposition, annealing temperature, O2 pressure) on the final surface.

CR2 A Spin-Crossover Complex on Surfaces: Structural and Electronic Differences Between Mono- and Multilayers

Bernien M, Hermanns C F, Krüger A, Krüger D, Nickel F, Walter W, Kuch W, Naggert H, Bannwarth A, Tuczek F, Gopakumar T G, Matino F, Mühlenberend S, Berndt R

The adsorption of the spin-crossover (SCO) complex [Fe(bpz)2(phen)] (bpz=dihydrobis(pyrazolyl) borate, phen=1,10-phenanthroline) on surfaces was studied by NEXAFS. We find that [Fe(bpz)2(phen)] in direct contact with a Au(111) surface dissociates into four-coordinate complexes, [Fe(bpz)2], and phen molecules. Molecules in the second layer on the other hand are intact and show a SCO transition.

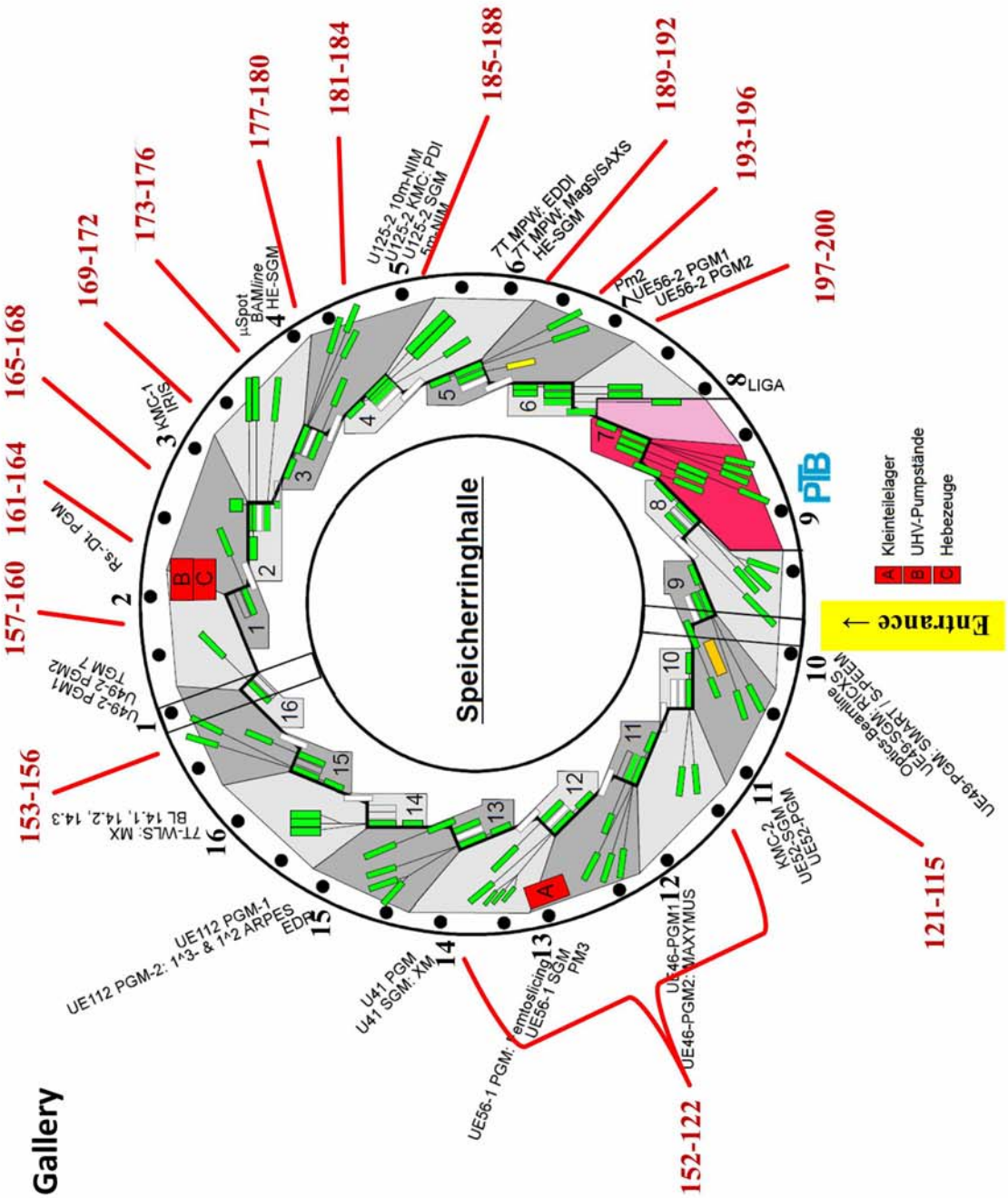
Speicherringhalle
Gallery
Entrance →
PTB
LIGA
Kleinteilelager
UHV-Pumpstände
Hebezeuge
A
B
C
153-156
157-160
161-164
165-168
169-172
173-176
177-180
181-184
185-188
189-192
193-196
197-200
121-115
152-122
U49-2 PGM1
U49-2 PGM2
TGM 7
7T-WLS: MX
BL 14.1, 14.2, 14.3
UE112 PGM-1
UE112 PGM-2: 1^3- & 1^2 ARPES
EDR
U41 PGM
U41 SGM: XM
UE56-1 PGM: femtoslicing
UE56-1 SGM
PM3
UE46-PGM1
UE46-PGM2: MAXYMUS
KMC-2
UE52-SGM
UE52-PGM
UE49-PGM: SMART / SPEEM
Optics-Beamline
UE48-SGM: RCXS
Rs-Dl: PGM
KMC-1
IRIS
µSpot
BAMline
HE-SGM
U125-2 10m-NIM
U125-2 KMC: PDI
U125-2 SGM
5m-NIM
7T MPW: EDDI
7T MPW: MagS/SAXS
HE-SGM
Pm2
UE56-2 PGM1
UE56-2 PGM2

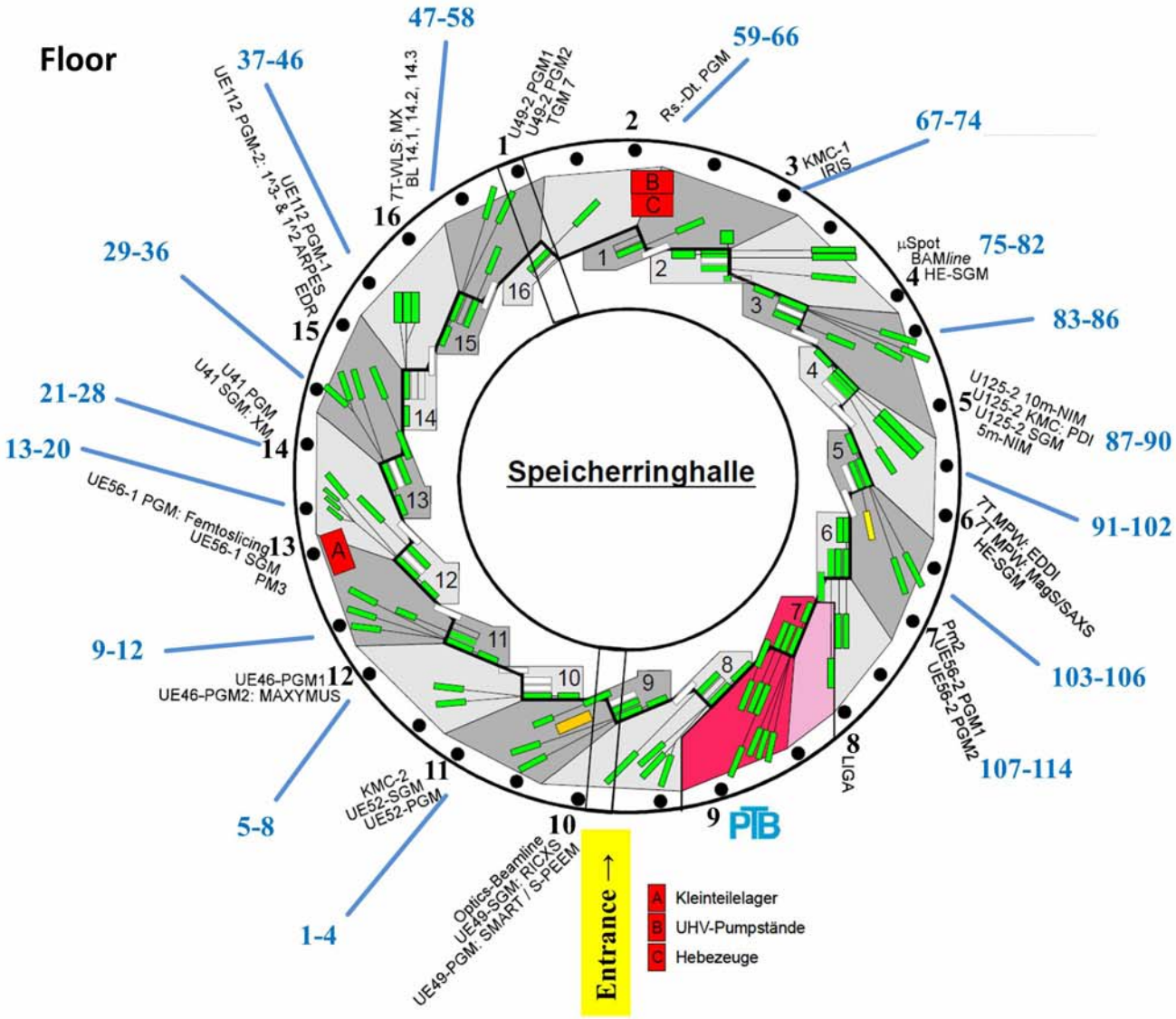
Floor
Speicherringhalle
Entrance →
PTB
A Kleinteilelager
B UHV-Pumpstände
C Hebezeuge
1-4
5-8
9-12
13-20
21-28
29-36
37-46
47-58
59-66
67-74
75-82
83-86
87-90
91-102
103-106
107-114
7T-WLS: MX
BL 14.1, 14.2, 14.3
U49-2 PGM1
U49-2 PGM2
TGM 7
Rs.-Dl. PGM
KMC-1
IRIS
µSpot
BAMline
HE-SGM
U125-2 10m-NIM
U125-2 KMC: PDI
U125-2 SGM
5m-NIM
7T MPW: EDDI
7T MPW: MagS/SAXS
HE-SGM
Pm2
UE56-2 PGM1
UE56-2 PGM2
LIGA
KMC-2
UE52-SGM
UE52-PGM
UE46-PGM1
UE46-PGM2: MAXYMUS
UE56-1 PGM: Femtoslicing
UE56-1 SGM
PM3
U41 PGM
U41 SGM: XM
UE112 PGM-1
UE112 PGM-2: 1^3- & 1^2 ARPES
EDR
Optics-Beamline
UE49-SGM: RICXS
UE49-PGM: SMART / S-PEEM

Vendor Exhibition
5th Joint BER II and BESSY II User Meeting

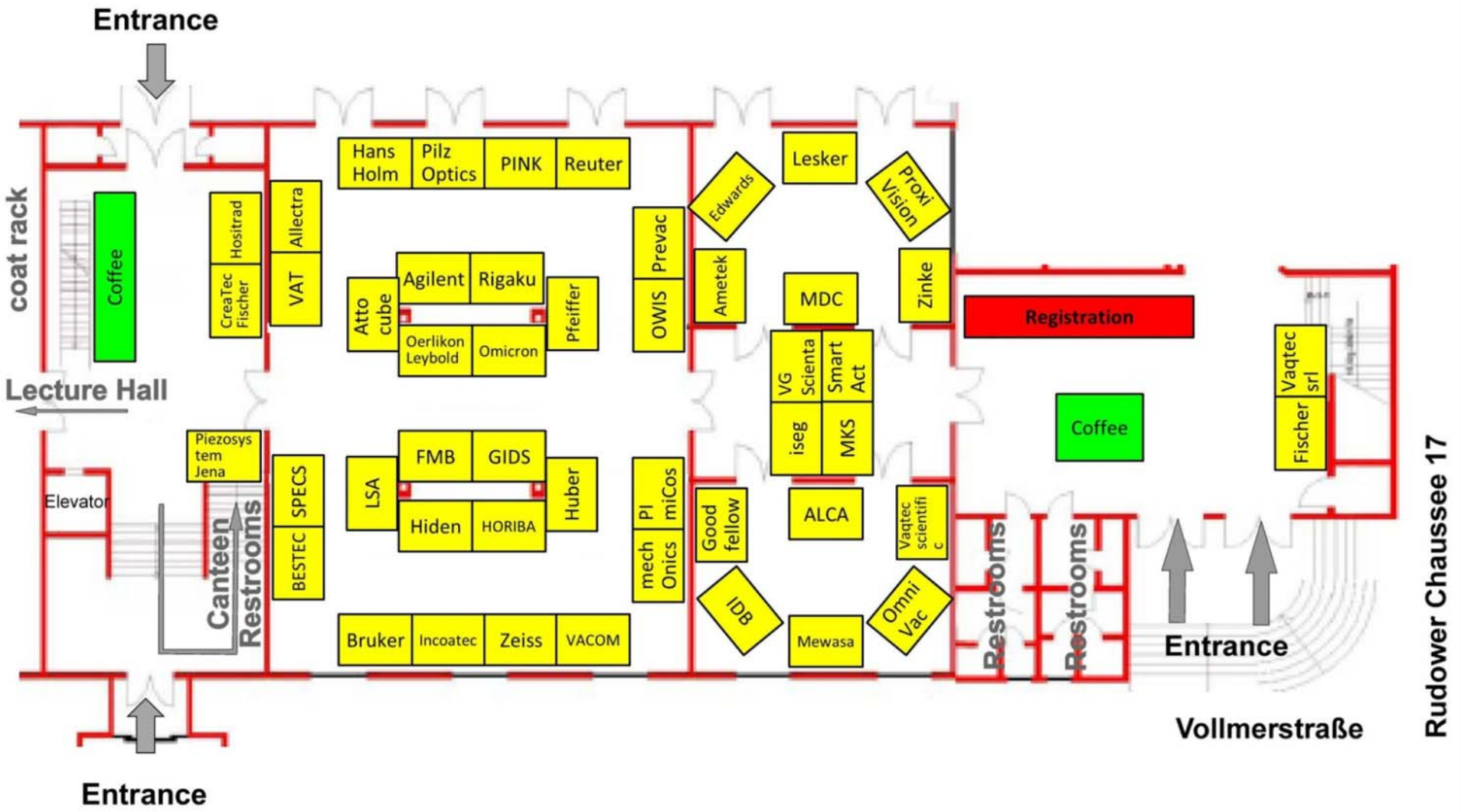


ZEISS


VAT


BESTEC


CREATEC
ENGINEERING SCIENCE


FMB Berlin


PRE VAC


10 -n
mbar
VACOM®


SPECS™


LSA
GmbH
Leischnig
Schaltschrankbau
Automatisierungstechnik


vaqtec
vacuum technology & components


INCOATEC
innovative coating technologies


MEWASA
SWISS MADE


PINK®


allectra


LCA
TECHNOLOGY


HORIBA
Scientific


PILZ-OPTICS


HOLM
THE VARIETY OF SILICON


VACUUM TECHNOLOGY
Hositrad


SmarAct
PERFECT MOTION


OWIS®


OXFORD
INSTRUMENTS
The Business of Science®


GIDS-GmbH
German Image Detector Systems


Surface Analysis and
Vacuum Technology
OmniVac


mechonics
competence
in micropositioning


VG SCIENTA
www.vgscienta.com


BRUKER


proxi
VISION


HUBER


AXO
AXO Dresden GmbH
Applied X-ray Optics
High Precision Deposition


PFEIFFER VACUUM


piezosystemjena
incredibly precise


HIDEN
ANALYTICAL


Rigaku


I.D.B.


ZINKE


JFA


MDC
Vacuum Products


Agilent Technologies

attocube
pioneers of precision

Kurt J. Lesker
Company Ltd

œrlikon
leybold vacuum

EDWARDS
Vacuum science... product solution.

Vendor Addresses

Agilent Technologies Vacuum Division
Lyoner Str. 20
60528 Frankfurt/Main
+49 351 413 96 17
johannes.schuricht@agilent.com
www.chem.agilent.com

ALCA Technology Srl
Via Lago di Garda 130
Schio (VI), Italy
+39 44 55 000 64
andrea.lanaro@alcatechnology.com
www.alcatechnology.com

Allectra GmbH
Traubeneichenstr. 62-66
16567 Schönfließ
+49 33056 415 980
b.luckscheiter@allectra.com
www.allectra.com

Ametek GmbH
Rudolf-Diesel-Str. 16
40670 Meerbusch
+49 5551 99 66 90
peter.koch@ametek.de
www.ortec-online.com

attocube systems AG
Königinstr. 11a
80539 München
+49 89 28 77 80 90
info@attocube.com
www.attocube.com

BESTEC GmbH
Carl-Scheele-Str. 14
12489 Berlin
+49 30 67 09 92 11
sabine.proll@bestec.de
www.bestec.de

Bruker Nano GmbH
Schwarzschildstr. 12
12489 Berlin
+49 30 67 09 90 59
alexandra.wirth@bruker-nano.de
www.bruker.com

Carl Zeiss Laser Optics GmbH
Carl-Zeiss-Straße 22
73447 Oberkochen
+49 7364 20 59 71
n.niewrzella@smt.zeiss.com
www.zeiss.com/lo

CreaTec Fischer & Co.GmbH
Industrie Str.9
74391 Erligheim Deutschland
+49 7143 96 70 134
neitzel@createc.de
www.createc.de

Edwards Vacuum
Crawley Business Quarter Manor Royal
Crawley
RH10 9LW West Sussex (UK)
+44 1293 60 32 91
helen.nicholls@edwardsvacuum.com
www.edwardsvacuum.com

FMB Feinwerk- und Meßtechnik GmbH
Friedrich-Wöhler-Str. 2
12489 Berlin
+49 30 67 77 30 57
j.jaehnigen@fmb-berlin.de
www.fmb-berlin.de

GIDS-GmbH German Image Detector Systems
Theodor-Haubach-Weg 2
21684 Stade
+49 41 417 76 124
kuznik@gids-gmbh.com
www.gids-gmbh.com

Goodfellow GmbH
Postfach 13 43
61213 Bad Nauheim
+49 30 80 01 00 05 79
Hildyard@goodfellow.com
www.goodfellow.com

Hans Holm GmbH
Gigerenz 1
84367 Tann
+49 8572 969 330
hans.holm@holm-silicon.de
www.holm-silicon.de

Hiden Analytical
Niedmannweg 13
82431 Kochel am See
+49 8857 693 01
roethlein@hiden.de
www.hiden.de

HORIBA Scientific
Hauptstr. 1
82008 Unterhaching
+49 6251 84 75 24
perrine.wenzel@horiba.com
www.horiba.com/de/scientific

Hositrad Vacuum Technology
Lindnergasse 2
93047 Regensburg Deutschland
+ 49 941 558 27
jurgen@hositrad.nl
www.hositrad.com

Huber Diffraktionstechnik GmbH & Co. KG
Sommerstrasse 4
83253 Rimsting
+49 8051 687 80
nh@xhuber.com
www.xhuber.com

IDB, Ingenieurbüro Dietmar Budzylek
Hermann Cossmann Str.19
41472 Neuss
+49 21 82 608 04
Chr.Budzylek@idbscb.de
www.idbscb.de

incoatec GmbH
Max-Planck-Str. 2
21502 Geesthacht
+49 4152 88 93 55
hahn@incoatec.de
www.incoatec.de

iseg Spezialelektronik GmbH
Bautzener Landstraße 23
01454 Radeberg / OT Rossendorf
+49 351 26 99 60
sales@iseg-hv.de
www.iseg-hv.com

Johann Fischer Aschaffenburg Präzisionswerk
Ruhlandstr. 72 - 78
63741 Aschaffenburg
+49 6021 860 50
matthias.fischer@jfa.de
www.jfa.de

Kurt J. Lesker Company
Burgess Road 15/16
TN35 4NR Hastings East Sussex (UK)
+44 0142 445 81 00
louisep@lesker.com
www.lesker.com

LSA GmbH
Äußerer Hofring 11
09509 Wolkenstein OT Hilmersdorf
+49 37369 17 20
l.leischnig@lsa-gmbh.de
www.lsa-gmbh.de

mechOnics ag
Unnützstr. 2b
81825 München
+49 89 420 24 207
muenzer@mechOnics.de
www.mechOnics.de

MDC Vacuum Limited
Am Rotdorn 39
44577 Castrop-Rauxel
+49 2305 94 75 08
galthoff@mdcvacuum.de
www.mdcvacuum.de

Mewasa AG
Straubstrasse 11
7323 Wangs (CH)
+41 81 720 48 82
t.kuenzler@mewasa.ch
www.mewasa.ch

MKS Instruments Deutschland GmbH
Schatzbogen 43
81829 München
+49 89 420 00 82 21
Sandra_Traber@mksinst.com
www.mksinst.com

Oerlikon Leybold Vacuum GmbH
Bonner Str. 498
50968 Köln
+49 30 4356090
Michael.Pschyrembel@oerlikon.com
www.oerlikon.com

Oxford Instruments Omicron NanoScience
Limburger Str. 75
65232 Taunusstein Germany
+49 6128 98 71 15
s.langnickel@omicron.oxinst.com
www.omicron.de

OmniVac
Espensteigstrase 16
67661 Kaiserslautern
+49 631 311 07 40
h.ruppender@omnivac.de
www.omnivac.de

OWIS GmbH
Im Gaisgraben 7
79219 Staufen i. Br.
+49 7633 950 48 80
mge@owis.eu
www.owis.eu

Pfeiffer Vacuum GmbH
Berliner Str. 43
35614 Asslar
+49 9342 96 10 34
Christiane.Friedrich@pfeiffer-vacuum.de
www.pfeiffer-vacuum.de

PI miCos GmbH
Freiburger Str. 30
79427 Eschbach
+49 7634 505 72 32
c.maucher@pimicos.com
www.pimicos.com

Piezosystem Jena GmbH
Stockholmer Strasse 12
07747 Jena
+ 49 3641 668 80
ipetras@piezojena.com
www.piezosystem.de

Pilz-Optics
Enzianstrasse 29
73485 Zöbingen-Unterschneidheim
+49 7966 803 96 09
info@pilz-optics.de
www.pilz-optics.de

PINK GmbH Vakuumtechnik
Gyula-Horn-Straße 20
97877 Wertheim
+49 9342 91 91 45
moetzel@pink.de
www.pink.de

PREVAC sp. z o.o.
Raciborska Str. 61
44-362 Rogow (PL)
+48 60 228 14 70
j.kowalska@prevac.pl
www.prevac.eu

ProxiVision GmbH
Robert-Bosch-Straße 34
64625 Bensheim
+49 6251 17 03 24
frank.fandrich@proxivision.de
www.proxivision.de

REUTER TECHNOLOGIE GmbH
Roentgenstr. 1
63755 Alzenau
+49 6023 50 44 46
m.debes@reuter-technologie.de
www.reuter-technologie.de

Rigaku Innovative Technologies
Indestr. 109
52249 Eschweiler Deutschland
+49 1729 34 73 23
paul.pennartz@rigaku.com
www.Rigaku.com

SmarAct GmbH
Schütte-Lanz-Strasse 9
26135 Oldenburg
+49 441 80 08 79 27
seefeld@smaract.de
www.smaract.de

SPECS Surface Nano Analysis GmbH
Voltastrasse 5
13355 Berlin
+49 30 467 82 40
christin.ellrich@specs.com
www.specs.com

VACOM Vakuum Komponenten & Messtechnik GmbH
Gabelsbergerstr. 9
07749 Jena
+49 3641 42 75 25
franziska.straubel@vacom.de
www.vacom.de

Vaqtec Srl
Corso Grosseto 437
10151 Torino, Italy
+39 32 994 51 836
r.cometti@vaqtec.com
www.vaqtec.com

vaqtec-scientific
Thulestr. 18b
13189 Berlin
+49 30 78 71 31 58
melzer@vaqtec-scientific.com
www.vaqtec-scientific.com

VAT Deutschland GmbH
Am Hochacker 4
85630 Grasbrunn b. München
+49 89 97 89 78 76 30
vsaissreiner@vatvalve.com
www.vatvalve.com

VG Scienta
Maunsell Road, Castleham Industrial Estate,
St Leonards-on-sea
TN38 9NN East Sussex (UK)
+49 1424 85 12 91
senay.ciftci@vgscienta.com
www.vgscienta.com

Zinke Anlagen- und Vakuumservice e.K.
Paradiesstr. 206 A
12526 Berlin
+49 30 670 235 80
service@zinke-berlin.de
www.zinke-berlin.de

List of Participants

Akaike	Kouki	akaike@riken.jp
Alekseeva	Olga	blackhole2010@yandex.ru
Alsmeier	Jan-Hendrik	jan-hendrik.alsmeier@helmholtz-berlin.de
Arion	Tiberiu	tiberiu.arion@cfel.de
Aristov	Victor	victor.aristov@gmail.com
Arlt	Tobias	tobias.arlt@helmholtz-berlin.de
Audehm	Patrick	audehm@is.mpg.de
Babenkov	Sergey	sergey.babenkov@desy.de
Baev	Ivan	ivan.baev@desy.de
Baran	Stanislaw	stanislaw.baran@uj.edu.pl
Barciszewski	Jakub	agent007@man.poznan.pl
Barrett	Matthew	matthew.barrett@helmholtz-berlin.de
Barthel	Thomas	tb@crystal-photonics.com
Bartkowiak	Maciej	maciej.bartkowiak@helmholtz-berlin.de
Bechtel	Michael	bechtel@is.mpg.de
Beckhoff	Burkhard	Burkhard Beckhoff
Behnke	Steffen	behnke@pdi-berlin.de
Behrens	Malte	behrens@fhi-berlin.mpg.de
Bera	Anup Kumar	anup.bera@helmholtz-berlin.de
Bernien	Matthias	bernien@physik.fu-berlin.de
Beye	Martin	martin.beye@helmholtz-berlin.de
Birke	Michael	michael.birke@desy.de
Blanco	Francisco	fran.blanco@uab.cat
Blanco Canosa	Santiago	santiago.blanco@helmholtz-berlin.de
Boguslaw	Penc	boguslaw.penc@uj.edu.pl
Bon	Volodymyr	volodymyr.bon@chemie.tu-dresden.de
Boschker	Jos	boschker@pdi-berlin.de
Böttcher	Stefan	boettcher@fhi-berlin.mpg.de
Bragaglia	Valeria	bragaglia@pdi-berlin.de
Brandt	Astrid	brandt@helmholtz-berlin.de
Braun	Walter	Walter.Braun@Helmholtz-Berlin.de
Brieger	Claudia	claudia.brieger@fu-berlin.de
Bruno	Giovanni	giovanni.bruno@bam.de
Brzhezinskaya	Maria	maria.brzhezinskaya@helmholtz-berlin.de
Buchold	Philipp	pbuchold@gmail.com
Buzanich	Günter	Guenter.Buzanich@bam.de
Bykova	Iuliia	bykova@is.mpg.de
Calvet	Wolfram	wolfram.calvet@helmholtz-berlin.de
Cardenes	Ruben	ruben.cardenes@upf.edu
Casu	Benedetta	benedetta.casu@uni-tuebingen.de
Charalampidou	Elli-Maria	ellimaria31@yahoo.gr
Chatterji	Tapan	chatterji@ill.fr

Chiang	Cheng-Tien	chiang@mpi-halle.de
Chiappisi	Leonardo	leonardo.chiappisi@tu-berlin.de
Chittas	Pantelis	pantelis_chittas@hotmail.com
Cramm	Stefan	s.cramm@fz-juelich.de
Czeslik	Claus	claus.czeslik@uni-dortmund.de
Darlatt	Erik	erik.darlatt@ptb.de
Darowski	Nora	nora.darowski@helmholtz-berlin.de
Dedkov	Yuriy	Yuriy.Dedkov@specs.com
Demo	Gabriel	guliver@mail.muni.cz
Dobbek	Holger	holger.dobbek@biologie.hu-berlin.de
Doganay	Hatice	h.doganay@fz-juelich.de
Dronskowski	Richard	drons@HAL9000.ac.rwth-aachen.de
Efimov	Vadim	efimovvv2006@mail.ru
Ehlert	Christopher	christopher.ehlert@bam.de
Ehrig	Karsten	karsten.ehrig@bam.de
Eichner	Adina	adina.eichner@pharmazie.uni-halle.de
Eisenblaetter	Gerald	eisenblaetter@uni-leipzig.de
Elovaara	Tomi	tkelov@utu.fi
Emmerling	Franziska	franziska.emmerling@bam.de
Engel	Nicholas	nicholas.engel@helmholtz-berlin.de
Erlkamp	Mirko	mirko.erlkamp@tu-dortmund.de
Fantin	Andrea	andrea.fantin@helmholtz-berlin.de
Feyerherm	Ralf	ralf.feyerherm@helmholtz-berlin.de
Fiechter	Sebastian	fiechter@helmholtz-berlin.de
Filatova	Elena	feo@EF14131.spb.edu
Fischer	Franziska	franziska.fischer@bam.de
Fittschen	Ursula	ursula.fittschen@chemie.uni-hamburg.de
Fleury Curado	Jessica	jessica.curado@bam.de
Florian	Timo	timo.florian@physik.hu-berlin.de
Förster	Ronald	foerster@helmholtz-berlin.de
Franke	Robert	robert.franke@helmholtz-berlin.de
Frano	Alex	a.frano@fkf.mpg.de
Friedrich	Matthias	friedrich@fhi-berlin.mpg.de
Fritsch	Katharina	katharina.fritsch@helmholtz-berlin.de
Gaal	Peter	peter.gaal@helmholtz-berlin.de
Gainar	Adrian	adrian.gainar@postgrad.manchester.ac.uk
Gast	Heike	gast@helmholtz-berlin.de
Genzel	Christoph	genzel@helmholtz-berlin.de
Gerbrecht	Stefanie	sgerbi1985@yahoo.de
Gericke	Eike	eike.gericke@helmholtz-berlin.de
Gerlach	Martin	Martin.Gerlach@ptb.de
Gil	Alina	a.gil@ajd.czest.pl
Glavatskyi	Illia	illya.glavatskyy@gmail.com
Gnutzmann	Tanja	tanja.gnutzmann@bam.de
Goering	Eberhard	goering@is.mpg.de
Gollwitzer	Christian	Christian.Gollwitzer@ptb.de

Gorgoi	Mihaela	mihaela.gorgoi@helmholtz-berlin.de
Gottwald	Alexander	alexander.gottwald@ptb.de
Götz	Andreas	a.goetz@campus.tu-berlin.de
Grimm	Nico	nico.grimm@helmholtz-berlin.de
Grötzsch	Daniel	daniel.groetzsch@tu-berlin.de
Gurieva	Galina	galina.gurieva@helmholtz-berlin.de
Guttmann	Peter	peter.guttmann@helmholtz-berlin.de
Habicht	Klaus	habicht@helmholtz-berlin.de
Habraken	Wouter	wouter.habraken@mpikg.mpg.de
Haeberle	Jörg	haeberle@tu-cottbus.de
Hahn	Marc	hahn@physik.fu-berlin.de
Handick	Evelyn	evelyn.handick@helmholtz-berlin.de
Hanke	Michael	hanke@pdi-berlin.de
Hartwig	Steffen	steffen.hartwig@helmholtz-berlin.de
Hauß	Thomas	hauss@helmholtz-berlin.de
Hävecker	Michael	michael.haevecker@helmholtz-berlin.de
Heine	Andreas	heinea@mailer.uni-marburg.de
Heinemann	Udo	heinemann@mdc-berlin.de
Hellmig	Michael	michael.hellmig@helmholtz-berlin.de
Hendel	Stefan	stefan.hendel@helmholtz-berlin.de
Hergenhahn	Uwe	uwe.hergenhahn@ipp.mpg.de
Hergenhahn	Uwe	uwe.hergenhahn@ipp.mpg.de
Herrmann	Theodor	therrmann@roperscientific.de
Hertwig	Andreas	andreas.hertwig@bam.de
Hesse	Ronald	rhesse@uni-leipzig.de
Hilger	André	hilger@helmholtz-berlin.de
Hinrichs	Karsten	hinrichs@isas.de
Hinz	Alexander	alm@tf.uni-kiel.de
Hirsch	Konstantin	Konstantin.Hirsch@helmholtz-berlin.de
Hoehl	Arne	arne.hoehl@ptb.de
Hoell	Armin	hoell@helmholtz-berlin.de
Hoffmann	Jens-Uwe	hoffmann-j@helmholtz-berlin.de
Holfelder	Ina	ina.holfelder@ptb.de
Holzweber	Markus	markus.holzweber@bam.de
Hönicke	Philipp	philipp.hoenicke@ptb.de
Hoppe	Michael	m.hoppe@fz-juelich.de
Horn	Karsten	horn@fhi-berlin.mpg.de
Hoser	Andreas	hoser@helmholtz-berlin.de
Houser	Josef	houser@mail.muni.cz
Hüsges	Anna Zita	huesges@cpfs.mpg.de
Huth	Paula	paula.huth@gmx.de
Iles	Gail N.	gail.iles@helmholtz-berlin.de
Janowitz	Christoph	christoph.janowitz@physik.hu-berlin.de
Jansing	Christine	c.jansing@fh-muenster.de
Jiang	Zheng	jiangzheng@sinap.ac.cn
Joester	Maike	maike.joester@chemie.hu-berlin.de

Johnson	Benjamin	benjamin@fhi-berlin.mpg.de
Jung	Christian	christian.jung@helmholtz-berlin.de
Jungwirth	Sebastian	jungwirth@physik.hu-berlin.de
Käämbre	Tanel	tanel.kaambre@ut.ee
Kabelitz	Anke	Anke.Kabelitz@bam.de
Kalbe	Henryk	henryk.kalbe@bam.de
Kallfaß	Christoph	kallfass_@gmx.net
Kalms	Jacqueline	jacqueline.kalms@charite.de
Kardjilov	Nikolay	kardjilov@helmholtz-berlin.de
Karpinsky	Dmitry	karpinski@ua.pt
Kaser	Hendrik	hendrik.kaser@ptb.de
Kast	Patrick	kast@fhi-berlin.mpg.de
Kataev	Elmar	kataev.elmar@gmail.com
Katja	Henzler	katja.henzler@helmholtz-berlin.de
Keiderling	Uwe	keiderling@helmholtz-berlin.de
Kent	Ben	ben.kent@helmholtz-berlin.de
Kepsutlu	Burcu	burcu.kepsutlu@helmholtz-berlin.de
Khan	Munirah	munirah.khan@helmholtz-berlin.de
Kiefer	Klaus	klaus.kiefer@helmholtz-berlin.de
Kiyan	Igor	Igor.Kiyan@helmholtz-berlin.de
Klaus	Manuela	klaus@helmholtz-berlin.de
Klee	Andreas	andreas.klee@campus.tu-berlin.de
Klein	Roman	roman.klein@ptb.de
Klemke	Bastian	Bastian.Klemke@helmholtz-berlin.de
Kloess	Gert	kloess@uni-leipzig.de
Klyushin	Alexander	klyushin@fhi-berlin.mpg.de
Kneipp	Janina	janina.kneipp@chemie.hu-berlin.de
Knop-Gericke	Axel	knop@fhi-berlin.mpg.de
Koch	Norbert	norbert.koch@physik.hu-berlin.de
Köhler	Leonard	leonard.koehler@helmholtz-berlin.de
Köhler	Ralf	ralf.koehler@helmholtz-berlin.de
Kolbe	Michael	michael.kolbe@ptb.de
Koller	Georg	georg.koller@uni-graz.at
Könnecke	René	rene.koennecke@helmholtz-berlin.de
Koren	Katrin	katrin.koren@ntc-weiz.at
Kotkowska	Olga	olga.kotkowska@gmail.com
Kraehnert	Ralph	ralph.kraehnert@tu-berlin.de
Kraffert	Kai	kraffert@physik.fu-berlin.de
Krist	Thomas	krist@helmholtz-berlin.de
Kronast	Florian	florian.kronast@helmholtz-berlin.de
Krumrey	Michael	Michael.Krumrey@ptb.de
Kuch	Wolfgang	kuch@physik.fu-berlin.de
Kühn	Julius	julius.kuehn@bam.de
Kunnus	Kristjan	kristjan.kunnus@helmholtz-berlin.de
Kupski	Oliver	okupski@gwdg.de
Lawicki	Arkadiusz	arkadiusz.lawicki@helmholtz-berlin.de

Leitner	Torsten	torsten.leitner@physics.uu.se
Leppert	Linn	linn.leppert@uni-bayreuth.de
Lewin	Arno	arno.lewin@ptb.de
Li	Chenghao	chenghao.li@mpikg.mpg.de
Lischke	Toralf	tlischke@fhi-berlin.mpg.de
Liu	Zhonghao	z.liu@ifw-dresden.de
Lopez-Mesas	Montserrat	montserrat.lopez.mesas@uab.cat
Lospichl, von	Anja	anja.lospichl@mailbox.tu-berlin.de
Lupulescu	Cosmin	cosmin.lupulescu@helmholtz-berlin.de
Lust	Enn	enn.lust@ut.ee
Maawad	Emad	emad.maawad@hzg.de
Maderitsch	Angelika	angelika.maderitsch@aon.at
Mahler	Willy	mahler@fhi-berlin.mpg.de
Makarova	Anna	aa-makarova@yandex.ru
Manke	Ingo	manke@helmholtz-berlin.de
Markötter	Henning	henning.markoetter@helmholtz-berlin.de
Menzel	Magnus	magnus.menzel@chemie.uni-hamburg.de
Merzlikin	Sergiy	merzlikin@mpie.de
Metje	Jan	jan.metje@helmholtz-berlin.de
Mezher	Michelle	michelle.mezher@helmholtz-berlin.de
Michel	Raphael	raphael.michel@mailbox.tu-berlin.de
Mishra	Durgamadhab	Durgamadhab.Mishra@rub.de
Molodtsova	Olga	olga.molodtsova@desy.de
Mühlethaler	Roland	roland.muehlethaler@mfn-berlin.de
Müller	Josefin	josefin.mueller@pharmazie.uni-halle.de
Müller	Matthias	matthias.mueller@ptb.de
Müller	Peter	peter.mueller@ptb.de
Müller	Katharina	katharina.muller@upmc.fr
Necas	David	yeti@physics.muni.cz
Nefedov	Alexei	alexei.nefedov@kit.edu
Neicke	Thomas	neicke@web.de
Neldner	Kai	kai.neldner@helmholtz-berlin.de
Netzeband	Christian	christian.netzeband@helmholtz-berlin.de
Neudachina	Vera	vera_neudachina@mail.ru
Neumann	Maciej	maciej.neumann@isas.de
Nguyen Thi	Yen	yen.nguyen-thi@bam.de
Nickel	Fabian	fabian.nickel@fu-berlin.de
Niederhausen	Jens	jniederh@physik.hu-berlin.de
Nietzold	Carolin	Carolin.Nietzold@bam.de
Nutsch	Andreas	andreas.nutsch@ptb.de
Ogata	Hideaki	hideaki.ogata@cec.mpg.de
Olar	Tetiana	tetiana.olar@helmholtz-berlin.de
Ovcharenko	Roman	r.e.ovcharenko@gmail.com
Ovsyannikov	Ruslan	ovsyannikov@helmholtz-berlin.de
Papp	Christian	christian.papp@fau.de
Partzsch	Sven	s.partzsch@ifw-dresden.de

Paßvogel	Malte	passvogelm@uni-greifswald.de
Paul	Dietrich	paul.dietrich@bam.de
Pavlicek	Jiri	jiri.pavlicek@img.cas.cz
Peisert	Heiko	heiko.peisert@uni-tuebingen.de
Penghui	Yang	penghui.yang@helmholtz-berlin.de
Petzold	Albrecht	albrecht.petzold@helmholtz-berlin.de
Picot	Thomas	thomas.picot@fys.kuleuven.be
Pietzsch	Annette	annette.pietzsch@helmholtz-berlin.de
Pollakowski	Beatrix	beatrix.pollakowski@ptb.de
Polonskyi	Oleksandr	olpo@tf.uni-kiel.de
Prevost	Sylvain	prevost.sylvain@gmail.com
Proessdorf	Andre	proessdorf@pdi-berlin.de
Prokes	Karel	prokes@helmholtz-berlin.de
Ptacek	Jakub	ptacekj@img.cas.cz
Pucher	Andreas	pucher@uni-potsdam.de
Puls	Jana	jana.puls@ptb.de
Qureshi	Bilal	bilal.qureshi@charite.de
Qviller	Atle	atlejq@ife.no
Rädel	Stephanie	stephanie.raedel@helmholtz-berlin.de
Rader	Oliver	rader@helmholtz-berlin.de
Radtke	Martin	martin.radtke@bam.de
Radu	Ilie	ilie.radu@helmholtz-berlin.de
Radu	Abrudan	radu-marius.abrudan@helmholtz-berlin.de
Raghuwanshi	Vikram Singh	vsingh4u@gmail.com
Rehders	Stefan	sr@tf.uni-kiel.de
Reichardt	Gerd	gerd.reichardt@helmholtz-berlin.de
Reiche	Ina	ina.reiche@upmc.fr
Reinholz	Uwe	uwe.reinholz@bam.de
Repchenko	Iurii	kent160@mail.ru
Riemer	Andrea	andrea.riemer@desy.de
Riemer	Sven	Sven.Riemer@gmx.net
Ries	Markus	markus.ries@helmholtz-berlin.de
Roczen	Maurizio	Maurizio.Roczen@physik.hu-berlin.de
Roewer	Martin	martin.roewer@helmholtz-berlin.de
Roske	Yvette	yroske@mdc-berlin.de
Rößler	Robert	robert.roessler@helmholtz-berlin.de
Roth	Friedrich	friedrich.roth@cfel.de
Roth	Christina	christina.roth@fu-berlin.de
Rump	Doreen	doreen.rump@bam.de
Rupp	Axel	rupp-a@helmholtz-berlin.de
Ryll	Hanjo	Hanjo.Ryll@Helmholtz-Berlin.de
Ryukhtin	Vasyl	ryukhtin@ujf.cas.cz
Sadykov	Ravil	rsadykov@inr.ru
Santander-Syro	Andres F.	andres.santander@csnsm.in2p3.fr
Santos	Karine	kdossan@gwdg.de
Sauer	Olaf-Peter	olaf-peter.sauer@helmholtz-berlin.de

Sautner	Viktor	vsautne@gwdg.de
Savas	Özgür	oezguer.savas@isas.de
Scheerer	Patrick	patrick.scheerer@charite.de
Schenderlein	Thomas	Thomas.Schenderlein@helmholtz-berlin.de
Scherb	Tobias	tobias.scherb@helmholtz-berlin.de
Schlegel	Moritz-Caspar	moritz-caspar.schlegel@helmholtz-berlin.de
Schmidbauer	Martin	martin.schmidbauer@ikz-berlin.de
Schmidt	Andrea	schmidt.andrea@charite.de
Schmidt	Harald	harald.schmidt@tu-clausthal.de
Schmidt	Ingo	ingo.schmidt@mpikg.mpg.de
Schmitz	Detlef	schmitz@helmholtz-berlin.de
Schmitz-Antoniak	Carolin	carolin.antoniak@uni-due.de
Schoekel	Alexander	a.schoekel@fu-berlin.de
Schreck	Simon	simon.schreck@helmholtz-berlin.de
Schulz	Jennifer	jennifer.schulz@helmholtz-berlin.de
Schumacher	Gerhard	schumacher@helmholtz-berlin.de
Schumann	Frank	schumann@mpi-halle.de
Schütz	Gisela	schuetz@is.mpg.de
Schwarzkopf	Olaf	olaf.schwarzkopf@helmholtz-berlin.de
Schwörer	Felicitas	schwoerer@stud.uni-heidelberg.de
Seidlhofer	Beatrix-Kamelia	beatrix-kamelia.seidlhofer@helmholtz-berlin.de
Seidt	Britta	britta.seidt@mpikg.mpg.de
Seifert	Stephan	stephan.seifert@bam.de
Senkovska	Irena	irena.senkovska@chemie.tu-dresden.de
Senkovskiy	Boris	senkovskiy@gmail.com
Siegel	Stefan	siegel@mpikg.mpg.de
Sikolenko	Vadim	vadim.sikolenko@helmholtz-berlin.de
Simon	Miriam	miriamsimon@mailbox.tu-berlin.de
Sivkov	Victor	svn@dm.komisc.ru
Smolek	Stephan	smolek@ati.ac.at
Sokolov	Andrey	andrey.sokolov@helmholtz-berlin.de
Sokolowski	André	andre.sokolowski@helmholtz-berlin.de
Solopow	Sergej	sergej.solopow@helmholtz-berlin.de
Soltwisch	Victor	Victor.Soltwisch@ptb.de
Sparta	Karine	karine.sparta@helmholtz-berlin.de
Squibb	Richard	richard.squibb@physics.uu.se
Staier	Florian	florian.staier@helmholtz-berlin.de
Stammer	Max	max-stammer@hotmail.de
Staude	Andreas	andreas.staude@bam.de
Steffien	Michael	michael.steffien@helmholtz-berlin.de
Steigert	Alexander	alexander.steigert@helmholtz-berlin.de
Steitz	Roland	steitz@helmholtz-berlin.de
Stemmler	Carsten	stemmler@pdi-berlin.de
Stephan	Christiane	christiane.stephan@helmholtz-berlin.de
Stöber	Stefan	stefan.stoeber@geo.uni-halle.de

Stockert	Oliver	oliver.stockert@cpfs.mpg.de
Streeck	Cornelia	cornelia.streeck@ptb.de
Strunskus	Thomas	ts@tf.uni-kiel.de
Svensson	Svante	Svante.svensson@physics.uu.se
Szczerbowska-Boruchowska	Magdalena	Magdalena.Boruchowska@fis.agh.edu.pl
Szytula	Andrzej	andrzej.szytula@uj.edu.pl
Telser	Joshua	jtelser@roosevelt.edu
Tesch	Marc F.	marc.tesch@fh-muenster.de
Thielemann-Kühn	Nele	nele.thielemann@helmholtz-berlin.de
Thornagel	Reiner	reiner.thornagel@ptb.de
Tietze	Thomas	tietze@is.mpg.de
Tietzel	Michael	mtietze1@gwdg.de
Tommaseo	Caterina	caterina.e.tommaseo@TU-Berlin.de
Tötzke	Christian	christian.toetzke@helmholtz-berlin.de
Trabant	Christoph	christoph.trabant@fu-berlin.de
Trapp	Marcus	marcus.trapp@helmholtz-berlin.de
Tratsiak	Katsiaryna	tionawow@gmail.com
Tröbs	Lisa	Lisa.Troebs@bam.de
Uehlein	Monika	monika.uehlein@helmholtz-berlin.de
Ulm	Gerhard	gerhard.ulm@ptb.de
Ümsür	Bünyamin	buenyamin.uemsuer@helmholtz-berlin.de
Ünal	Ahmet Akin	akin.uenal@helmholtz-berlin.de
Unger	Wolfgang	wolfgang.unger@bam.de
Unterumsberger	Rainer	rainer.unterumsberger@ptb.de
Valentyn	Novosad	novosad@anl.gov
Valle Rios	Laura Elisa	laura.valle-rios@helmholtz-berlin.de
Vetterlein	Matthias	m.vetterlein@prevac.eu
Vogel	Christian	christian.vogel@bam.de
Vogel	Dirk	vogel@mpie.de
Vollmer	Antje	antje.vollmer@helmholtz-berlin.de
Voloshina	Elena	elena.voloshina@hu-berlin.de
Vyalikh	Denis	denis.vyalikh@gmail.com
Wagermaier	Wolfgang	wolfgang.wagermaier@mpikg.mpg.de
Wallacher	Dirk	dirk.wallacher@helmholtz-berlin.de
Wanke	Martina	martina.wanke@physik.tu-chemnitz.de
Weigand	Markus	mweigand@is.mpg.de
Weiss	Manfred	msweiss@helmholtz-berlin.de
Welke	Martin	martin.welke@uni-leipzig.de
Wernecke	Jan	jan.wernecke@ptb.de
Wessel	Andreas	andreas.wessel@mfn-berlin.de
Wilke	Manuel	manuel.wilke@bam.de
Wilks	Regan	regan.wilks@helmholtz-berlin.de
Willenberg	Britta	britta.willenberg@helmholtz-berlin.de
Winkler	Stefanie	stefanie.winkler@helmholtz-berlin.de
Wöckel	Claudia	claudia.woeckel@uni-leipzig.de

Xiao	Jie	jie.xiao@helmholtz-berlin.de
Yadav	Om Prakash	yadavop02@yahoo.com
Zabel	Hartmut	hartmut.zabel@rub.de
Zada	Birgitt	birgitt.zada@helmholtz-berlin.de
Zahn	Dietrich R. T.	zahn@physik.tu-chemnitz.de
Zamudio-Bayer	Vicente	vicente.zamudio-bayer@helmholtz-berlin.de
Zander	Stefan	stefan.zander@helmholtz-berlin.mpg.de
Zhang	Bin	binzhang@zedat.fu-berlin.de
Zimmermann	Peter	pz@atom.physik.tu-berlin.de
Züttel	Andreas	andreas.zuettel@empa.ch

Friends of Helmholtz-Zentrum Berlin e.V.

The purpose of the Association of Friends of Helmholtz-Zentrum Berlin includes the support of the development of science and research, especially by the support of scientific activities at BESSY II. The association is a link between HZB and the general public and it shall develop the cooperation between HZB, its friends and sponsors and other national and international institutions. In particular, it is dedicated to support young scientists.

Main activities of the association include the annual bestowals of science awards. In memory of the former scientific director of BESSY, who died in September 1988, the association awards annually the Ernst-Eckhard-Koch-Prize. This prize is given for outstanding Ph.D. theses completed during the current or past year in the field of research with synchrotron radiation and performed at either BESSY II or HASYLAB (Hamburg) as the main places of activities of Ernst-Eckhard Koch. Furthermore, the association bestows the Innovation-Award on Synchrotron Radiation since 2001, which is announced Europe wide for an outstanding technical achievement or experimental method that promises to extend the frontiers of research with synchrotron radiation.

All natural or juristic persons may become member of the association. The regular annual membership fee amounts to 10 € for undergraduate and graduate students, 40 € for other natural persons and, as a rule, 150 € for juristic persons. In its work, the association depends also on donations which can also be addressed with a specific purpose, such as "Ernst-Eckhard-Koch-Prize" (Account-No.: 414 44 40 at the Deutsche Bank AG, BLZ 100 700 00). Fees and donations are enjoying tax privileges.

If somebody else feels associated with Helmholtz-Zentrum Berlin and its circle of friends we kindly ask him to support our activities by becoming a member.

The Board of the Association

An den Vorstand
Freundeskreis Helmholtz-Zentrum Berlin e.V.
Albert-Einstein Straße 15
12489 Berlin
Germany

Tel.: +49-30-8062 - 12901
Fax.: +49-30-8062 - 12920
e-mail: freundeskreis@helmholtz-berlin.de
Internet: http://www.helmholtz-berlin.de/freundeskreis

Mitgliedschaft

Hiermit beantrage ich die Aufnahme in den Verein Freundeskreis Helmholtz-Zentrum Berlin e.V.

Membership

Herewith I apply for admission to the Association Friends of Helmholtz-Centre Berlin

Angaben zur Person / personal data	
	Anrede: / salutation: Nachname: / last name: Vorname: / first name:
	Geburtsdatum: /date of birth: (DD-MM-YYYY) Herkunftsland:/Staatsangehörigkeit: /nationality
	Titel: / title: Berufsbezeichnung: / profession:
Institution / institution	
Name: / name:	
Abteilung: / department:	
Straße: / street:	
PLZ: / zip: Ort: / city: district:	
Land: / country:	
Telefon: / phone: Fax: / fax:	
Homepage: / e-mail: homepage of institution:	

Die jährlichen Mitgliedsbeiträge betragen zur Zeit für natürliche Personen EUR 40,-, für juristische Personen EUR 150,-, EUR 100,- oder EUR 50,-, für Studenten EUR 10,-. / The regular annual membership fees amount to EUR 40,- for natural persons, EUR 150,--/100,-/50,- for legal entities, EUR 10,- for students.

Art der Person: / Character of person: natural person _____ legal entity _____
Mitgliedsbeitrag : / Membership fees: Euro _____

Im Rahmen freiwilliger Höherstufung/ voluntary upgrading: Euro _____

Datum: / date: Unterschrift: / signature:

HZB User Committee Election 2013

The HZB User Committee collects matters of concern to individual users working both at BER II and BESSY II, conveys an assessment summary of these matters and suggests appropriate measures to the Scientific Directors. The User Committee always encourages users to comment on topics that are currently being discussed within the panel, and between panel members and the HZB management. Feedback on these issues can be an important point in decision-making. The User Committee can be contacted by e-mail (usercommittee@helmholtz-berlin.de). Members are elected annually at the Joint BER II and BESSY II users meeting. At current the User Committee consists of the following colleagues:

Dr. Burkhard Langer (spokes person)

Benedetta Casu

Christiane Helm

Yvette Roske

Oliver Stockert

Denis Vyalikh

For replacement of three members and extention by one member the following candidates are nominated for the current election

Heloisa Bordallo

Eva Kovacevic

Christian Papp

Carolin Schmitz-Antoniak

Thomas Strunskus

All users of BER II and BESSY II present at the Joint User Meeting can vote for one of the above candidates. We encourage all participants to take part in the election.

This page is intentionally left blank for your notes…

Helmholtz-Zentrum Berlin
Lise-Meitner Campus
Wannsee

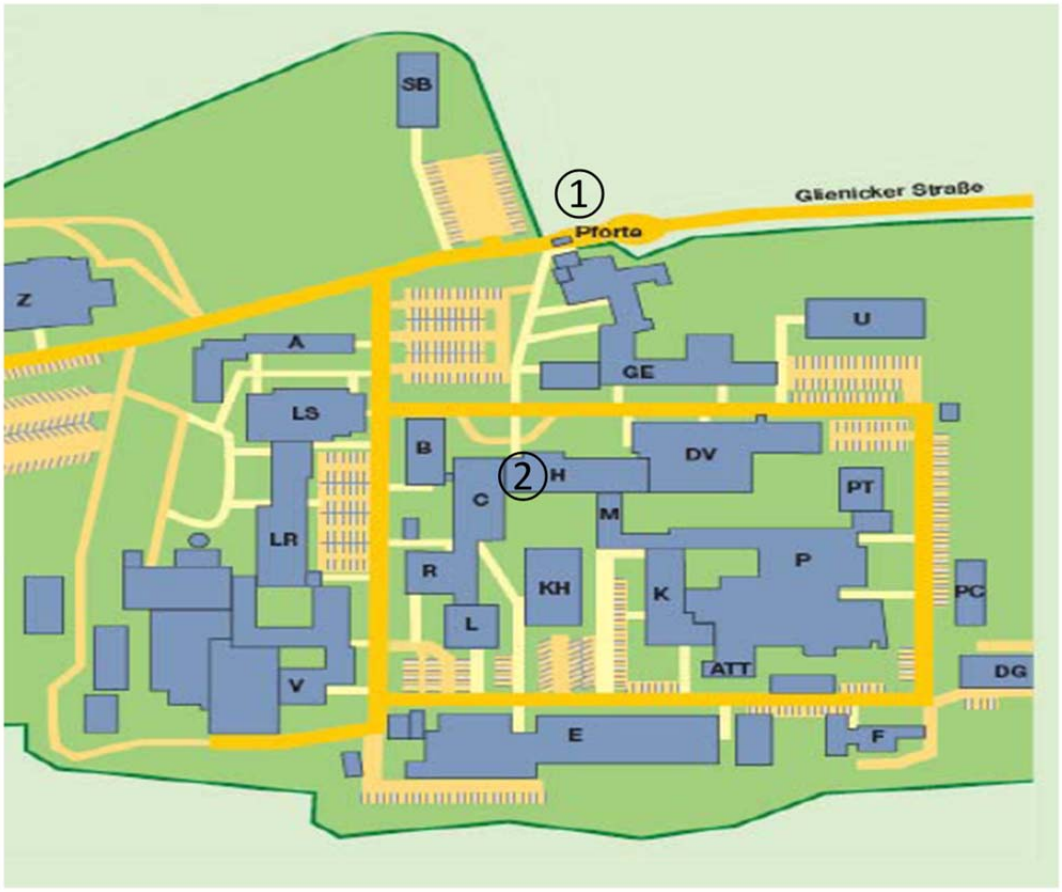

① Main entrance
② Lecture building (H): LMC-Foyer
Cafe Jahn
Lecture Hall

BER II
Hahn-Meitner-Platz 1
14109 Berlin

tel +49 (0)30 8062-42304
fax +49 (0)30 8062-42523
neutrons@helmholtz-berlin.de

Helmholtz-Zentrum Berlin
Wilhelm Conrad Röntgen Campus
Adlershof

① Train Station Adlershof
② Lectures: Humboldt Uni, room 0‘101
③ Conference Dinner: Wista, Newton room
④ BESSY II

Hotels:
⑤ Airporthotel
⑥ Berolina
⑦ Dorint

BESSY II
Albert-Einstein-Str. 15
12489 Berlin

tel +49 (0)30 8062-12931
fax +49 (0)30 8062-14673
photons@helmholtz-berlin.de

HZB Helmholtz Zentrum Berlin

Call for Proposals 2014/II

The HZB User Coordination invites the submission of proposals for the next joint proposal round for the large scale facilities **BESSY II** and **BER II** for beamtime from October 2014 to February 2015. The submission will be open soon.

Next deadline for submission: 1 March 2014

Beamtime applications have to be submitted by using the online **General Access Tool** (**GATE**).
For guidance in writing a proposal please refer to the Guide for beamtime application.

www.helmholtz-berlin.de/user/beamtime/proposals/index_en.html